

2

AD-A218 873

NAVAL POSTGRADUATE SCHOOL

Monterey, California



THESIS

ON THE EFFECTIVENESS OF THE PRODUCTION
OF ANTARCTIC BOTTOM WATER IN THE
WEDDELL AND ROSS SEAS

by

David B. St.Pierre

September 1989

Thesis Advisor
Co-Advisor

Arne Foldvik
Robert H. Bourke

Approved for public release; distribution is unlimited.

DTIC
ELECTE
MAR 8 1990
S B D

Unclassified

security classification of this page

REPORT DOCUMENTATION PAGE				
1a Report Security Classification Unclassified			1b Restrictive Markings	
2a Security Classification Authority			3 Distribution Availability of Report	
2b Declassification Downgrading Schedule			Approved for public release; distribution is unlimited.	
4 Performing Organization Report Number(s)			5 Monitoring Organization Report Number(s)	
6a Name of Performing Organization Naval Postgraduate School		6b Office Symbol (if applicable) 35	7a Name of Monitoring Organization Naval Postgraduate School	
6c Address (city, state, and ZIP code) Monterey, CA 93943-5000			7b Address (city, state, and ZIP code) Monterey, CA 93943-5000	
8a Name of Funding Sponsoring Organization		8b Office Symbol (if applicable)	9 Procurement Instrument Identification Number	
8c Address (city, state, and ZIP code)			10 Source of Funding Numbers	
			Program Element No	Project No
			Task No	Work Unit Accession No
11 Title (include security classification) ON THE EFFECTIVENESS OF THE PRODUCTION OF ANTARCTIC BOTTOM WATER IN THE WEDDELL AND ROSS SEAS				
12 Personal Author(s) David B. St.Pierre				
13a Type of Report Master's Thesis		13b Time Covered From 10	14 Date of Report (year, month, day) September 1989	
15 Page Count 138				
16 Supplementary Notation The views expressed in this thesis are those of the author and do not reflect the official policy or position of the Department of Defense or the U.S. Government.				
17 Cosatt Codes			18 Subject Terms (continue on reverse if necessary and identify by block number)	
Field	Group	Subgroup	Antarctic; Weddell Sea; Ross Sea, bottom water	
19 Abstract (continue on reverse if necessary and identify by block number)				
<p>The northward propagation of Antarctic Bottom Water (AABW), from its primary source in the Weddell Sea, has been documented since the early part of this century. Despite the striking similarities between the Weddell and the Ross Seas, AABW is mainly produced in the Weddell Sea. The question is posed as to why the Weddell Sea is so effective in the production of AABW as compared to the Ross Sea. Differences are determined by analyzing various physical mechanisms and forcing functions in both basins with respect to the two predominant theories of AABW formation, Foster and Carmack's shelf break process theory and Foldvik and Gammelsrød's theory of ice shelf processes. Results reveal that the strong tidal forcing at the Weddell Sea ice shelf barrier combines with the wind stress field and with the special under-ice-shelf and continental shelf bathymetries of the Weddell Sea to become the critical elements of the AABW formation process. The shelf break process theory is found to predict the formation of intermediate or deep waters in both basins. The ice shelf process theory is found to account for the formation of Weddell Sea Bottom Water (WSBW), the parent constituent of AABW, with a prediction of an Ice Shelf Water outflow rate of approximately $0.7 \times 10^6 \text{ m}^3 \text{ s}^{-1}$ (due to tidal action at the barrier allowing ice production by high surface freezing levels and tidal forcing of sea water under the ice shelf) and a production rate of WSBW of $5 \times 10^6 \text{ m}^3 \text{ s}^{-1}$ which agrees with observations and current estimates.</p>				
20 Distribution Availability of Abstract			21 Abstract Security Classification	
<input checked="" type="checkbox"/> unclassified unlimited <input type="checkbox"/> same as report <input type="checkbox"/> DTIC users			Unclassified	
22a Name of Responsible Individual Robert H. Bourke			22b Telephone (include Area code) (408) 646-3270	22c Office Symbol 68Bf

DD FORM 1473, 84 MAR

83 APR edition may be used until exhausted
All other editions are obsolete

security classification of this page

Unclassified

Approved for public release; distribution is unlimited.

On the Effectiveness of the Production
of Antarctic Bottom Water in the
Weddell and Ross Seas

by

David B. St.Pierre
Lieutenant Commander, United States Navy
B.S., Loyola University of Chicago, 1974
M.B.A., Cornell University, 1976

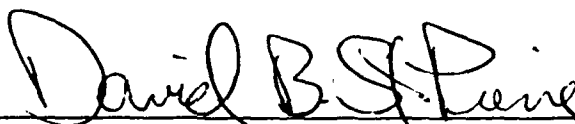
Submitted in partial fulfillment of the
requirements for the degree of

MASTER OF SCIENCE IN METEOROLOGY AND OCEANOGRAPHY

from the

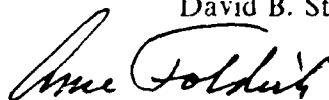
NAVAL POSTGRADUATE SCHOOL
September 1989

Author:

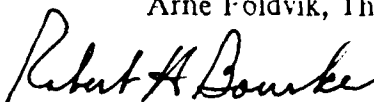


David B. St.Pierre

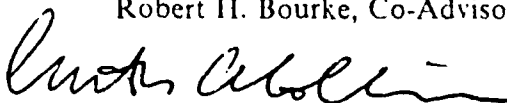
Approved by:



Arne Foldvik, Thesis Advisor



Robert H. Bourke, Co-Advisor



Curtis A. Collins, Chairman,
Department of Oceanography

ABSTRACT

The northward propagation of Antarctic Bottom Water (AABW), from its primary source in the Weddell Sea, has been documented since the early part of this century. Despite the striking similarities between the Weddell and the Ross Seas, AABW is mainly produced in the Weddell Sea. The question is posed as to why the Weddell Sea is so effective in the production of AABW as compared to the Ross Sea. Differences are determined by analyzing various physical mechanisms and forcing functions in both basins with respect to the two predominant theories of AABW formation, Foster and Carmack's shelf break process theory and Foldvik and Gammelsrød's theory of ice shelf processes. Results reveal that the strong tidal forcing at the Weddell Sea ice shelf barrier combines with the wind stress field and with the special under-ice-shelf and continental shelf bathymetries of the Weddell Sea to become the critical elements of the AABW formation process. The shelf break process theory is found to predict the formation of intermediate or deep waters in both basins. The ice shelf process theory is found to account for the formation of Weddell Sea Bottom Water (WSBW), the parent constituent of AABW, with a prediction of an Ice Shelf Water outflow rate of approximately $0.7 \times 10^6 \text{ m}^3 \text{ s}^{-1}$ (due to tidal action at the barrier allowing ice production by high surface freezing levels and tidal forcing of sea water under the ice shelf) and a production rate of WSBW of $5 \times 10^6 \text{ m}^3 \text{ s}^{-1}$ which agrees with observations and current estimates.

Accession For	
NTIS GRA&I	<input checked="" type="checkbox"/>
DTIC TAB	<input type="checkbox"/>
Unannounced	<input type="checkbox"/>
Justification	
By	
Distribution/	
Availability Codes	
Dist	Avail and/or Special
A-1	

TABLE OF CONTENTS

I. INTRODUCTION	1
A. A UNIQUE SOURCE OF ANTARCTIC BOTTOM WATER	1
B. CLASSICAL THEORY OF BOTTOM WATER FORMATION	2
C. GOAL AND OBJECTIVES	4
D. APPROACH	4
1. Literature Search	4
2. Data Acquisition and Analysis	4
3. Determination	4
II. BACKGROUND.	7
A. ANTARCTIC OCEANOGRAPHY AND CLIMATOLOGY	7
1. Geography	7
2. Meteorology.	7
3. Sea Ice	8
4. Currents, Water Structure and Tides	8
5. Water Masses.	10
B. ANTARCTIC BOTTOM WATER	10
1. Basic Characteristics	10
2. Distribution.	11
3. Tracing Antarctic Bottom Water	11
C. PHYSICAL REQUIREMENTS OF AABW FORMATION	13
1. Mechanisms	13
a. Convection	13
b. Pressure-related Instability	13
c. Wind-induced Downwelling	13
d. Chimneys	13
e. Double-diffusion	14
f. Cabbeling	14
g. Glacial Melting Freezing	14
h. Miscellaneous processes	14
2. Water Masses	15

3. Theory and Evidence	16
4. Shelf Break Process Theory	17
5. Ice Shelf Process Theory	18
D. FORCING FUNCTION REQUIREMENTS	19
1. General	19
2. Geography.	19
3. Surface Air Temperature and Its Effect on the Growth of Sea Ice	20
4. Surface Winds	21
a. Climatological Surface Winds	21
b. Katabatic Winds	22
5. Sea Ice Concentration	23
6. Hydrography.	24
7. Under-Ice-Shelf Bathymetry.	24
8. Tidal Forcing.	25
III. DATA ACQUISITION, ANALYSIS METHODOLOGY AND LIMITA- TIONS	50
A. FORCING FUNCTION DATA SOURCES AND DATA PRESENTA- TION	50
1. Geography.	50
2. Surface Air Temperatures	50
3. Surface Winds	50
4. Ice Concentration	51
5. Hydrography	51
6. Under-Ice-Shelf Bathymetry	52
7. Tides	52
B. METHOD OF DATA ANALYSIS	53
1. Zonation	53
2. Tidal Comparison Statistic	56
C. LIMITATIONS OF DATA AND METHODOLOGY	57
1. NCAR Temperature and Wind Fields.	57
2. Satellite Blended Ice Concentrations	57
3. Hydrographic Data Limitations	57
4. Limitations on Tidal Information	58

IV. RESULTS OF ANALYSIS	61
A. GEOGRAPHY	61
1. Continental Shelf	61
2. Shelf Bathymetry	61
3. Latitude Considerations	62
4. Ice Shelves	62
B. SURFACE AIR TEMPERATURE	62
C. SURFACE WINDS	67
D. ICE CONCENTRATION	67
E. HYDROGRAPHY	68
1. Horizontal Circulation and Water Masses	68
2. Vertical Circulation and Water Masses	68
F. UNDER-ICE-SHELF BATHYMETRY	70
G. TIDES	70
1. Barrier Comparisons	70
2. Zonal Comparisons	71
V. DISCUSSION	101
A. UNIQUENESS OF THE WEDDELL SEA	101
1. Non-Unique Forcing Functions	101
a. Geography	101
b. Hydrography	101
c. Surface Air Temperatures	101
2. Surface Winds Revisited	101
3. Hydrography Revisited	102
4. Austral Summer Ice Concentration Revisited	102
5. Continental Shelf and Under-Ice-Shelf Bathymetry Revisited	103
6. Tidal Forcing Revisited	104
7. Summary of the Uniqueness of The Weddell Sea	104
B. RELEVANT THEORY	105
1. Shelf Break Process	105
2. Ice Shelf Process	106
VI. CONCLUSIONS	110

APPENDIX A. FREEZING DUE TO TIDES AT THE ICE SHELF BARRIER	112
A. ICE PRODUCTION	112
B. ICE GROWTH COEFFICIENT	114
APPENDIX B. PLUME MIXING WITH WARM DEEP WATER	115
LIST OF REFERENCES	117
INITIAL DISTRIBUTION LIST	124

LIST OF TABLES

Table 1.	WATER MASSES INVOLVED IN THE FORMATION OF AABW ..	16
Table 2.	MAJOR TIDAL CONSTITUENTS	53
Table 3.	ZONE DIMENSIONS (KM)	54
Table 4.	ZONE TO CROSS SECTION CROSS REFERENCE	55
Table 5.	ROSS SEA HYDROGRAPHIC STATION LOCATIONS	55
Table 6.	WEDDELL SEA HYDROGRAPHIC STATION LOCATIONS	56
Table 7.	CONTINENTAL SHELF SIZE	61
Table 8.	PERCENTAGE OF SHELF AREA VERSUS DEPTH	61
Table 9.	AVERAGE ZONAL AND BASIN SURFACE AIR TEMPERATURES (°C) FOR JANUARY THROUGH APRIL	64
Table 10.	AVERAGE ZONAL AND BASIN SURFACE AIR TEMPERATURES (°C) FOR MAY THROUGH AUGUST	65
Table 11.	AVERAGE ZONAL AND BASIN SURFACE AIR TEMPERATURES (°C) FOR SEPTEMBER THROUGH DECEMBER	66
Table 12.	AVERAGE TIDAL AMPLITUDE (CM) IN THE ROSS AND WEDDELL SEAS	72
Table 13.	TIDAL PHASE COMPARISONS BETWEEN THE ROSS AND WEDDELL SEAS	73

LIST OF FIGURES

Figure 1.	The northward flow of Antarctic Bottom Water	5
Figure 2.	A schematic illustration of the classical view of AABW formation	6
Figure 3.	Topography of the Southern Ocean shown with ice shelf orientation	27
Figure 4.	Mean surface winds (knots) for August and February	28
Figure 5.	Mean surface air temperatures (°C) for August and February	29
Figure 6.	Mean sea surface temperatures (°C) for August and February	30
Figure 7.	Prevailing wind directions for the Southern Ocean and Antarctica	31
Figure 8.	Average atmospheric pressure (millibars) for January (top) and July (bottom)	32
Figure 9.	Sea ice coverage around Antarctica illustrating absolute and mean minimum and maximum extents	33
Figure 10.	Surface circulation around Antarctica (knots)	34
Figure 11.	Antarctic Circumpolar Current showing the Weddell and Ross Sea gyres	35
Figure 12.	A schematic of the vertical structure and motion of the Southern Ocean	36
Figure 13.	Tidal ranges around Antarctica (feet)	37
Figure 14.	Types of tides in the Southern Ocean	38
Figure 15.	A schematic of the water masses in the Southern Ocean	39
Figure 16.	Temperature evolution of Antarctic Bottom Water shown by temperature regimes	40
Figure 17.	A schematic of wind-induced downwelling along an Antarctic ice shelf	41
Figure 18.	A schematic illustrating the formation of deep convection chimneys	42
Figure 19.	A schematic illustrating various double-diffusive processes involved in the formation of AABW	43
Figure 20.	A schematic illustrating various cabbeling processes involved in the formation of AABW	44
Figure 21.	A schematic illustrating glacial melting freezing processes involved in the formation of AABW	45
Figure 22.	A schematic summary of the physical process effecting AABW formation	46
Figure 23.	A schematic illustrating the shelf break process mixing scheme involved in the formation of AABW	47
Figure 24.	A schematic illustrating the ice shelf processes involved in the formation	

of AABW	48
Figure 25. Katabatic wind regimes of the Antarctic continent	49
Figure 26. Map of the Ross Sea showing zonation scheme.	59
Figure 27. Map of the Weddell Sea showing zonation scheme.	60
Figure 28. Continental shelf bathymetry for the Ross Sea	74
Figure 29. Continental shelf bathymetry for the Weddell Sea	75
Figure 30. Climatological surface wind velocities in the Ross and Weddell Seas for January through March.	76
Figure 31. Climatological surface wind velocities in the Ross and Weddell Seas for April through June.	77
Figure 32. Climatological surface wind velocities in the Ross and Weddell Seas for July through September.	78
Figure 33. Climatological surface wind velocities in the Ross and Weddell Seas for October through December.	79
Figure 34. Mean monthly ice concentration contours for January to June	80
Figure 35. Mean monthly ice concentration contours for July to December	81
Figure 36. Yearly cycle of area covered by sea ice in the Ross and Weddell Seas ..	82
Figure 37. Interannual variation of mean sea ice concentration in the Ross and Weddell Seas	83
Figure 38. Mean summer surface circulation for the Ross and Weddell Seas	84
Figure 39. Mean summer surface salinities for the Ross and Weddell Seas	85
Figure 40. Mean summer sea surface temperature (°F) for the Ross and Weddell Seas	86
Figure 41. Mean summer sea surface densities (sigma-t) for the Ross and Weddell Seas	87
Figure 42. Hydrographic station locator map shown for the Ross Sea.	88
Figure 43. Hydrographic station locator map shown for the Weddell Sea	89
Figure 44. Temperature, salinity, and density (sigma-t) cross-sections for Track 1 ..	90
Figure 45. Temperature, salinity, and density (sigma-t) cross-sections for Track 2 ..	91
Figure 46. Temperature, salinity, and density (sigma-t) cross-sections for Track 3 ..	92
Figure 47. Temperature, salinity, and density (sigma-t) cross-sections for Track 5 ..	93
Figure 48. Temperature, salinity, and density (sigma-t) cross-sections for Tracks 4 and 6 in the Ross Sea	94
Figure 49. Temperature, salinity, and density (sigma-t) cross-sections for Track 4 in the Weddell Sea.	95

Figure 50. Contours (meters) of bottom depth	96
Figure 51. Semi-diurnal corange map for the Ross Sea (top) and Weddell Sea (bottom)	97
Figure 52. Semi-diurnal cotidal map for the Ross Sea (top) and Weddell Sea (bottom)	98
Figure 53. Diurnal corange map for the Ross Sea (top) and Weddell Sea (bottom)	99
Figure 54. Diurnal cotidal map for the Ross Sea (top) and Weddell Sea (bottom)	100
Figure 55. Possible flow path under the Weddell Sea ice shelves	109

I. INTRODUCTION

...if we assume the world's oceans contain 10^9 km^3 of sea water, have a residency time of 1000 years and a vertical ventilation rate of 1 mm s^{-1} due to the thermohaline convection of bottom waters, then the area of sinking surface water needed to maintain this regime is 10^4 km^2 . What we are talking about is a surface area as small as the size of Rhode Island needed to produce all the bottom waters of the free oceans!

Gascard (1989)

...the observed, dynamically active zone in front of the 500 km long Ronne Ice Shelf in the Weddell Sea has a surface area of 10^4 km^2 . Rhode Island just moved to the Antarctic!

Foldvik (1989)

A. A UNIQUE SOURCE OF ANTARCTIC BOTTOM WATER

As soon as observations of the temperature and salinity of the waters around the Antarctic continent were acquired at the beginning of this century, it became evident that the coldest bottom water was to be found near the western and northern margins of the Weddell Sea. In fact, the bottom temperatures were found to increase progressing eastward from the Weddell Sea, continuing all around the circumpolar ocean. This pattern of increasing bottom temperatures with increasing eastward progression was combined with simultaneous increases in salinity and decreases in oxygen content to support the hypothesis that the Weddell Sea was the major source of Antarctic Bottom Water (AABW). Though some highly saline shelf water has been found in the Ross Sea and evidence of bottom water from this source has been detected in the deep ocean, the amount has been remarkably small (Deacon, 1977).

Hence, the Weddell Sea has been regarded as the primary source of AABW ever since the pioneering work of Brennecke (1982 translation of original 1921 work), Mosby (1934) and Deacon (1937). This bottom water has been shown to spread northward into the Atlantic, Pacific and Indian Oceans by Deacon (1937, 1963), Wüst (1978 translation of original 1938 work) and Reid and Lynn (1971) (Figure 1).

B. CLASSICAL THEORY OF BOTTOM WATER FORMATION

Ever since Count Rumford in 1800 obtained the first temperature measurements of oceanic waters at low and temperate latitudes and inferred that cold water flowed from high latitudes towards the equator in the deep ocean, the problem of bottom water formation has intrigued oceanographers (Foldvik and Gammelsrød, 1988, p. 12).

Historically, all theories for the formation of AABW have included two processes:

- **COOLING.** Whenever high salinity water found in warm regions is transported into the polar oceans, cooling and mixing with the cold polar water will produce dense water whose characteristic are comparable to deep water.
- **FREEZING.** Reducing sea water to its freezing point augments the density of that water through temperature-induced volume contraction and through a salinity increase due to brine rejection during the freezing process.

When a parcel of sea water is cooled it becomes denser. When freezing of the parcel commences, the salinity of the adjacent unfrozen parcels is increased through brine rejection of the frozen parcel. When the effects of cooling and freezing are combined, the unfrozen parcels become even denser and sink. If this scenario is applied to the Antarctic coast where the coldest waters in the world's free oceans are found, dense water will sink to the bottom and flow along the bottom of the ocean basins towards the equator and beyond. This water is called Antarctic Bottom Water (AABW).

A number of perplexing problems concerning the role of freezing ice in the formation of AABW remains, not the least of which is actually observing the process. Though less saline than the Warm Deep Waters of the great oceans (e.g., the warm salty outflow from the Mediterranean Sea into the Atlantic Ocean), the salinity of AABW is too high for it to be the result of a simple mixture of surface and deep waters. Neither have deep waters with appropriate temperature-salinity properties been found at the surface where they could be cooled without dilution to form AABW.

At first look, it appears remarkable that the effect of intense cooling all around the Antarctic continent should be confined to the surface layer. No obvious mechanism for direct cooling of the deep waters is apparent. But there are places on the continental shelf of Antarctica where prolonged or intense vertical mixing reduces the temperature of the deep water sufficiently to facilitate the production of very

dense mixtures. Conditions near the southern and western margins of the Ross and Weddell Seas are particularly favorable. At these high latitude locations the continental shelves are broad and wide and the deep water near the continental slope, arriving as a westerly flow, is already cooled and can mix with the higher salinity, near-freezing surface water to produce dense bottom water.

Bottom waters are cold and form at high latitudes. This is not an *a priori* condition just because the coldest waters are found at high latitudes. In the same vein, just because some waters have higher salinities does not mean that they will produce bottom water. Bottom water is produced in the Antarctic because the coldest waters in the world are found there under the floating ice shelves, coupled with the fact that cold sea water is more compressible than warm sea-water, a feature of sea water explained by the variability of the coefficient of thermal expansion with pressure (Gill, 1973). Thus, if the source water for AABW were to differ in temperature and salinity but had the same surface density as a warmer water mass, it would be denser than this other water mass at depth because of its initially lower temperature.

The classical view of the formation of AABW presented by Brennecke (1982 translation) and Mosby (1934) assumed that strong winds maintained open leads in the water which produced excessive sea ice whose salt rejection during the freezing process would lead to an increase of salinity in the Antarctic shelf water. When the salinity exceeded 34.62 PSU, the shelf water would sink beneath the intermediate water (Warm Deep Water) to become bottom water (see Figure 2).

This simple view has been dismissed by Carmack (1977) who showed that brine-enriched shelf water does not simply run down the shelf but is mixed with the Warm Deep Water to form a water denser than either of its parent constituents. It is this denser water that flows down the continental slope entraining ambient water to become AABW.

Past scientific discussion has been focused on the mechanisms which are active in producing this dense bottom water, such as freezing of sea water (Foster and Carmack, 1976a,b), interactions between sea water and ice shelves (Foldvik and Kvinge, 1974) or double diffusion related to melting sea ice (Gill, 1973). However, a more relevant question appears to be: Why is the Weddell Sea so dramatically more effective than the Ross Sea or other Antarctic ice shelf regions in producing

bottom water?¹ The climates are similar, the depths and the areas of the shelves are comparable. Even the areas covered by their respective floating ice shelves appear to be the same, so why is so little AABW produced in the vicinity of the Ross Sea?

C. GOAL AND OBJECTIVES

The goal of this thesis is to answer the question why the Weddell Sea is more effective than the Ross Sea in producing Antarctic Bottom Water. To reach this goal two objectives must be met. First, a study must be made to determine what is unique about the Weddell Sea as compared to the Ross Sea. Secondly, an examination of the theories for AABW formation should be conducted to determine which one does the best to explain why the Weddell Sea's unique qualities are crucial to the formation of AABW.

D. APPROACH

To achieve these objectives of determining unique Weddell Sea qualities and best formation theory based on those unique qualities, three steps are required.

1. Literature Search

- Review the general Antarctic/Southern Ocean environment to determine the setting for the formation of AABW.
- Determine the characteristics, distribution and methods of tracing AABW to establish clues to learn what qualities might be indicators of its formation.
- Analyze the theories of AABW as to their physical mechanisms. Determine which mechanisms appear to dominate.
- Determine the forcing functions required by each of these theories.

2. Data Acquisition and Analysis

- Collect data on the specific forcing functions of the Ross and Weddell Seas, their adjacent coast lines and ice shelves.
- Analyze the data and determine what differences exist between the two regions.

3. Determination

- Determine what is unique about the Weddell Sea from the data analysis.
- Determine which of the theories of AABW formation best describes the formation process by determining which forcing function requirements are met in the Weddell Sea but not in the Ross Sea.

¹ This question was raised by Foldvik and Gammelsrød (1988) and became the seed of this research.

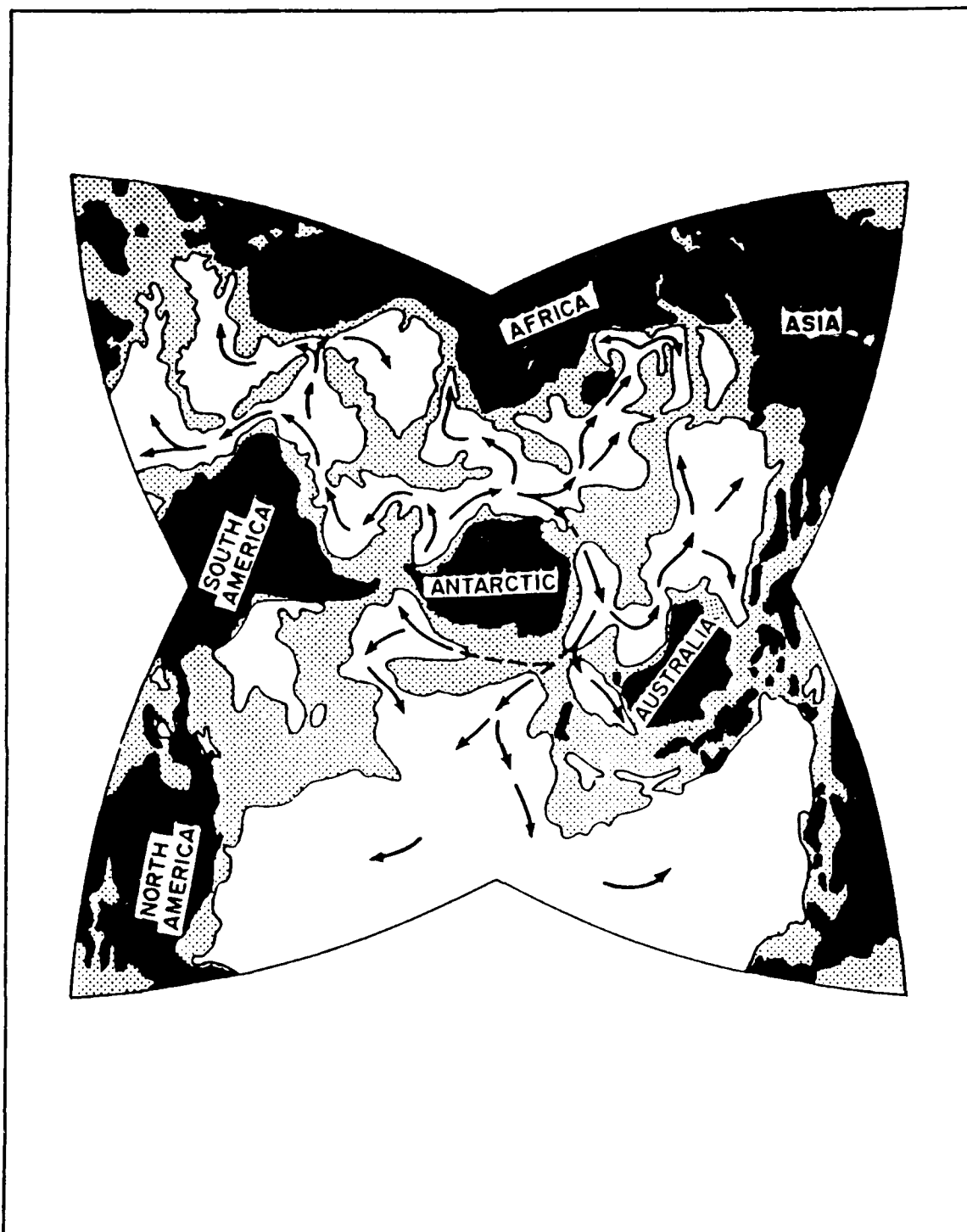


Figure 1. The northward flow of Antarctic Bottom Water from its source region in the Weddell Sea (after Tchernia, 1980).

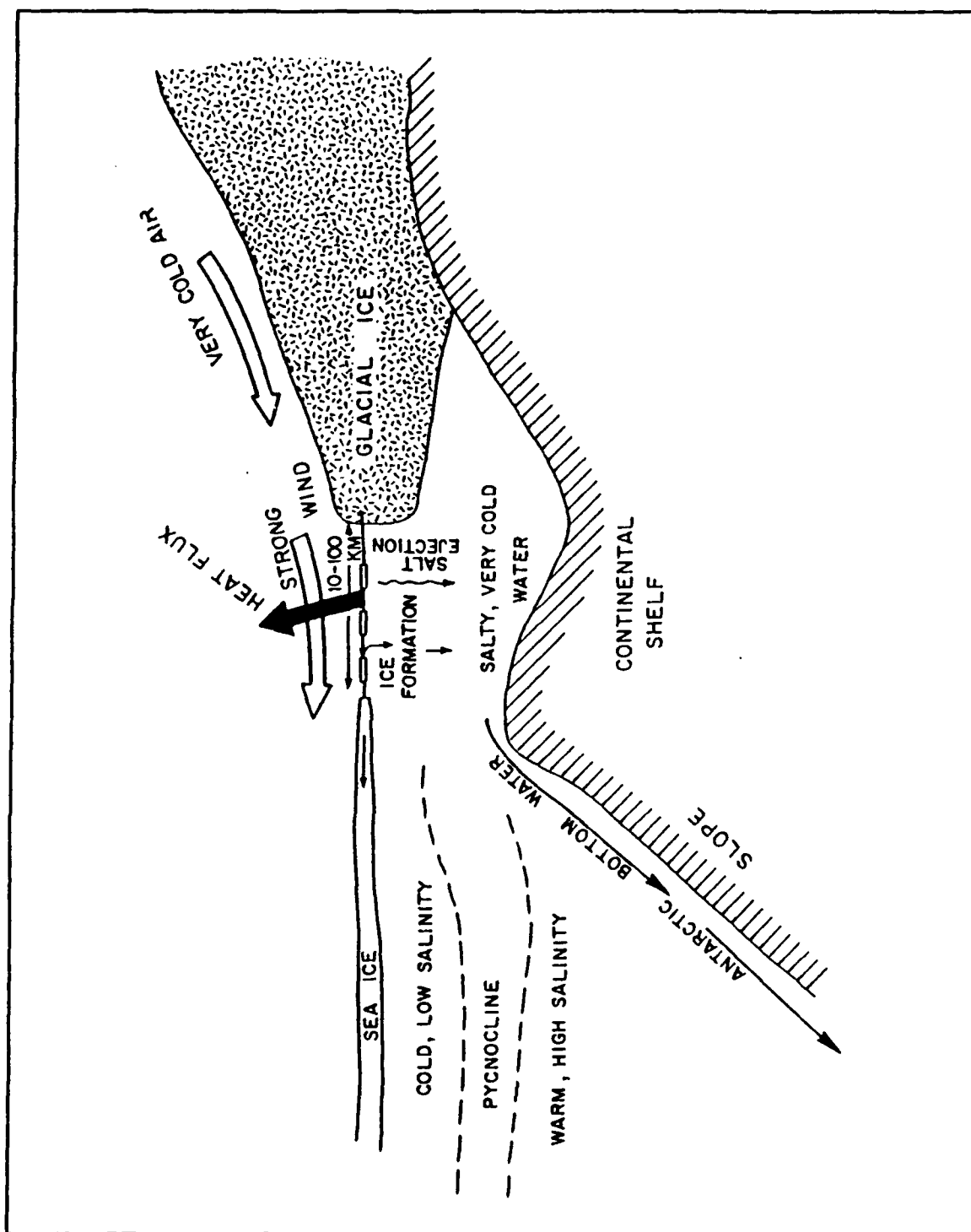


Figure 2. A schematic illustration of the classical view of AABW formation (after Gordon, 1988).

II. BACKGROUND

A. ANTARCTIC OCEANOGRAPHY AND CLIMATOLOGY

1. Geography

Antarctica is totally surrounded by the Southern Ocean which is a confluence of the southernmost portions of the Pacific, Atlantic and Indian Oceans. The Weddell, Bellingshausen, Amundsen and Ross Seas are adjacent to the continent (Figure 3). The Southern Ocean is unique among the world's oceans because of the configuration of land and water which permits a circumpolar zonal flow which contains approximately 10 % of all the world's sea water (DMA, 1985, p. 7). The Antarctic continent provides the southern boundary of the Southern Ocean while the northern boundary is defined by the Polar Front, also termed the Antarctic Convergence. The total area of the Southern Ocean is vast, $38 \times 10^6 \text{ km}^2$, with a volume of $140 \times 10^6 \text{ km}^3$ (Carmack, 1986, p. 644).

The bathymetry of the Southern Ocean consists of four major basins each exceeding 4500 m in depth and separated from each other by broad ridges and plateaus (Figure 3 details this morphology). The continental shelves surrounding Antarctica are relatively narrow and are two to four times deeper than the average oceanic shelf depth, extending to 1000 m. Two exceptions are the two broad (500 km longshore dimension) and deep (500 m) shelves of the Weddell and Ross Seas. These two shelf embayments contain massive floating ice shelves of glacial origin which thicken rapidly towards the continent. At the edge of the continental shelf the continental slope steepens rapidly to 3000-4000 m depth in a horizontal traverse of 100-200 km.

2. Meteorology.

The Antarctic continent is the coldest region of the world. Frequent passage of intense cyclonic storms offshore, a strong outflow of cold air from the continent (katabatic winds) and precipitation in excess of evaporation make the Antarctic climate the most adverse climate in the world. Maps are presented that reflect the austral winter (August) and austral summer (February) mean surface winds (Figure 4), mean air temperature (Figure 5) and mean sea surface temperature (Figure 6).

The boundary between the polar continental and polar maritime air masses (the Antarctic coast) and the polar maritime and tropical maritime air masses (polar

front $\sim 50^{\circ}\text{S}$) represents an area of frequent and intense storm activity throughout the year. Storms generally are generated north of 70°S and circle the continent from west to east. Lows forming along the polar front tend to move southeasterly towards the continent. (DMA, 1985)

The lack of a meridional barrier for atmospheric flow over the Southern Ocean leads to a basic zonal wind regime (Figure 7). These mean wind fields flow clockwise around the quasi-permanent low pressure areas in both austral summer (January) and winter (July) (Figure 8) and, through zonal forcing of the sea surface, produce a westward flowing coastal current called the East Wind Drift. North of the lows the winds are westerly and produce an eastward surface circulation called the West Wind Drift.

3. Sea Ice

Sea Ice covers a large portion of the Antarctic waters and is the greatest single factor contributing to the isolation of the Antarctic continent (Figure 9). Most of the pack ice is newly formed every year and therefore has a maximum thickness of only one to two meters² and may contain many large polynyas and leads. During the austral winter sea ice completely surrounds the continent making an almost impassable barrier that extends northward from 65°S up to 55°S in some locations, occupying about 60 % of the Southern Ocean. During the austral summer ice melts to cover less than 10 % of the Southern Ocean. (Foldvik and Gammelsrød, 1988, p. 12)

Floating ice shelves hundreds of meters thick project off the continent and cover over 10^6 km^2 . These are the source of iceberg calving in the Southern Ocean (Tchernia, 1980).

4. Currents, Water Structure and Tides

The general surface circulation of the Southern Ocean is shown in Figure 10. The Antarctic Circumpolar Current or West Wind Drift is the world's largest current. This current completely encircles Antarctica reaching to the ocean floor. Closer to Antarctica, the East Wind Drift is a complex flow due to the irregularities of the Antarctic coastline and basins causing gyres to be formed in the Weddell and Ross Seas which Deacon (1937) found to be barotropic in both cases (Figure 11).

² On the continental shelf local production of sea ice may be quite different from the observed ice thickness (Foldvik and Gammelsrød, 1988). This will be discussed later.

Westerly winds that frictionally drive the Antarctic Circumpolar Current (ACC) have a northerly component due to the Coriolis force. These northward flows move up the west side of South America as the Humboldt Current, up the east side of South America as the Falklands Current, up the west side of Africa as the Benguela Current and equatorward between Australia and New Zealand. The northern limit of the Southern Ocean, called the Polar Front, occurs where the Antarctic surface waters of the ACC thrust under the warmer subantarctic waters. A region of weak divergence, the Antarctic Divergence, exists between the eastward flowing ACC and the westward flowing East Wind Drift and significant upwelling of Warm Deep Water occurs here (Gordon and Goldberg, 1970).

The upwelling of Warm Deep Water is shown schematically in a meridional cross section depicting the general vertical structure and motions of the Southern Ocean (Figure 12). As Foldvik and Gammelsrød (1988, pp. 5-6) state:

"...this deep water upwelling is perhaps the single most important oceanographic process of the Antarctic and fundamental to its biology...this process allows the deep water contact with the surface layers and the associated air-sea interactions...note that oxygen minimum and the temperature maximums coincide and rise at the Antarctic Divergence together with the underlying salinity maximum. The cold, low-salinity high-oxygen Antarctic surface water moves north towards the Antarctic Convergence...where it sinks and contributes to the formation of the low-salinity, intermediate water of the world's oceans. North of the Antarctic Convergence we find the warmer subantarctic surface water towards the Subtropical Convergence where temperature increases rapidly. Near the bottom the very cold Antarctic Bottom Water is moving north from its primary generating source in the Weddell Sea. Sandwiched between these two Antarctic water masses...is a broad compensating flow of high-salinity warm...Deep Water. The south-flowing...Deep Water mixes with the Antarctic Waters above and below and contributes to the Antarctic Circumpolar Water which, in terms of volume, is the dominating water mass in the Southern Ocean."

The major horizontal movement of the subsurface waters is generally in the same direction as the surface currents; however, with increasing depth and changing bottom configuration, the subsurface current directions may deviate considerably from the surface directions. The speed of the current decreases with depth (Deacon, 1937). Finally, as can be seen in Figure 13, the tidal regimes of the Southern Ocean are not only far more active in the Atlantic sector than any other, but the other

sectors show none of the complexity of the Atlantic sector. The type of tides around the Antarctic coast is shown in Figure 14³.

5. Water Masses.

Much of the water column of the Southern Ocean can be separated into three main layers consisting of Surface Water (14%), Warm Deep Water (or Circumpolar Deep Water) (58%) and Antarctic Bottom Water (28%) (Carmack, 1977, p. 15). Pickard and Emery (1982, pp.136-137) further define the origin of these layers citing surface waters as originating from local ice melting and freezing, deep water as originating from the basins to the north of the Polar Front which is subsequently upwelled into the Antarctic Circumpolar Current, and bottom water originating from a mixture of Antarctic continental shelf water with the Warm Deep Water of the Antarctic Circumpolar Current.

Another water mass, unique to the Antarctic region, is found on the continental shelves near the ice shelf barriers and has an in-situ temperature below the freezing point at one atmosphere. It has been termed Ice Shelf Water. A representative breakdown of Southern Ocean water mass structures and temperature salinity ranges is presented in Figure 15. (The Weddell Sea is used here for reference. Different regions around the continent have similar structures with appropriate appellations.)

B. ANTARCTIC BOTTOM WATER

1. Basic Characteristics

From Sverdrup et al. (1942, pp. 605-613) and Gordon (1972, pp. 1-17) certain basic characteristics of the water mass known as Antarctic Bottom Water (AABW) are defined:

- AABW is the densest of all free ocean bottom waters having a density (σ_t) ~ 27.9 .
- AABW has a potential temperature less than 0 °C and a salinity between 34.6 and 34.7 PSU.
- AABW is formed by some process that mixes Antarctic surface waters to reach temperatures around -1.9 °C and salinities around 34.6 PSU, then entrains Warm Deep Water to warm its temperature to approximately -1 °C and increase its salinity to approximately 34.65, then flows equatorward increasing its temperature and salinity marginally.

³ It will be shown that the type of tide that occurs at the ice shelf barrier in the Weddell Sea is of a different type than shown in Figure 14.

- Current estimates of AABW formation rates range from $5 \times 10^6 \text{ m}^3 \text{ s}^{-1}$ (Carmack, 1977, p. 15), $7 \times 10^6 \text{ m}^3 \text{ s}^{-1}$ (Michel, 1978 p. 6192), $4.5 - 8 \times 10^6 \text{ m}^3 \text{ s}^{-1}$ (Weiss et al., 1979, p. 1110), to $13 \times 10^6 \text{ m}^3 \text{ s}^{-1}$ (Gordon, 1988, p. 44).

AABW originating from the Weddell Sea (and possibly the Ross Sea and other regions around the Antarctic coast) has been traced into the great abyssal plains (Figure 1) (Carmack, 1977; Jacobs et al., 1970; Gordon and Tchernia, 1972). The Weddell Sea source makes a contribution to the total production of AABW ten times greater than that of the Ross Sea (Carmack, 1977, p.36) and may represent 80% of its total production (Foldvik and Gammelsrød, 1988, p. 12).

2. Distribution.

The lowest bottom water temperatures are in the region of the Weddell Sea at 4000 m. The mean potential temperature of the bottom water rises as it circulates eastward around the continent until it reaches 0°C in the region of 90°W (Figure 16). Deacon (1937, p. 109) showed that the deep current exiting the Weddell Sea moves towards the east even in regions between the Antarctic Divergence and the continent, and that it passes the basins of the Indian and Pacific Oceans without receiving new contributions of bottom water from other parts of the Antarctic continental shelf. Gordon (1972) states that AABW characteristics of temperature, salinity and dissolved oxygen evolve by reason of the gradual mixing with the circumpolar waters above it. Tchernia (1980, p. 74) states that because of the high density of AABW, it can flow towards the bottom of all the oceanic basins whenever its movements are not impeded by ridges (Figure 1). This bottom water mixes to some extent with the deep waters along its path and its influence extends beyond the equator all the way to 40°N in the Atlantic and 50°N in the Pacific. It is from this dense bottom water that the deep waters of the major oceans derive their low temperatures.⁴

3. Tracing Antarctic Bottom Water

According to Worthington (1981, p. 54), no AABW can be traced unchanged to its point of origin in the Weddell Sea because its temperature and salinity become mixed with deep water as part of its formation process. This means that to determine the precise origin of a parcel of AABW other geochemical or biological tracers must be used. Some of these tracers have not only pinpointed the origin of

⁴ Three-quarters of the world's ocean volume (deep and bottom waters) is influenced by AABW whose zones of formation represent no more than .005% of its total area (Tchernia, 1980).

AABW but have made it possible to infer the process by which the AABW had been formed.

Broecker (1981, p. 434) found that by acting as tracers of circulation, mixing and metabolic processes, biological products, radioactive carbon, tritium, nitrates, phosphates, silicates, alkalinity and dissolved oxygen could be the keys to models designed to unscramble the mixtures found in the deep and bottom waters and thus determine the origins of the various mixing constituents (and their formation processes (Deacon, 1984))⁵. Weiss et al. (1979, p. 1093) and Chen and Rodman (1985) determined that location, but not formation process, could be determined by these tracers. However, they found that deuterium and isotopes of oxygen (18 and 16) could be used to infer formative processes relative to freezing and melting of sea ice and of evaporation and precipitation as they effect salinity and temperature of the components that mix to form AABW.

Oxygen 18 and 16 are especially effective as illustrative of formation processes for the following reason. As an air mass moves away from the equator, water molecules incorporating the heavier oxygen 18 are preferably removed by precipitation. The snow that falls at high latitude (forming glaciers) therefore holds more of the lighter isotope. Thus the low and middle latitude, poleward flowing ocean waters become more enriched with oxygen 18. The glacial melt water from the high latitudes, however, will be low in oxygen 18 relative to oxygen 16. Therefore if $^{18}\text{O}/^{16}\text{O}$ ratios are measured, a determination can be made as to whether the formation process involved shelf water by itself (high $^{18}\text{O}/^{16}\text{O}$ ratios) or whether glacial melt water was required (low $^{18}\text{O}/^{16}\text{O}$ ratios). Schlosser (1986) also claimed ^4He showed a strong signal when glacial water was involved.

With the minor exception of Jacobs and Fairbanks' (1985) progressive use of $^{18}\text{O}/^{16}\text{O}$ ratios for tracing bottom water production from under the Ross Ice Shelf, no comprehensive attempt has been made to trace the origin of AABW to its source process. Foldvik and Gammelsrød (1988, p. 16) imply that such comprehensive knowledge of $^{18}\text{O}/^{16}\text{O}$ ratios of AABW could determine which processes were involved in its formation. They believe that the results of such an experiment would show that AABW has a very low $^{18}\text{O}/^{16}\text{O}$ ratio, indicating that glacial melt water from under the ice shelves plays an important part in the formation of AABW.

⁵ In fact, most of the authors cited in this section have determined the Weddell Sea origin of AABW through these techniques.

C. PHYSICAL REQUIREMENTS OF AABW FORMATION

1. Mechanisms

Due to the refutation of the classical AABW formation theory, an explosion of new theoretical work has commenced. To account for the formation of AABW, three questions must be answered (Warren, 1981, p. 17):

1. How the density of the shelf water is increased to the point where it can sink through the relatively warm and saline water at mid-depth.
2. How the water moves off the shelf.
3. How it descends with entrainment to the floor of the Weddell Sea.

The following physical processes associated with circulation and mixing have been presented by various authors as attempts to answer one or more of these questions. Currently there are two predominant theories that attempt to answer all three questions and they will be presented at the end of this chapter.

a. Convection

When cooling of surface water and eventual surface freezing weakens the vertical stability of the water column, the surface water will sink. This water is replaced by warmer water from below, eventually overturning the entire water column and achieving homogeneity (Solomon, 1983; Gordon, 1978; Killworth, 1977a; Gill, 1973; Foster, 1972b).

b. Pressure-related Instability

Variations in the coefficient of thermal expansion make cold sea water more compressible than warm sea water. If two volumes of water with different temperatures and salinities have the same density at the surface, when brought to depth, the colder water will be denser (Gill, 1973).

c. Wind-induced Downwelling

Due to the Ekman flux, the predominantly westward flowing geostrophic wind drives the surface water to the left in the Southern Hemisphere and causes downwelling at the ice shelf barrier or coast (Figure 17) (Deacon, 1977; Killworth, 1977a).

d. Chimneys

Baroclinic instabilities generate cyclonic eddies which bring nearly neutral stability, deeper water close to the surface (doming) where surface freezing and brine convection can cause mixing to the bottom (Figure 18). Chimneys are narrow

columns of deep convective mixing formed by these intense buoyancy fluxes (Gascard, 1978; Killworth, 1979; Martinson et al., 1981).

e. Double-diffusion

When two or more components of different molecular diffusivity make opposite contributions to the vertical density gradient, the process acts to release potential energy of the destabilizing components. Two types can exist. Salt fingering occurs when warm saline water overlies cold, fresh water (temperature stabilized). Salt layering (diffusive instability) occurs when cold fresh water overlies warm saline water (salt stratified) (Carmack, 1986, p.681; Foster and Carmack, 1976b, p. 41; Foldvik, Gammelsrød, and Tørresen, 1985b, p. 189; Foldvik, Gammelsrød, Slotsvik, and Tørresen, 1985, p. 224). Three possible combinations of these two double-diffusive mechanisms that could lead to the formation of bottom water are shown in Figure 19.

f. Cabbeling

Due to the non-linearity in the equation of state of sea water, it is possible for the mixture of two parcels of sea water with the same density, but different temperatures and salinities, to have a greater density than that of the constituent parcels (Figure 20). This process is called cabbeling (Gill, 1973; Foster, 1972a; Hofenoff, 1956).

g. Glacial Melting/Freezing

Melting under the ice shelf generally tends to increase the static stability of the underlying water column. However, freezing occurring under the ice shelf releases a flux of salt into the underlying sea water and induces a convective motion due to the vertical instability of the water column near the base of the ice shelf (Figure 21) (Foldvik and Kvinge, 1974; Carmack, 1986, p. 666; Lewis and Perkins, 1985; Gill, 1973, pp. 123-126).

h. Miscellaneous processes

Other processes such as isopycnal mixing caused by the breaking of internal waves (Jacob and Georgi, 1977; Carmack and Killworth, 1978), shear (barotropic) instabilities (Foster and Carmack, 1976b, 1977) and continental shelf waves excited by tidal forcing (Middleton et al., 1982) have been proposed as forcing mechanisms as well.

The possible physical processes involved in the production of AABW are summarized in Figure 22.

2. Water Masses

As outlined above, a variety of physical processes work on the water masses found in the Antarctic regime. To understand the details of these processes, a familiarity with the water masses on the continental shelf is required. Water masses are traditionally identified by a core property, i.e., that part of a layer where some oceanographic characteristic reaches an extreme value. This method assumes that the core represents both the main axis of the spreading and the maximum percentage of a particular water type within a layer. Water masses may also stand out as densely patterned areas or modes on a potential temperature-salinity diagram. Divisions (boundaries) between water masses may be based on slope changes in the potential temperature-salinity (θ - S) curve, volumetric considerations, or simply be defined as the mid-point between two cores (Carmack, 1977, p. 18).

Eight water masses are of particular interest for the formation of AABW. Though Weddell Sea values are presented here, a similar structure exists in the Ross Sea with slightly different values but with the same relative ratios between masses. As previously defined, AABW is defined as having a potential temperature less than 0.0°C and a salinity between 34.6 and 34.7. Weddell Sea Bottom Water (WSBW), from which AABW is ultimately derived, has approximately the same salinity as AABW but a potential temperature between -1.3 to -0.7°C . It is observed as a thin, near-bottom layer along the western and northern perimeter of the Weddell Sea, and is easily identified by a large temperature gradient. (Carmack and Foster, 1977, p. 153)

Above the bottom water is found Warm Deep Water (WDW) ($\theta \sim 0.5^{\circ}\text{C}$, $S > 34.68$) which is the dominate water mass in the Antarctic region. Overlying the WDW is near surface Winter Water (WW) with temperatures near freezing ($\theta \sim -1.9^{\circ}\text{C}$) and salinities in the range 34.36 to 34.52. A low salinity shelf water on the eastern shelf termed Eastern Shelf Water (ESW) ($\theta \sim -1.8^{\circ}\text{C}$, $S < 34.5$) is advected westward and subjected to freezing. Western Shelf Water (WSW) ($\theta \sim -1.9^{\circ}\text{C}$, $S > 34.7$) is formed by brine rejection due to intense freezing of WW on the shelf in the southwestern part of the Weddell Sea. The coldest water of this melange is Ice Shelf Water (ISW) ($\theta \sim -2.3$ to -1.9°C , $S > 34.65$), formed under the floating ice shelves and, by definition, potentially supercooled, i.e., it has a potential temperature lower than the surface freezing point ($\theta \sim -1.9^{\circ}\text{C}$). Finally, over the deeper waters of the shelf WW and warm and saline WDW combine to form Modified Weddell Deep

Water (MWDW) ($\theta \sim -0.7^{\circ}\text{C}$, $S > 34.59$). (Foldvik, Gammelsrød, Slotsvik, and Tørresen, 1985, and Foldvik, Gammelsrød, and Tørresen, 1985a)

Table 1 summarizes the potential temperature and salinities described above to aid in later analysis.

Table 1. WATER MASSES INVOLVED IN THE FORMATION OF AABW

Type	Abbreviation	$\theta (^{\circ}\text{C})$	S (PSU)
Antarctic Bottom Water	AABW	< 0.0	34.6 - 34.7
Weddell Sea Bottom Water	WSBW	-1.3 - -.7	34.6 - 34.7
Eastern Shelf Water	ESW	~ -1.8	< 34.5
Winter Water	WW	~ -1.9	34.36 - 34.52
Western Shelf Water	WSW	~ -1.9	> 34.7
Ice Shelf Water	ISW	-2.3 - -1.9	~ 34.65
Warm Deep Water	WDW	~ 0.5	> 34.68
Modified Weddell Deep Water	MWDW	~ -0.7	> 34.59

3. Theory and Evidence

A detailed theory of ice freezing, convective mixing and large scale ice flux divergence leading to the formation of dense WSBW was first presented by Gill (1973). Building on this work Foster and Carmack (1976a, b and 1977; also Carmack and Foster, 1975a) offered a theory of AABW formation that will be referred to as the "shelf break process" theory for the purposes of this discussion. It is based on frontal zone mixing at the shelf break between the dense WSW and MWDW. This process produces a dense water mass which continuously changes its characteristics by mixing with the surrounding WDW while sinking down the slope. Under the action of the Coriolis force the cold dense water would flow westward and follow the perimeter in a clockwise direction. Apparent reported observations of this process have been made in the above citations and by Jacobs (1989), Killworth (1977b), Foster and Middleton (1980), Foster et al. (1987) and Jacobs and Fairbanks (1985).

Foster and Carmack (1976) reported observing newly formed WSBW from this process at 2000-3000 m on the slope near 40°W . Foldvik, Gammelsrød, and Tørresen (1985a) specifically believe that this newly formed WSBW was merely a continuation of the cold ISW outflow from under the Filchner Ice Shelf.

Foldvik and Gammelsrød (1988) have offered an alternative theory based on recent observations that show large volumes of WSBW are formed through a process which does not involve shelf break mixing. Ice Shelf Water appears to flow down the continental slope as organized plumes forming WSBW through mixing with overlying WDW. (For purposes of definition, "organized" formation or flow is a focused, jet-like channeled flow constrained by bathymetry to follow depressions around rises or islands on the shelf.) Apparent observations were reported by Foldvik and Gammelsrød (1988), Foldvik, Gammelsrød, and Tørresen, (1985a, b, c), Foster and Middleton (1978), Foldvik and Kvinge (1977) and an observation of a similar process, but on a smaller scale, at the Ross Sea Ice Shelf was made by Jacobs et al. (1979). This theory will be referred to as the "ice shelf process" theory for the purposes of this discussion.

One exception to these reports was made by Carmack and Foster (1975b) who reported seeing no such evidence of outflowing ISW while taking measurements at the Filchner Ice Shelf. However, the timing of their observation appears to be such that the internal seiche within the Filchner Depression obscured or perhaps blocked the outflow of ISW. Their six day data stream was exactly half the period of the Filchner Depression's 12 day internal seiche (Foldvik, Gammelsrød, and Tørresen, 1985c, p.197). Thus, their failure to discover any plumes of outflowing ISW are potentially explainable.

Both theories appear to agree that the dense water produced by their respective processes will flow downslope beneath the less dense WDW and will be topographically steered (cascading) into a geostrophically balanced current which hugs the continental slope. Here it will mix with the WDW above it forming WSBW as it flows clockwise around the Weddell Sea (Coriolis forcing it to the west up against the slope) and ultimately out of the basin, warming slightly due to mixing, as AABW.

The next two sections outline the elements of these two theories up to the agreed upon cascading process and production of AABW from WSBW.

4. Shelf Break Process Theory

The following model offered by Foster and Carmack (1977) attempts to account for the formation of WSBW solely due to processes that occur at the continental shelf break. The steps listed are in the order they must occur. The various temperature and salinity mixing processes which occur are portrayed in Figure 23

(similar portrayal of this process can also be accomplished with oxygen-salinity analysis (Foster and Middleton, 1979, p. 750)).

1. Surface ESW flowing from the eastern side of the continental shelf is cooled in winter at the surface until it freezes and becomes WW. This water lies directly over WDW.
2. Due to cabbeling and double-diffusion, WW is mixed with the underlying WDW to form MWDW.
3. Due to some external forcing mechanism such as continental shelf waves excited by the tides or mass conservation due to the outflow of dense water down the slope, the MWDW will extend a tongue up onto the western continental shelf into the WSW which was previously formed by intense freezing of WW over the shelf.
4. Due to mechanical stirring on the under side of this tongue by tides, breaking internal waves or shear instabilities, the MWDW will mix with the WSW to form WSBW.
5. Depending on the rate of mixing, the denser WSBW will commence an organized descent down the continental slope.

5. Ice Shelf Process Theory

At the present time no observations exist of the actual circulation under the ice shelves, but the following model offered by Foldvik and Gammelsrød (1988) attempts to account for the organized formation of WSBW from ISW.

1. Dense water is formed near the western ice shelf barrier due to surface cooling, freezing and convective mixing.⁶
2. This process can be made more intense if off-shore winds are present which can carry away the ice but leave behind the rejected brine or by tidal action which cyclically converges new ice at the barrier by on-shelf currents and subsequently opens leads by off-shore currents. Due to intense freezing at the barrier, WSW is formed and flows shoreward towards deeper areas under the shelf driven by the action of gravity and tidal forcing.
3. As the WSW penetrates beneath the ever thickening ice shelf⁷, it comes into contact with the underside of the glacial ice shelf and is cooled further (temperatures within the ice shelf can reach -20°C). Since the freezing point of sea-water is depressed with increasing pressure (about 0.75°C km) below that of the freezing point of sea water at one atmosphere, this cooling is most readily accomplished by melting of the glacial ice at the interface as well as through heat conduction.

⁶ See Foldvik and Kvinge (1974) for a thermohaline convection mechanism based on the depression of the freezing point of sea water with increasing pressure (depth) at the barrier.

⁷ Since the thickness of the floating ice shelf increases shoreward, it follows that the bottom depth must also increase shoreward.

4. Tidal mixing, melting, and cooling beneath the ice shelf bring that portion of the water column near the base of the ice shelf to the local freezing point producing ISW. This process will continue as long as the temperature of this water column remains above the in-situ freezing point, i.e., along the descending path where the depth of the ice-water interface increases (Figure 24).
5. The ISW continues flowing poleward downslope, then turns eastward due to Coriolis effects.
6. If the topography under the ice shelf allows, the ISW will organize itself into a plume and flow out from under the ice shelf, over the shelf break, and then downslope at a high rate ($10^6 \text{ m}^3\text{s}^{-1}$). The ISW will flow down-slope due to its initial higher density than the overlying WDW. However, its extremely low temperature, therefore higher compressibility, will drive it across isobaths towards the greatest depths. If the topography is unfavorable, the ISW will stagnate in depressed basins on the shelf and/or dilute itself with other shelf waters during its downward flow thus losing its signal as the densest water.

D. FORCING FUNCTION REQUIREMENTS

1. General

The shelf break process theory of Foster and Carmack and the ice shelf process theory of Foldvik and Gammelsrød both require the application of specific forcing functions in order for their theories to work at a particular location. By identifying these forcing functions, data can be collected which describe how these functions vary at each location and also determine their relative impact. If all the forcing functions are determined to constructively contribute to bottom water production at a specific location, then AABW should be produced if the theory is correct. If, however, for a given theory the forcing functions are all present but AABW is not produced, then the theory might instead indicate the formation of intermediate or deep water. Unfortunately the expanded list of possibilities can not lead to an unequivocal decision about which theory is more appropriate but it can suggest which is the more likely.

An investigation of the two predominant theories has revealed the forcing functions necessary for their respective operation. They are detailed in the following pages.

2. Geography.

Geography is a critical forcing function for both theories and the following items are of utmost importance.

- Wide continental shelves (not including ice shelves), abrupt shelf breaks and steep continental slopes, and channels in the shelf bathymetry are required. These correspond to required shelf residency of the source water, dynamic forcing of WDW up onto the shelf that can only occur in abrupt frontal zones

and focusing the seaward flow preventing excessive entrainment by descending waters.

- Latitudinal location that will impart the requisite Coriolis flow off-shelf as well as provide the low level of solar radiation necessary for the surface freezing and heat flux.
- For the ice shelf process theory, size and topography of the ice shelf are factors controlling the amount of ice/water interface, i.e., amount of area and residence time that would be available for the production of ice shelf water.

3. Surface Air Temperature and Its Effect on the Growth of Sea Ice

Both shelf break and ice shelf process theories require surface water to be reduced to its freezing point in order to increase the water density through temperature reduction and through the addition of salinity from brine rejection that occur during freezing of sea water.

The growth of new sea ice is a measure of the effectiveness of this forcing function. The growth of sea ice is dependent upon such parameters as air temperature, initial ice thickness, snow depth and density, wind speed, sea water salinity and the specific heats of sea ice and sea water. Most important is air temperature. Zubov's formula takes air temperature, translated into accumulated frost degree days, and determines the theoretical ice thickness as follows:

$$T_j = \frac{-50 + \sqrt{2500 + 32 \sum_{i=1}^j dd_i}}{2} \quad \{1\}$$

where T_j equals the ice thickness in cm on day j and dd_i is the number of frost degree days (one day with mean temperature -1°C) accumulated in $^\circ\text{C}$ on day i (Bowditch, 1984, p. 850).

When surface air temperatures at the air-sea interface fall below the freezing temperature of sea water at $\sim -1.9^\circ\text{C}$, one of the necessary forcing functions for both theories of AABW formation becomes active. Comparisons between the climatological surface air temperatures in the Ross and Weddell Seas can indicate the relative effectiveness of this function in each basin. The increase in ice thickness goes as the square root of the accumulated cold temperature. If significant differences in air temperature or frost degree days can be found between the two basins, then Zubov's equation can produce a meaningful comparison even though it does not account for the advection of new ice. That parameter must be derived from the relative wind and tide fields.

4. Surface Winds

a. Climatological Surface Winds

In general, low temperatures combined with strong winds produce greater ice production than low temperatures alone. The turbulent mixing of the ocean surface caused by the wind forcing increases the effectiveness of the freezing. Comparison of surface wind speeds would provide a general measure of effectiveness; however the dynamics of the relationship between ice production and turbulent mixing caused by winds is not linear and therefore relative differences between the two wind regimes become difficult to support unless clearly differing regimes are found. However, wind direction appears to be more straightforward.

To allow the maximum production of dense water through surface freezing requires a direct contact between the surface of the sea water and the cold air at all times. To obtain this maximum production, a divergent sea ice flow is required to maintain continuously open leads. Although surface currents have some effect upon the drift of sea ice, the principal factor is the wind velocity.

Wind imparts a stress on the ice to force its movement. A measure of wind stress (τ) on sea ice is needed to predict ice motion. Wind stress is a function of surface roughness and stability of the atmosphere above the surface (Overland, 1985) as well, but has been empirically related to the surface wind vector (U) by a drag coefficient (C_D) as follows:

$$\tau = C_D \rho U^2 \quad \{2\}$$

where ρ is the air density. (Guest and Davidson, 1987, p. 6943)

The Coriolis force influences the direction the ice will move relative to the wind direction. Ekman showed theoretically that the surface drift of the ice due to winds is directed 45 degrees to the left of the wind direction in the Southern Hemisphere (Pond and Pickard, 1983, p. 108). In practice this deviation angle has been shown to vary from 18° to 90° depending upon the force of the surface wind, thickness and concentration of the ice and ocean current (Bowditch, 1984, p. 853). The relation between the surface wind speed, ice thickness and the theoretical drift angle shows that the drift angle increases with increasing ice thickness, decreasing wind speed and increasing latitude (Gill, 1982, p. 321).

Relating this scenario to atmospheric pressure we find that since cross-isobar deflection of surface winds over the ocean is approximately 20° (Bowditch,

1984, p. 853), the deflection of the ice varies from approximately parallel to the isobars to 70° to the left of the isobars with low pressure on the right and high pressure on the left in the Southern Hemisphere. On the Antarctic coast this implies that ice will be pushed to the west by the prevailing easterlies and at an average deflection angle of 30° to the left of the wind direction. Tchernia (1980, p. 61) estimates the ice will drift at a rate of 2% of the wind speed. Thus, a considerable amount of ice can be advected onto the ice shelf barriers. Hence, it would appear crucial to compare the climatological wind regimes of the Ross and Weddell Seas.

b. Katabatic Winds

Katabatic winds are gravity driven, frictionally retarded winds in the boundary layer (Schwerdtfeger, 1984, p. 63). They exist independent of the normal geostrophically forced wind fields. Parrish and Bromich (1987) found that intense radiative cooling of the air over the ice slopes of the Antarctic Continent were ripe conditions for generating these flows. They produced a detailed map showing which topographic regions of the Antarctic could produce strong and persistently recurring winds (Figure 25). Kurtz and Bromich (1985) established that these winds were responsible for newly formed ice to be advected away from the shoreline causing a coastal polynya in the Ross Sea thus allowing continuous new ice production. Sechrist (1989) reported a daily katabatic wind during his six month stay at the Druzhnaya research station at the barrier of the Filchner Ice Shelf in the Weddell Sea. Notably this wind blew 12 hours a day at speeds in excess of 50 mph⁸ but was contained within one meter of the surface⁹. By these reports it is clear that katabatic wind regimes along an ice barrier are potentially significant forcing functions to increase new ice production.

Due to the total lack of available data on katabatic wind regimes along the Ross and Ronne Ice Shelf barriers, this forcing function could not be reviewed in this thesis. However, it should be noted that Parrish and Bromich's map of potential katabatic wind regimes show a total absence of katabatic wind potential approaching the Ross or Ronne Ice Shelf barriers and that the only ice shelf barrier that should experience some of these winds is a small area of the Filchner Ice Shelf which appears to be corroborated by Sechrist (Figure 25).

⁸ Schwerdtfeger (1984, p. 73) found almost identical values in his coastal observations.

⁹ Lettau (1966, p. 9) corroborates this magnitude when he found maximum coastal katabatic winds contained within 4 m of the surface.

If the assumption made by Parrish and Bromich about the lack of katabatic wind fields at the Ross and Ronne Ice Shelf barriers is valid, then katabatic winds would not be expected at either location. The lack of an analysis of this forcing function, therefore, should not be fatal to any conclusions drawn.

5. Sea Ice Concentration

As a measure of the relative efficiency of the surface freezing process required by both shelf break and ice shelf process theories, the sea ice concentration in the Weddell and Ross Seas must be compared. As a forcing function, thermal efficiency (as governed by the ice thickness and concentration) at the air-sea interface directly impacts the various thermodynamic and dynamic processes involved in ice growth and decay which in turn directly effects the efficiency of brine rejection and sensible heat reduction of the surface waters.

Though this thermal efficiency has been modeled by Zubov, Anderson, Lebedev, Maykut and Untersteiner (Gascard, 1989 and Bowditch, 1984), ice concentration as a measure of thermal effectiveness of a basin's total heat flux, and thus its quantitative ability to produce dense surface water, has not been.

Only gross measures of the effectiveness of one basin over another to produce dense surface waters are available for interbasin comparison. Mean ice concentration and the probability of occurrence of ice of any thickness can be approximately determined by analyzing satellite infrared imagery and ship and aerial reports of local ice concentrations for the basins in question. Since all the basins in the Antarctic are dominantly divergent in nature for sea ice, with the exception of the area in front of the Larsen Ice Shelf in the western Weddell Sea, only first year sea ice is considered to be present. This means that Antarctic interbasin comparisons are not hampered by inequities of comparing ice regimes of different thermal efficiency (thicknesses and related ages). If the assumption is made that ice found in the Weddell and Ross Seas at the same time have comparable thermal efficiencies, then the effectiveness of those basins in the production of dense surface waters will only be a function of ice concentration (if all else is considered equal, i.e., holding all other forcing functions as equal for the purposes of analysis.) Various means of computing these concentrations are available and are dependent on the source of data.

The amount of ice present not only indicates the amount of freezing taking place at the surface but is also indicative of the amount of sea surface which is exposed to the cold atmosphere permitting production of brine-enriched shelf water.

When the sea surface becomes completely ice covered, the insulating effect of this thermal blanket severely reduces the production of dense shelf water.

This leads to the perplexing conclusion that large concentrations of sea ice can lead to low levels of shelf water production because sea ice acts as a thermal insulator to restrict the exchange of heat between the atmosphere and the ocean, whereas the surface freezing that created the large volume of sea ice led to high levels of shelf water production. Therefore an examination of ice concentration might point out differences between the Ross and the Weddell Seas, but those differences might not be easily attributable to their effect on the production of bottom water.

6. Hydrography.

Both formation theories require specific circulation patterns and temperatures, salinities and densities of the water column on the continental shelf. Sub-surface horizontal circulation of water masses is crucial to both theories and can be inferred from horizontal and vertical cross sections of temperature, salinity and density. Deacon (1937) showed that surface horizontal circulation patterns were adequate for describing the subsurface circulation due to the barotropic nature of the Antarctic seas. It follows then that if limited horizontal profile data at varying depths are available, then surface circulation data should suffice for interbasin comparisons when combined with vertical cross sections spaced progressively from one side of the basin to the other.

Vertical circulation patterns require much more complete data acquisition in order to obtain an accurate representation of the water column structure at varying locations within a basin. Therefore, well chosen vertical cross sections and horizontal surface circulation data are required to adequately compare the hydrography of the Ross and Weddell Seas.

7. Under-Ice-Shelf Bathymetry.

The shelf break process theory does not require special under ice shelf bathymetry since it does not require the presence of an ice shelf. The ice shelf process theory does require such under ice shelf bathymetry for two reasons:

- The forces of gravity, Coriolis, and friction must take over from the forcing function that initially moved the Western Shelf Water under the ice shelf for the production of Ice Shelf Water. Only a special under-ice-shelf bathymetry can provide the necessary environment to allow gravity, Coriolis and friction to operate effectively.

- The topography under the shelf must focus the Ice Shelf Water flow so no stagnation or substantial entrainment is allowed to occur with the environment. A high speed plume will result if the bathymetry is correct.

Comparisons of under ice shelf regimes between the Ross and the Weddell Seas are necessary to measure the effectiveness of this forcing function in each basin.

8. Tidal Forcing.

To understand how tidal forcing can effect the formation of AABW certain definitions and concepts must be reviewed.

Each tidal force is considered as a separate constituent force and the harmonic analysis of actual observations reveal the response of each constituent of the tide to its corresponding force. At any one place the response remains constant and is shown for each constituent by harmonic constants which are in the form of phase angles for the time relation and amplitudes for the height. The magnitude and frequency of these tidal generating forces are sinusoidal components which when added together yield water level η at time t as follows:

$$\eta = D + \sum a_n \cos(\sigma_n t + \delta_n) \quad \{3\}$$

where n equals the tidal constituent¹⁰, D equals the difference in height between mean sea level and mean low water, a_n equals the amplitude of constituent n , σ_n equals the frequency of constituent n and δ_n equals the phase angle of constituent n (Duxbury, 1971, p. 326).

Tidal waves may be reflected and refracted from the land barriers and pass back through the advancing wave, or oscillate in an ocean basin to create a standing wave. Resonance tides can occur when the frequency of a tidal constituent matches the fundamental period of oscillation of the basin. Dimensions of some natural basins are within the requirements of resonance thus permitting standing tidal waves to be generated. Tidal waves are influenced by the Coriolis force and will rotate in an ocean basin with the turning Earth.

Rotation occurs about a nodal or **amphidromic point** at which no significant vertical change in the water level due to tides occur. Radiating from these points are **cotidal** lines which join all positions at which high water occurs simultaneously.

¹⁰ As the number of tidal constituents used in this series is increased, so will the accuracy of the prediction of η .

Positions of common tidal range, called **corange**, cut across the cotidal lines forming approximately concentric circles of equal tidal range which increases with distance from its amphidromic point. This rotation of the tidal crest about the amphidromic point is indicated by the movement of the tidal crest from one cotidal position to the next. Due to Coriolis forcing, crests rotate clockwise in the Southern Hemisphere. When the tide crests simultaneously with the Moon's (or Sun's) passage over the Greenwich Meridian, convention has declared that this is a cotidal line of $0^\circ = 360^\circ$ with increasing phase clockwise (Schwiderski, 1978, p. 69).

The speed of progression of the wavefront is governed by the shallow-water wave equations and have a mid ocean average speed of 200 ms^{-1} extending to a depth of 4 km (Duxbury, 1971, p. 332-333). Tidal currents associated with the tidal wave are also rotary. Since successive high waters and low waters are not always at the same elevation, the flow strength is not constant. Despite the complex nature of the tide, reasonable estimates of its current can be made. To approximate the average flow rate at a given cross section of a tidal channel, it is necessary to calculate the volume of water (tidal prism) required to raise the inland tide from low to high water requiring the volume to pass through a cross section area in a certain time:

$$\text{average tidal flow rate} = \frac{\text{tidal prism}}{\text{channel area} \times \text{time period between low and high tide}} \quad \{4\}$$

Tidal mechanisms can bring a tongue of Warm Deep Water up on to the shelf, directly or by resonance. Tidal forcing can periodically remove new ice from the ice shelf barrier as well as drive shelf water under the ice shelf. It can cause mixing of shelf water. Tidal forcing is an integral part of both AABW formation theories and a comparison of Ross Sea and Weddell Sea tidal regimes appears crucial.

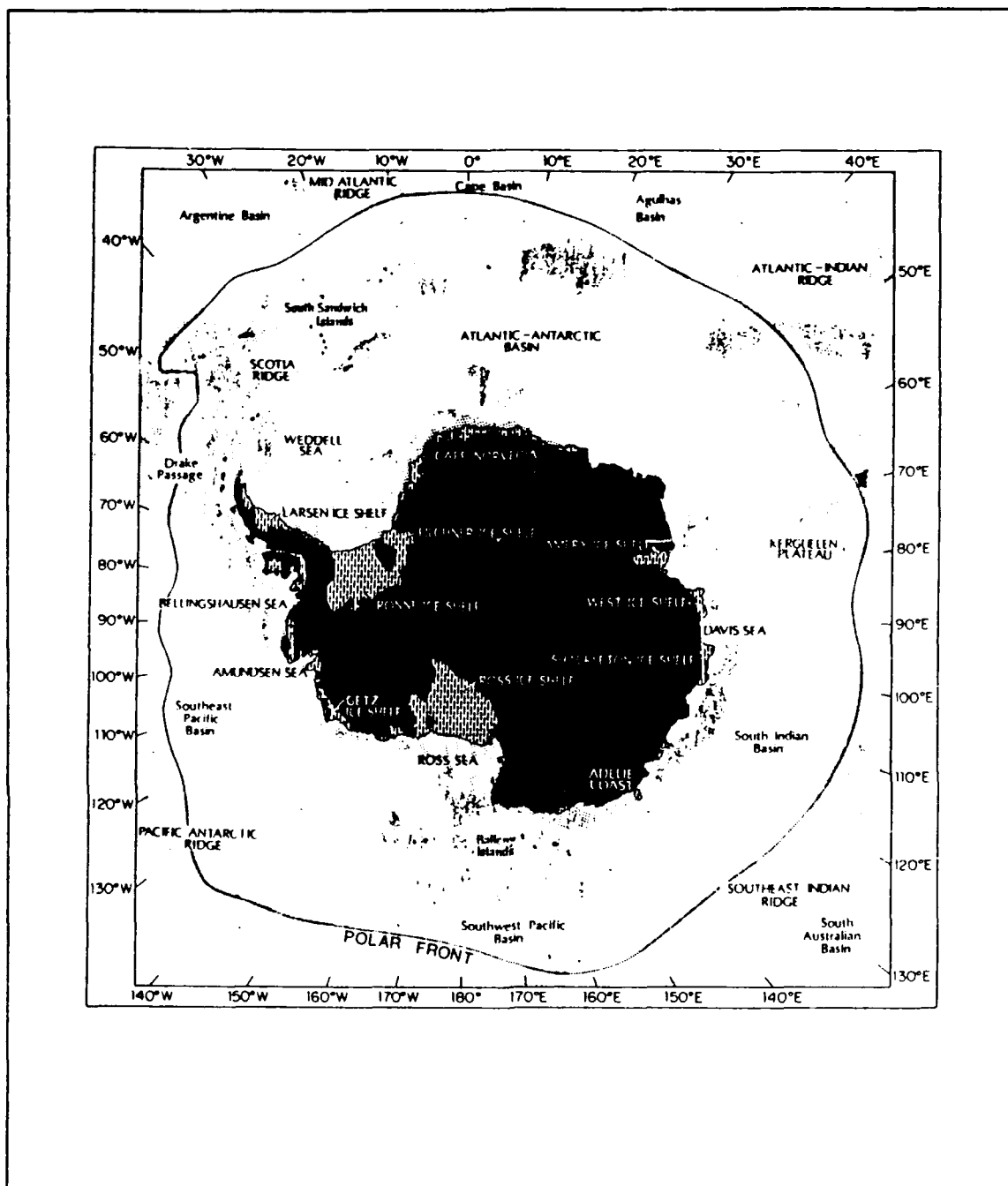


Figure 3. Topography of the Southern Ocean shown with ice shelf orientation (after Tchernia, 1980). Note: The Polar Front is depicted by the dotted line surrounding the Antarctic continent. Depths less than 1000 m are indicated by coarse stippling; depths 1000-4000 m are indicated by fine stippling. Continental ice shelves are illustrated by broken hatched lines.

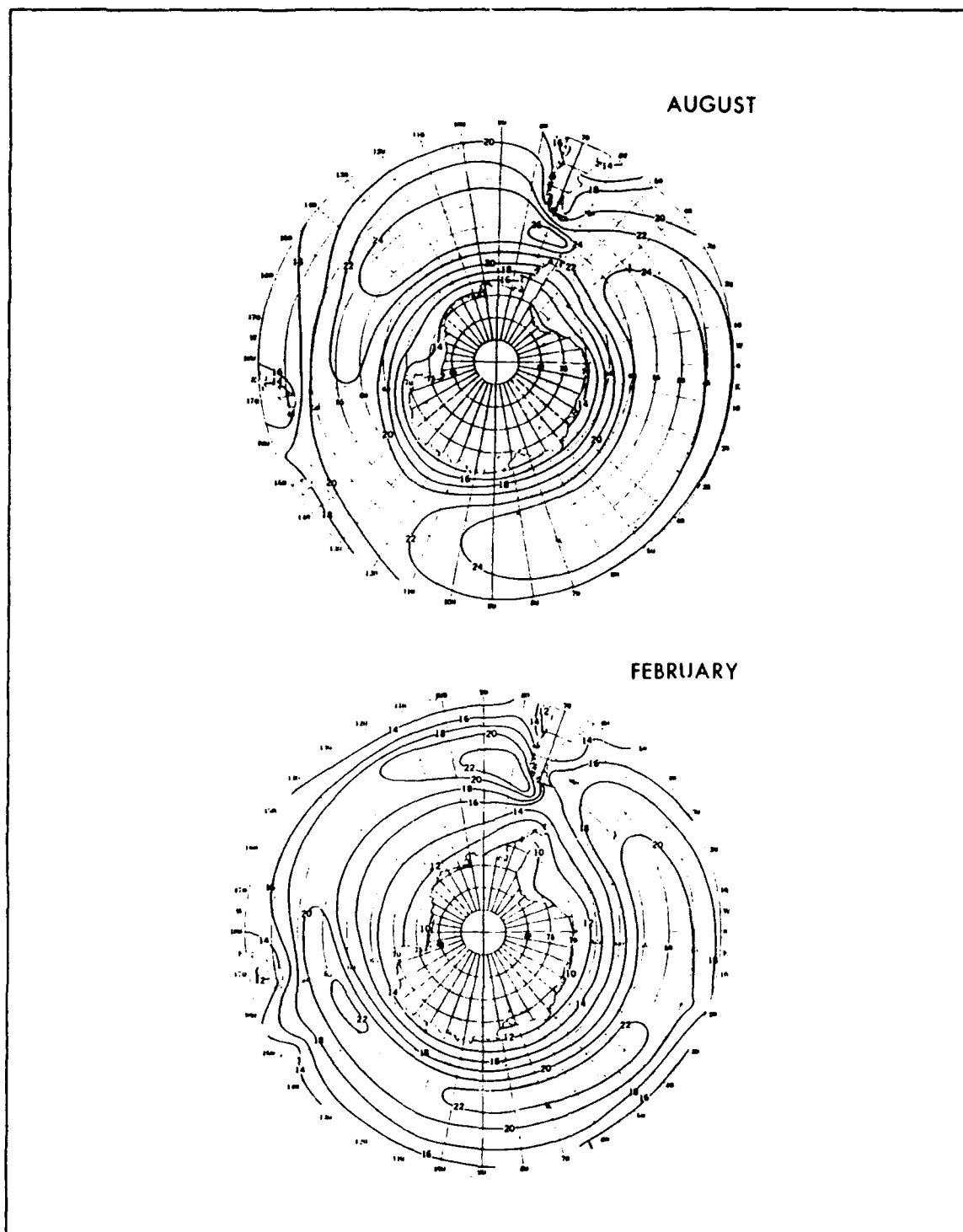


Figure 4. Mean surface winds (knots) for August and February (after DMA, 1985).

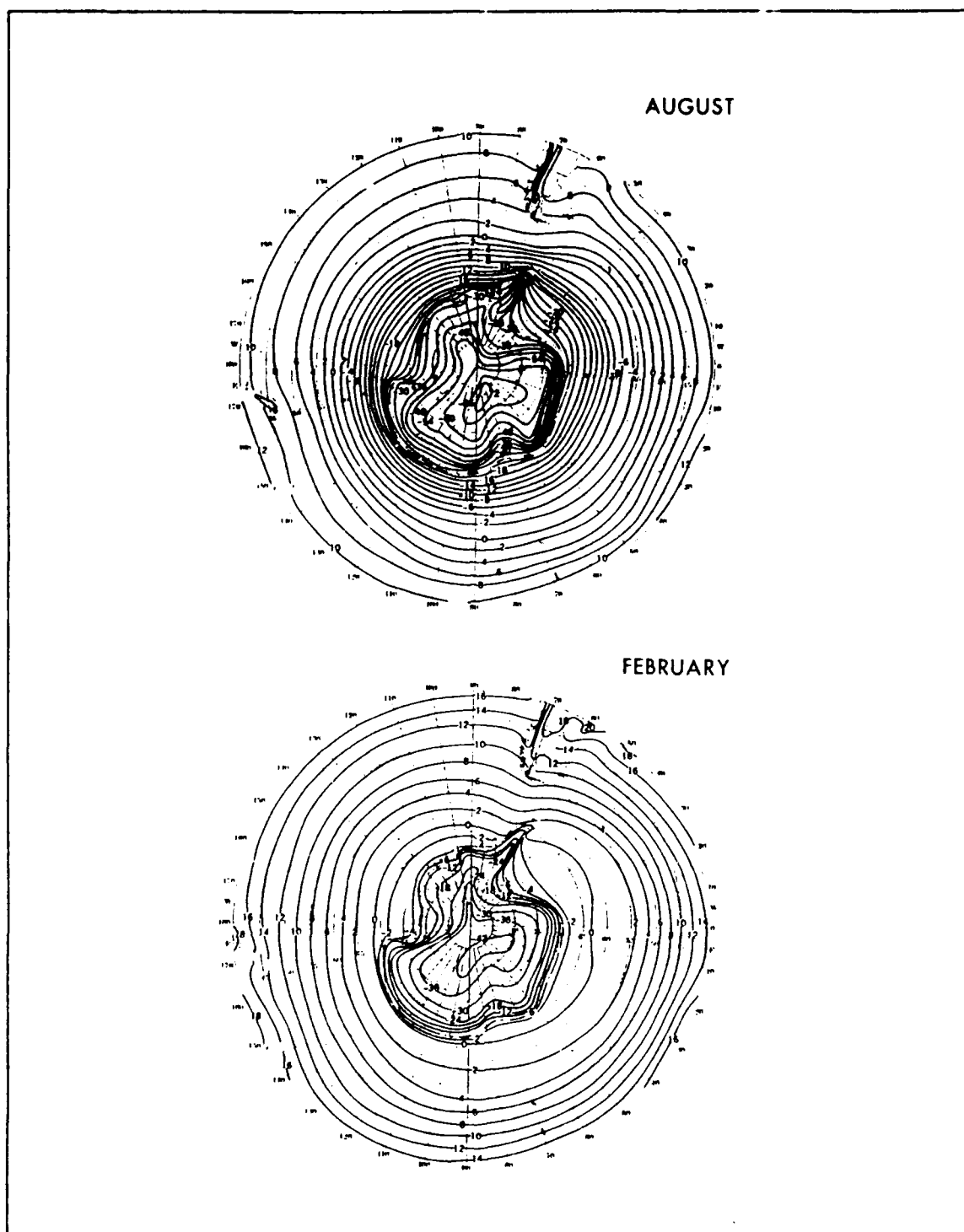


Figure 5. Mean surface air temperatures ($^{\circ}\text{C}$) for August and February (after DMA, 1985).

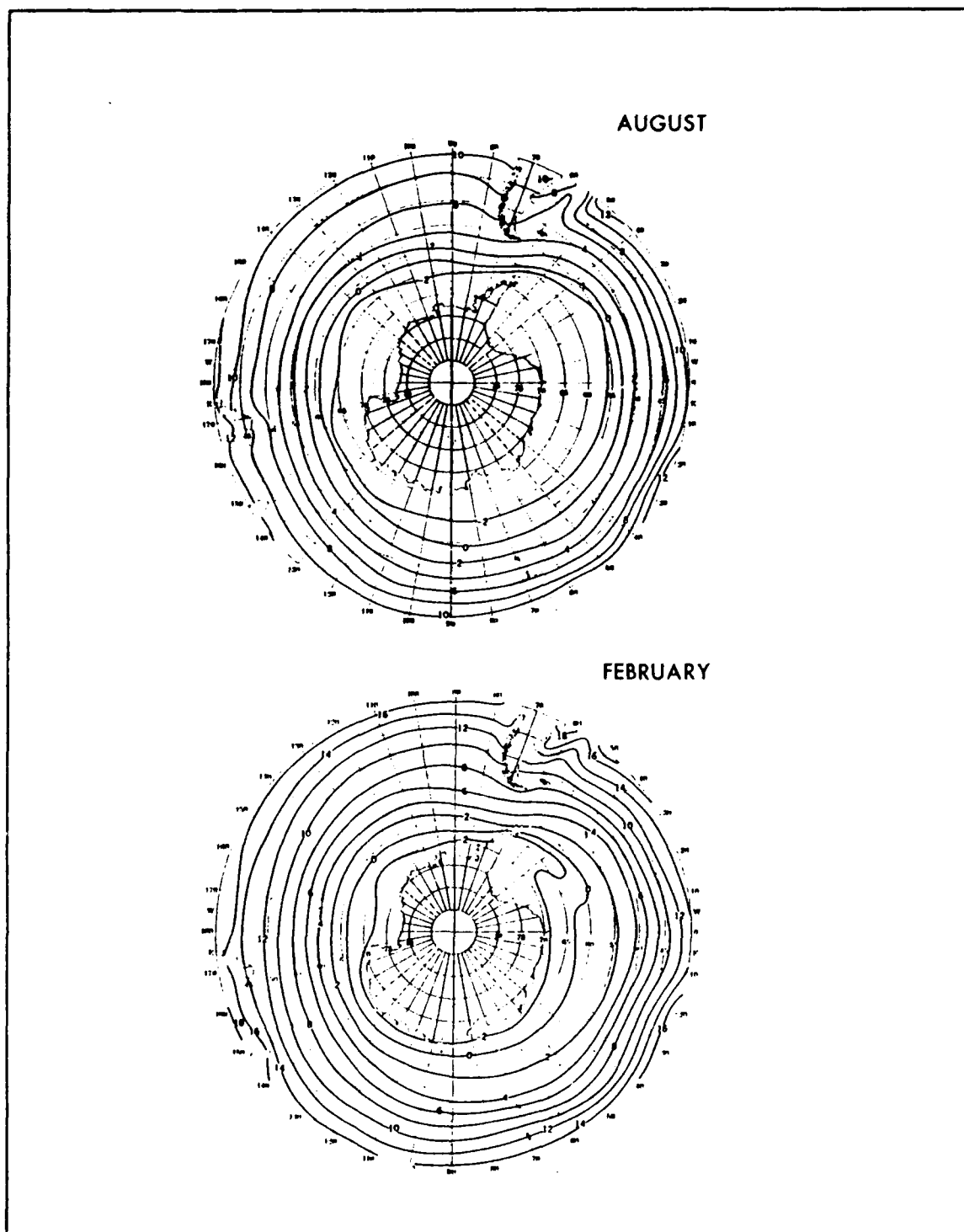


Figure 6. Mean sea surface temperatures ($^{\circ}\text{C}$) for August and February (after DMA, 1985).

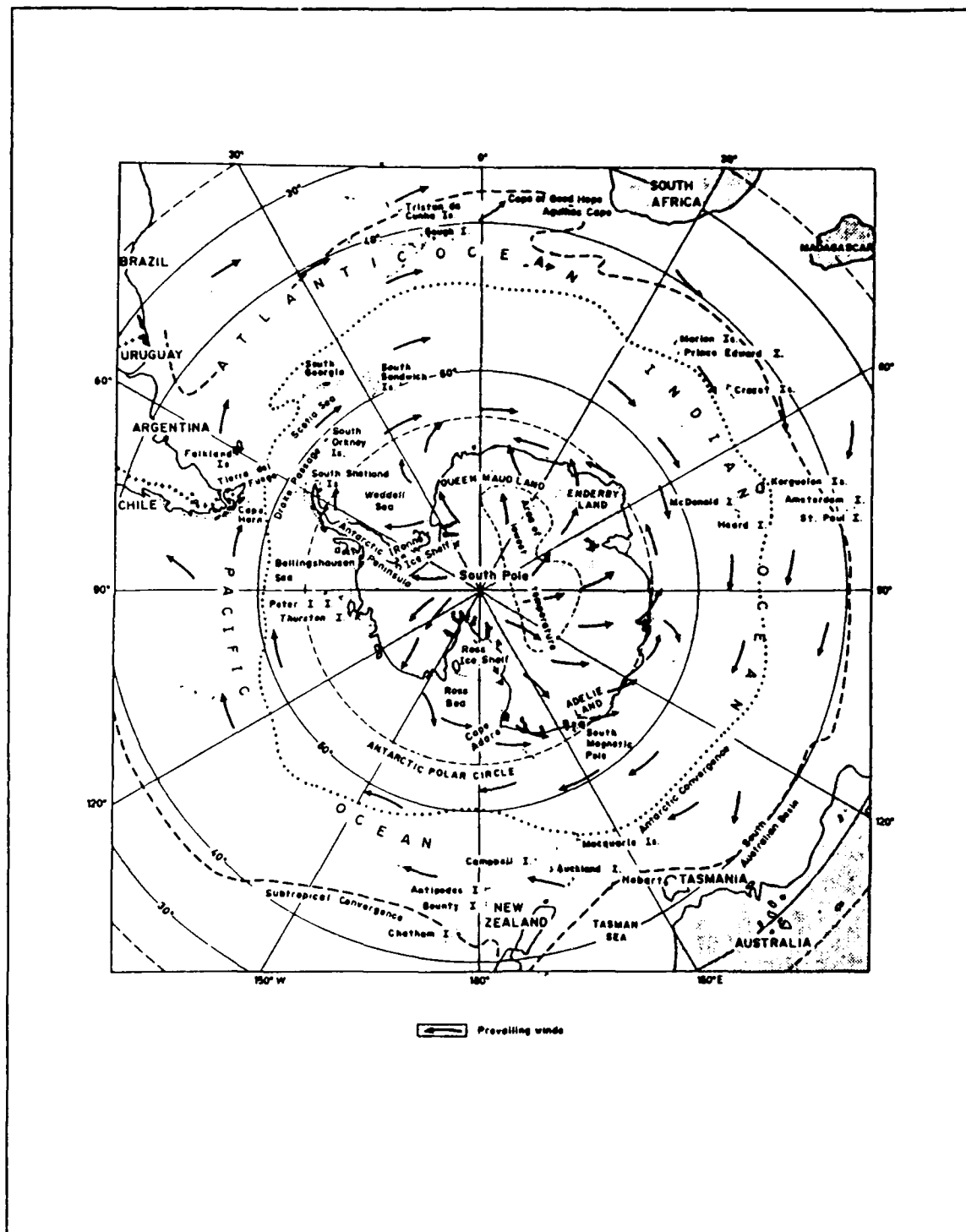


Figure 7. Prevailing wind directions for the Southern Ocean and Antarctica (after Tchernia, 1980).

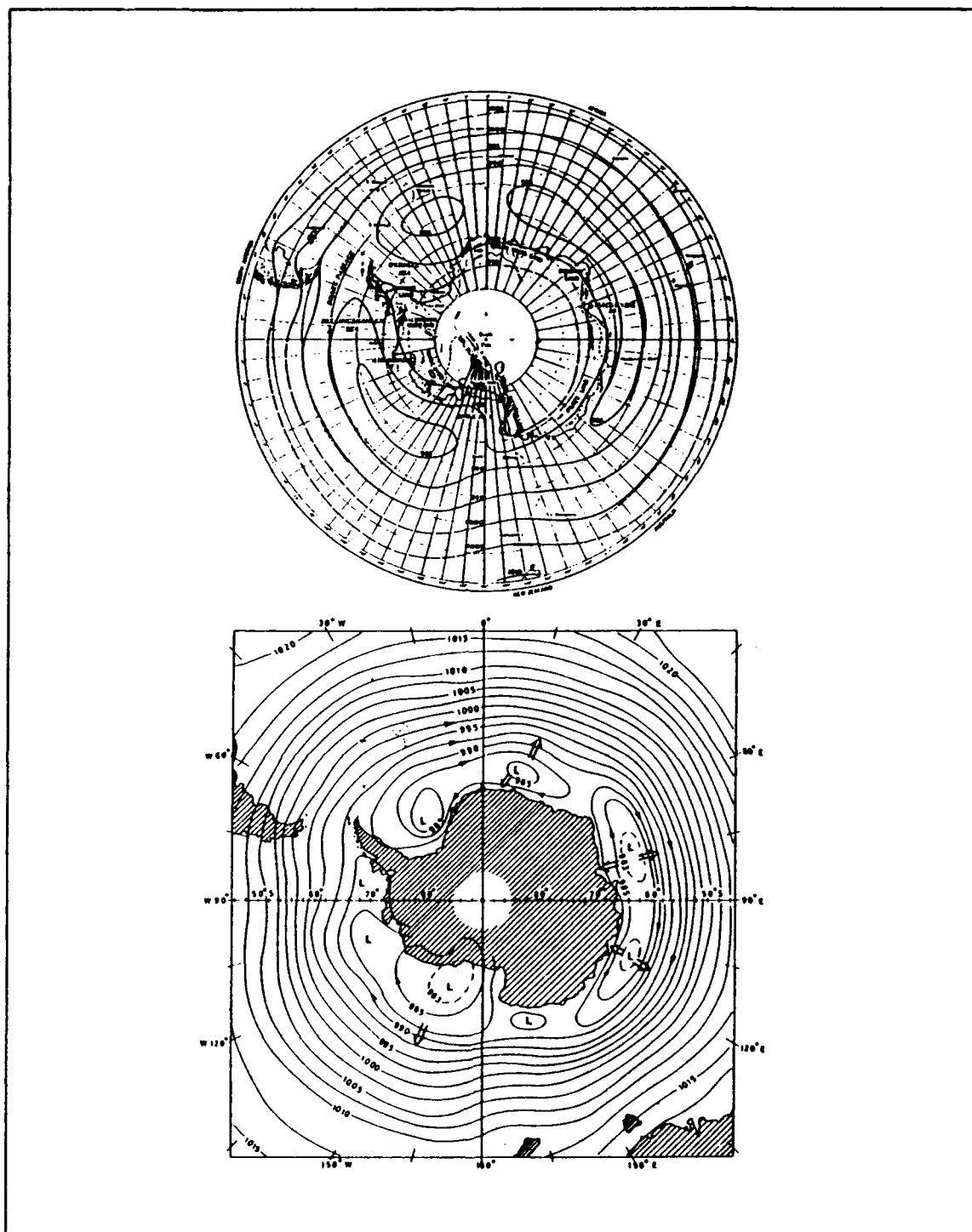


Figure 8. Average atmospheric pressure (millibars) for January (top) and July (bottom) (January after Hofmeyr, 1957; July after Foldvik and Gammelsrød, 1988).

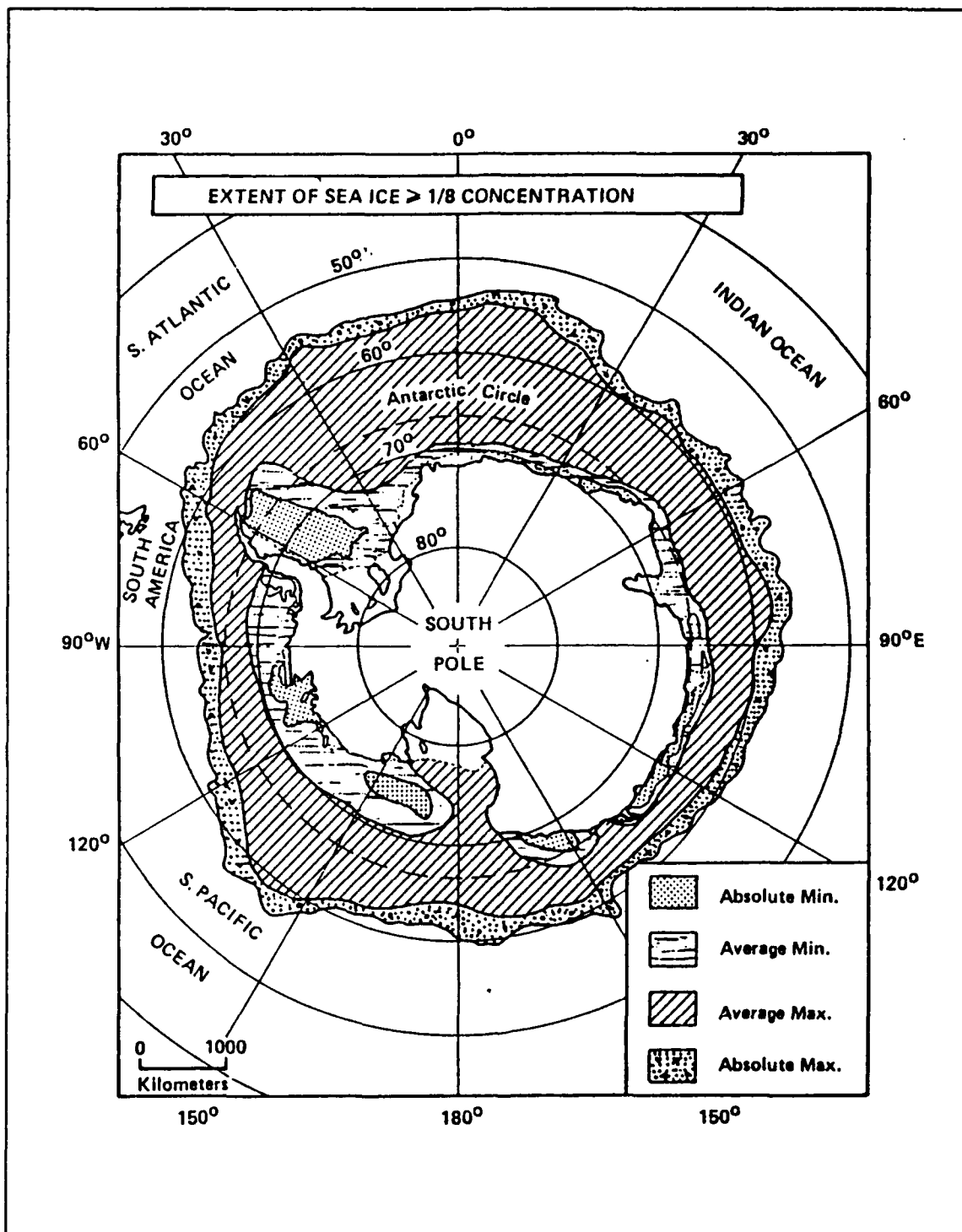


Figure 9. Sea ice coverage around Antarctica illustrating absolute and mean minimum and maximum extents (after CIA, 1978).

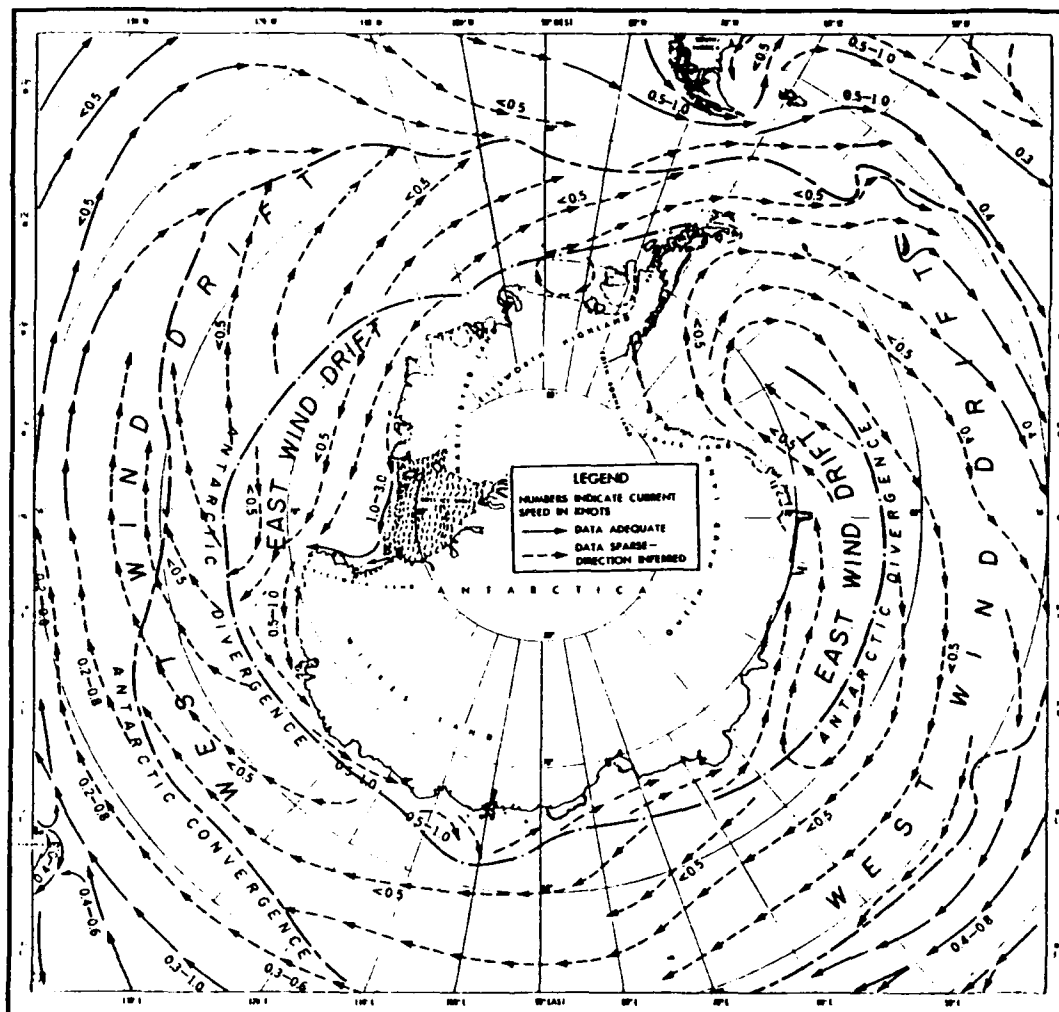


Figure 10. Surface circulation around Antarctica (knots) (after U.S. Navy Hydrographic Office, 1957).

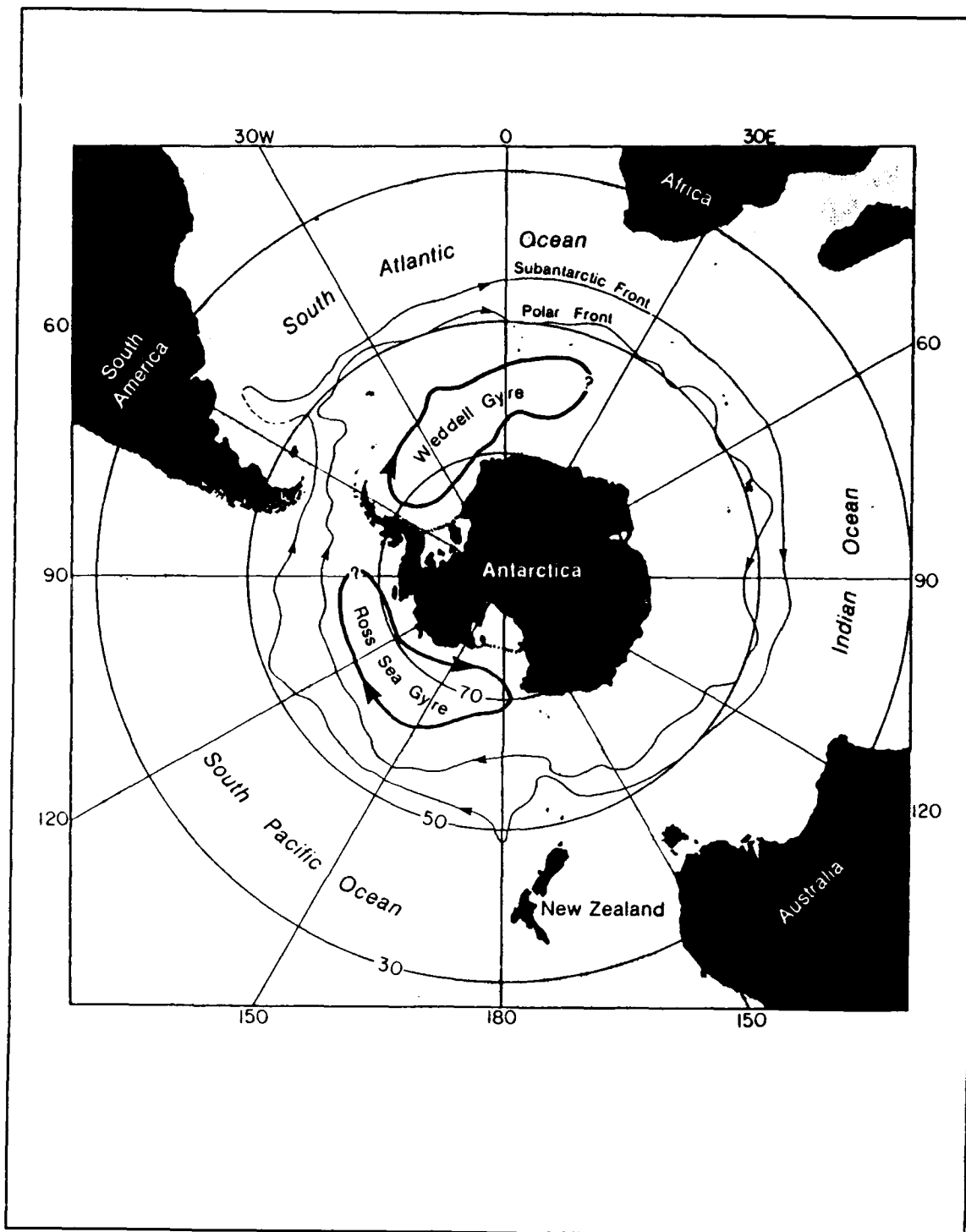


Figure 11. Antarctic Circumpolar Current showing the Weddell and Ross Sea gyres (after Whitworth, 1988).

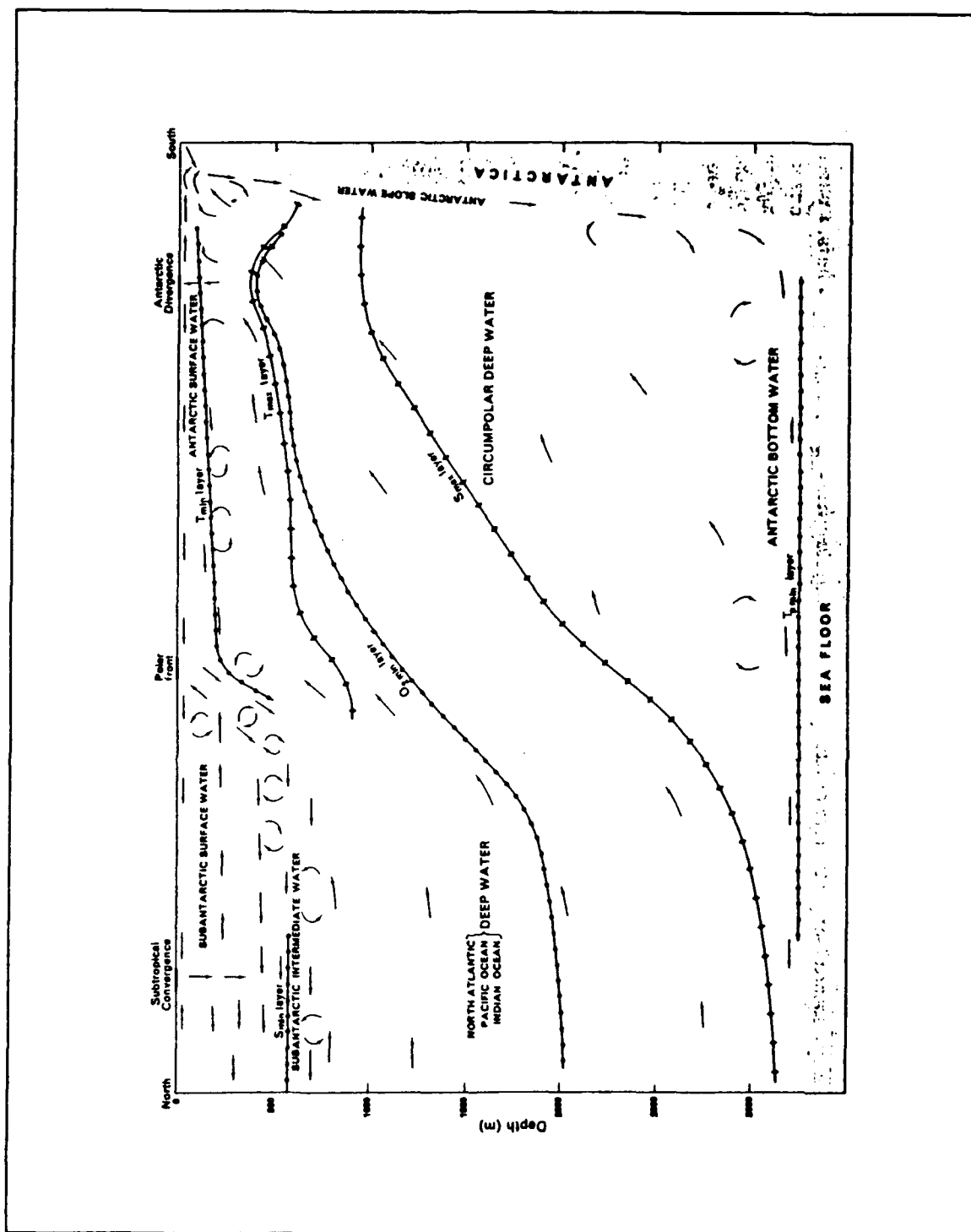


Figure 12. A schematic of the vertical structure and motion of the Southern Ocean (after Gordon, 1967).

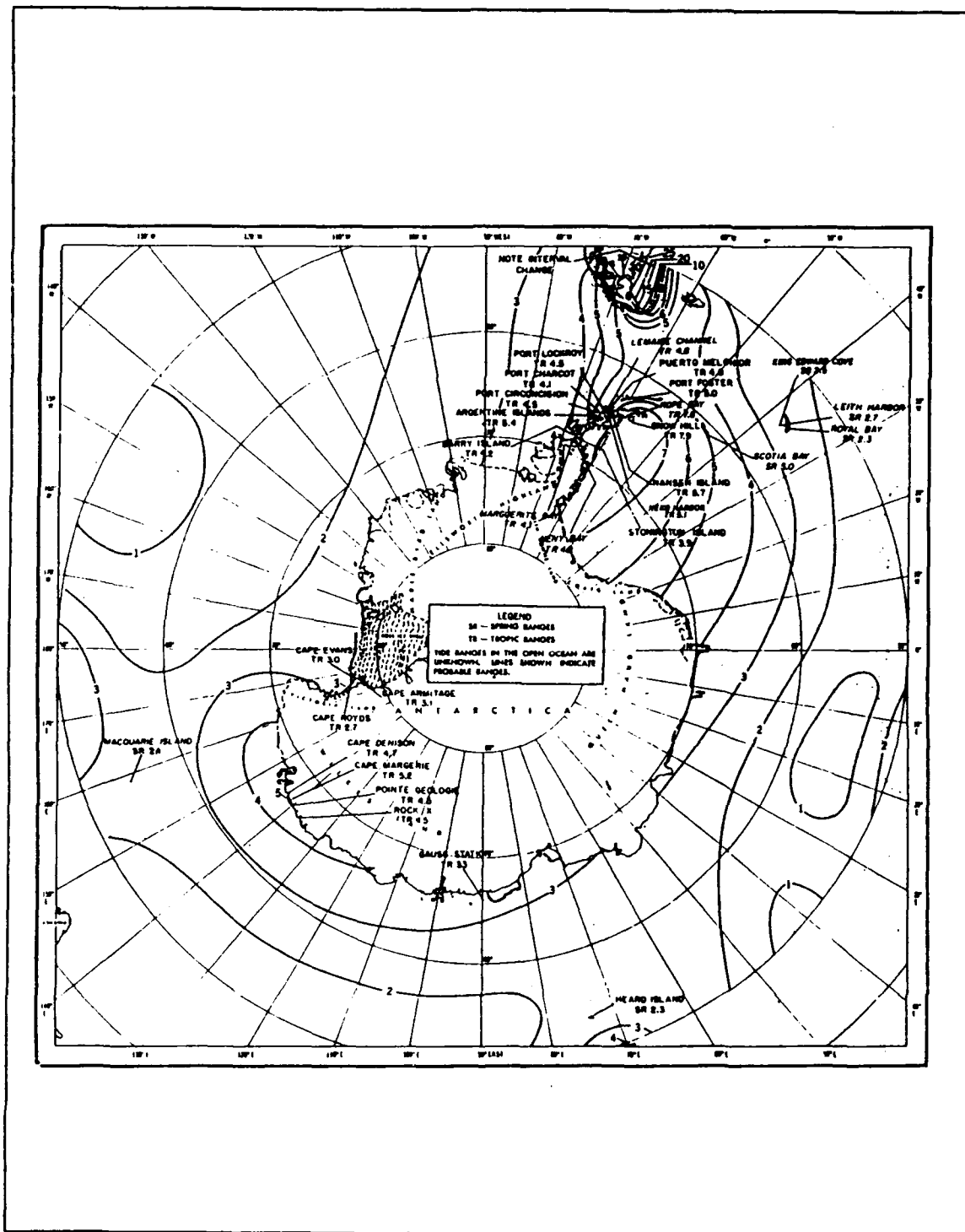


Figure 13. Tidal ranges around Antarctica (feet) (after U.S. Navy Hydrographic Office, 1957).

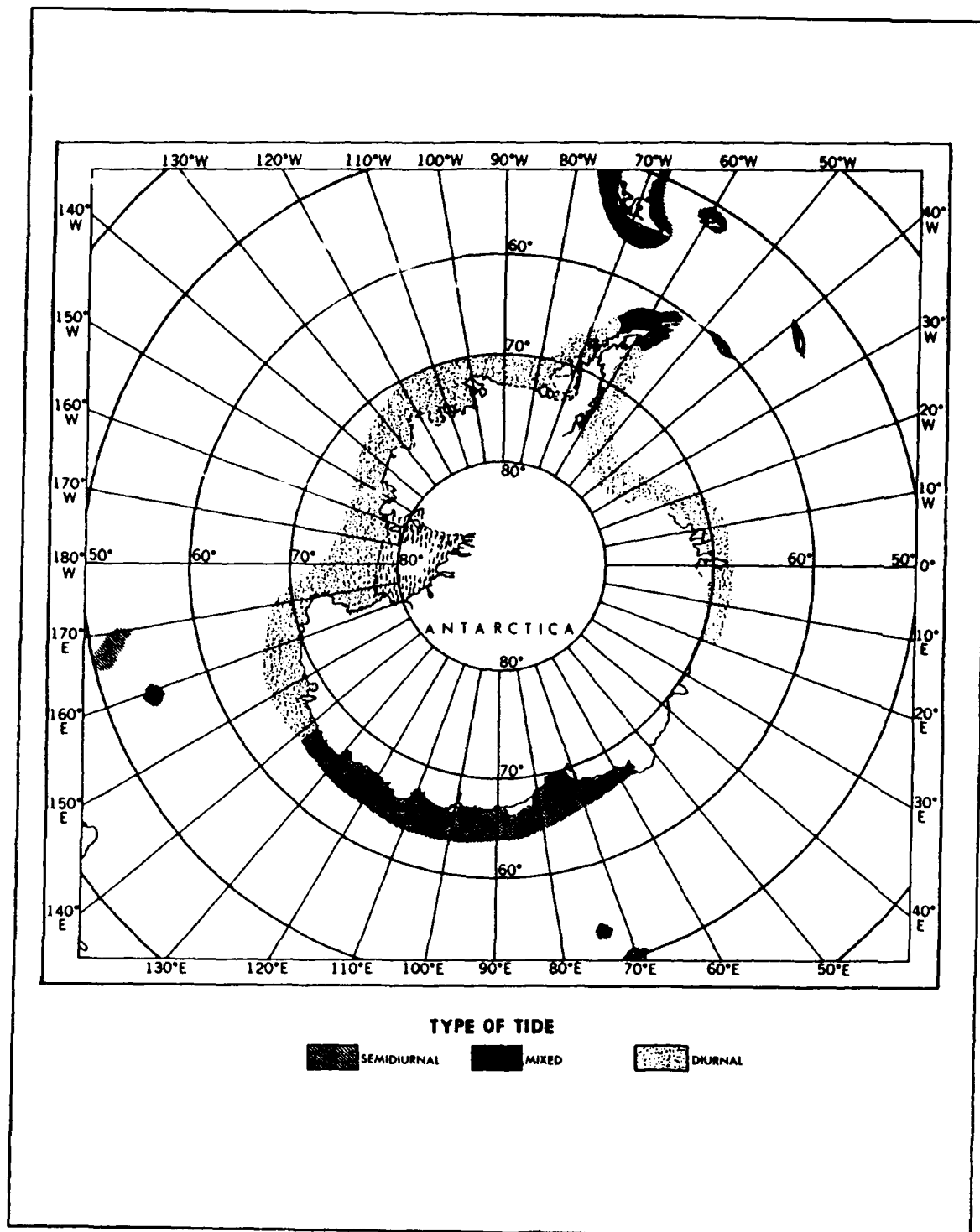
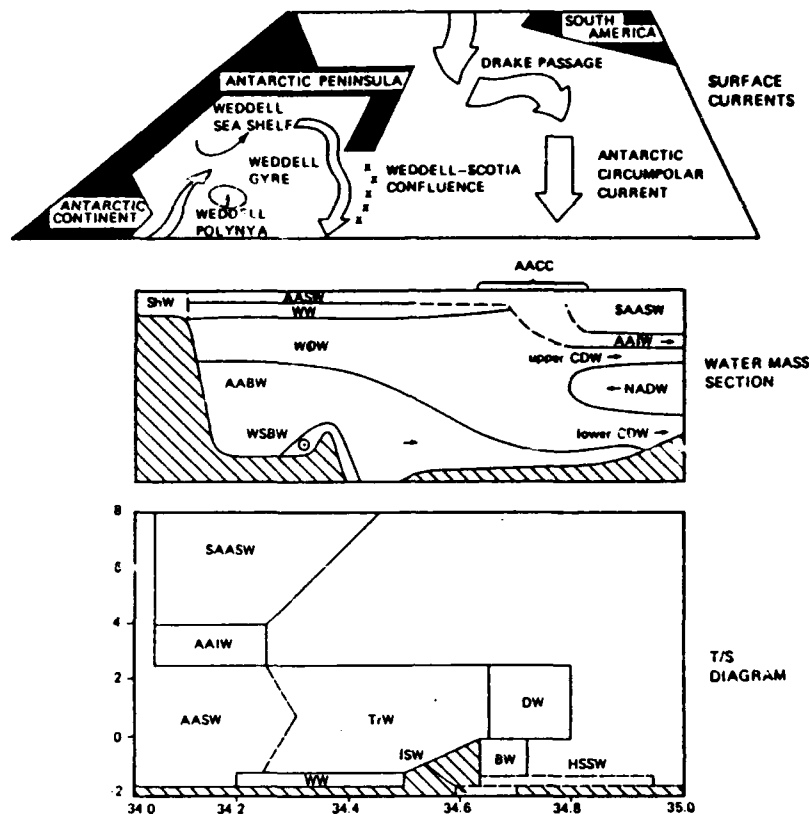


Figure 14. Types of tides in the Southern Ocean (after DMA, 1985).



(a) the surface circulation in the vicinity of the Atlantic-Antarctic Ocean; (b) water mass structure on a section extending from the Weddell Sea into the South Atlantic Ocean; (c) the classification of water masses on a T/S correlation diagram. The following abbreviations are used: Sub-Antarctic Surface Water (SAASW); Antarctic Surface Water (AASW); Antarctic Winter Water (WW); Antarctic Intermediate Water (AAIW); Deep Water (DW) includes North Atlantic Deep Water (NADW), upper and lower Circumpolar Deep Water (CDW) and Warm Deep Water (WDW); Bottom Water (BW) includes Antarctic Bottom Water (AABW) and Weddell Sea Bottom Water (WSBW); Shelf Water (ShW) includes Ice Shelf Water (ISW) and High Salinity Shelf Water (HSSW); and Transitional Water (TrW).

Figure 15. A schematic of the water masses in the Southern Ocean (after Carmack, 1986).

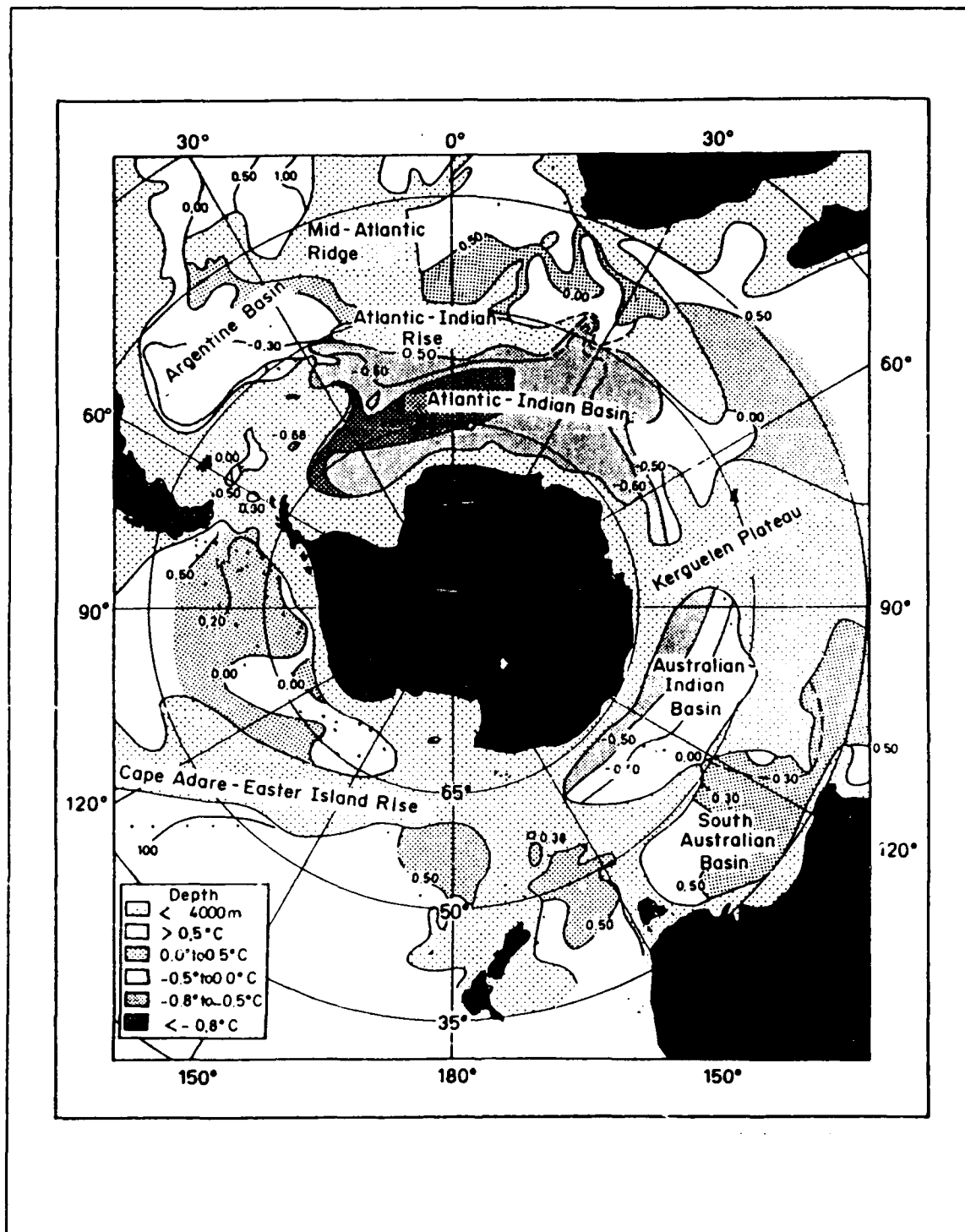


Figure 16. Temperature evolution of Antarctic Bottom Water shown by temperature regimes (after Deacon, 1937, plate XLIV).

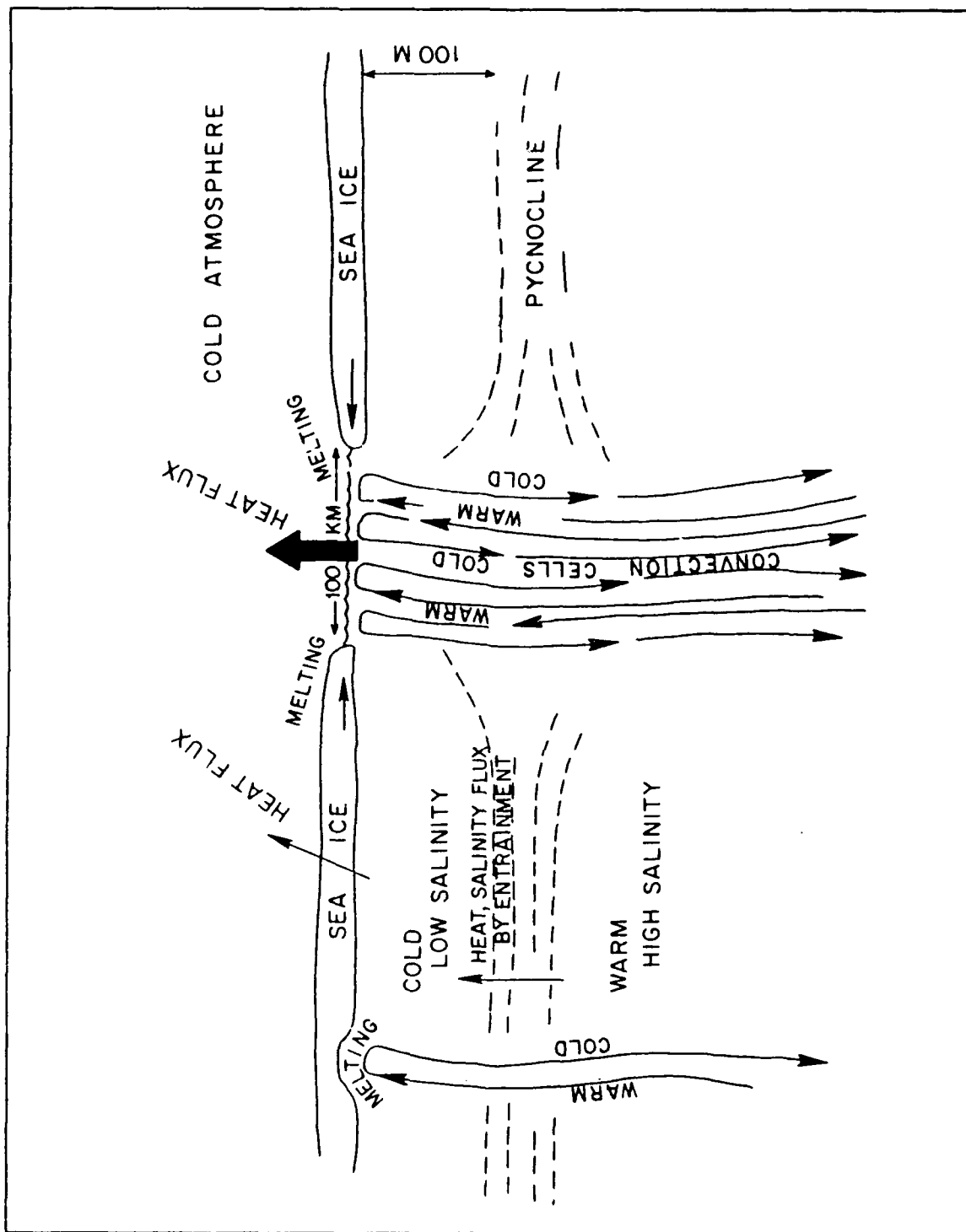


Figure 18. A schematic illustrating the formation of deep convection chimneys (after Gordon, 1988).

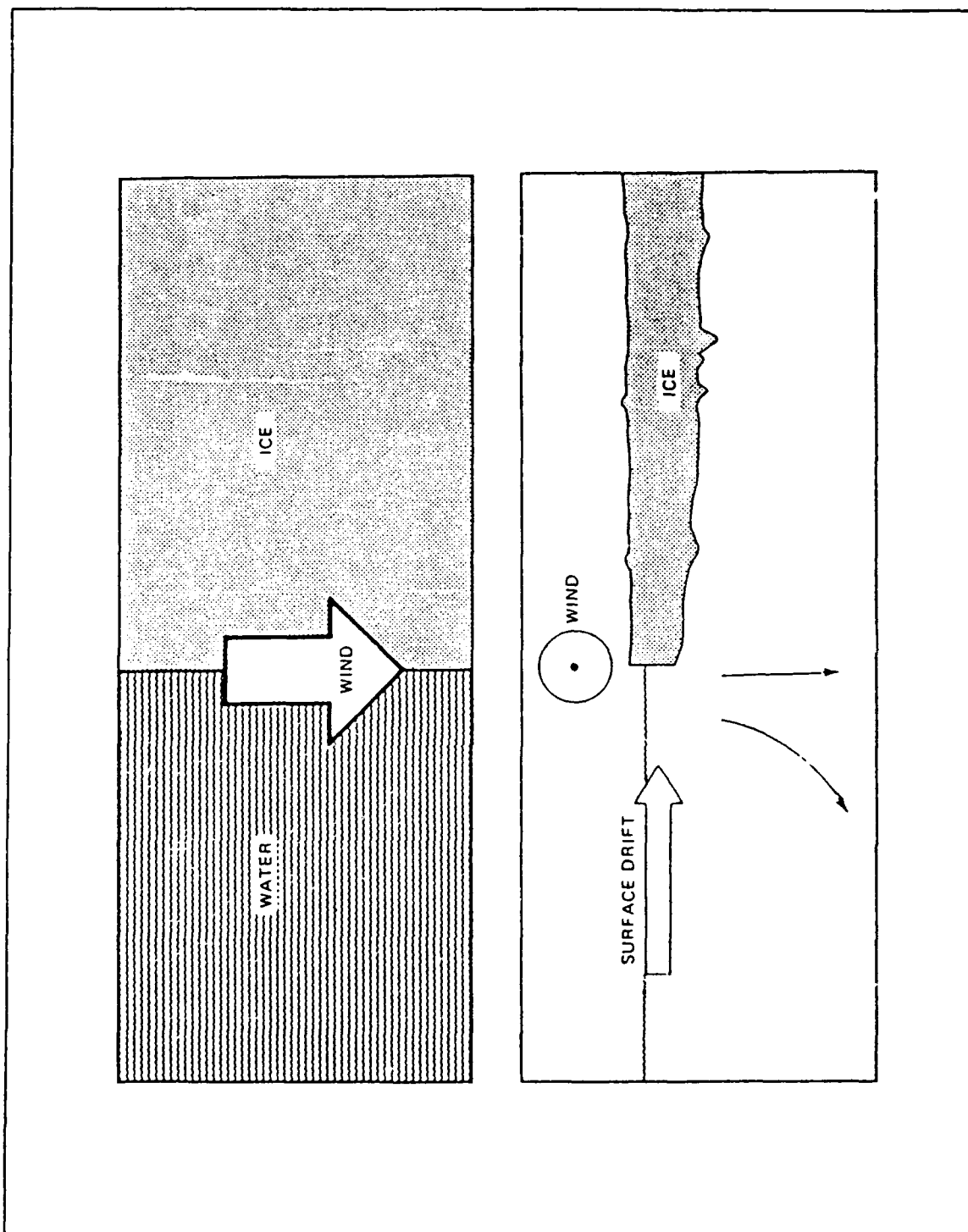
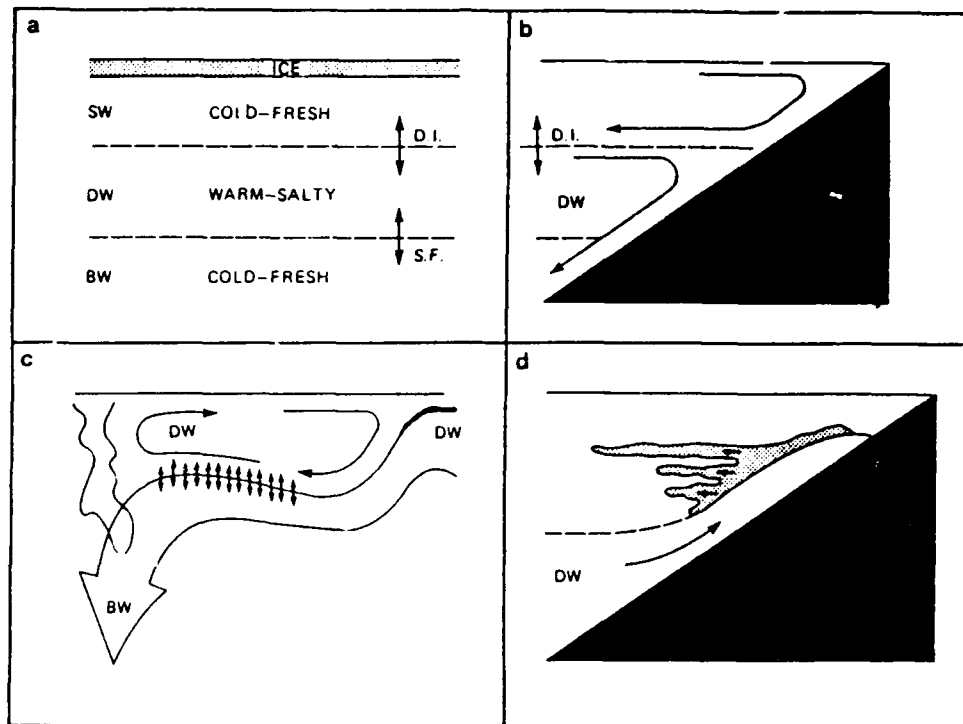
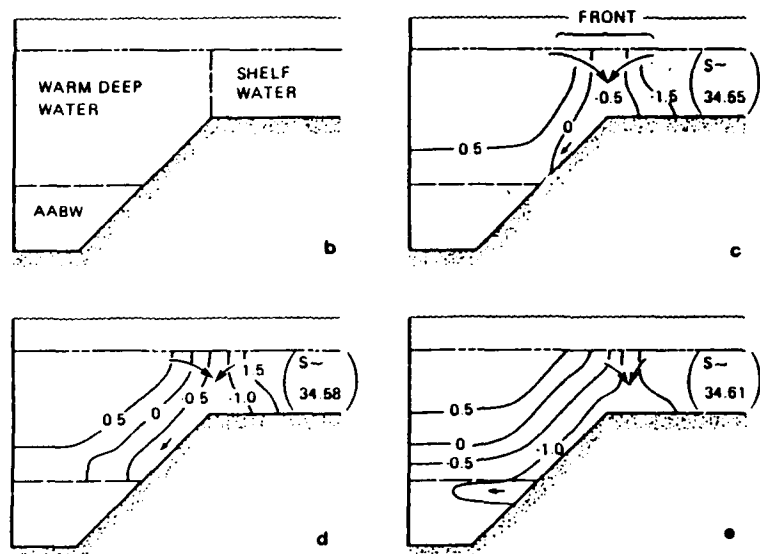
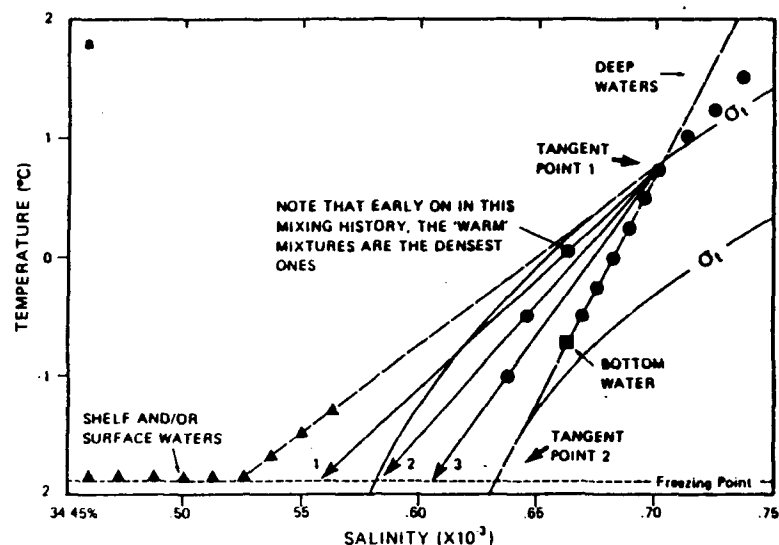


Figure 17. A schematic of wind-induced downwelling along an Antarctic ice shelf (after Carmack, 1986).



Surface Water (SW), Deep Water (DW) and Bottom Water (BW): (a) the case of double-diffusive instabilities at the interface between SW and DW, and salt finger instabilities below the core of DW with BW; (b) diffusive instability that leads to BW formation along the continental slope; (c) subsurface modification of DW involving two large-scale, convective regimes coupled by a double-diffusive process; (d) the potential for lateral interleaving associated with transient upwelling events.

Figure 19. A schematic illustrating various double-diffusive processes involved in the formation of AABW (after Carmack, 1986).



(a) T/S correlation diagram showing the principal water masses, tangents to lines of constant density (broken lines), and mixing curves (1, 2, and 3) between Warm Deep Water of constant salinity and shelf water of variable salinity; (b) vertical section showing the distribution of water masses near the shelf-break; (c, d, e) circulations due to mixing between Warm Deep Water and Shelf Waters of variable (increasing) salinities.

Figure 20. A schematic illustrating various cabbeling processes involved in the formation of AABW (modification on Carmack, 1986).

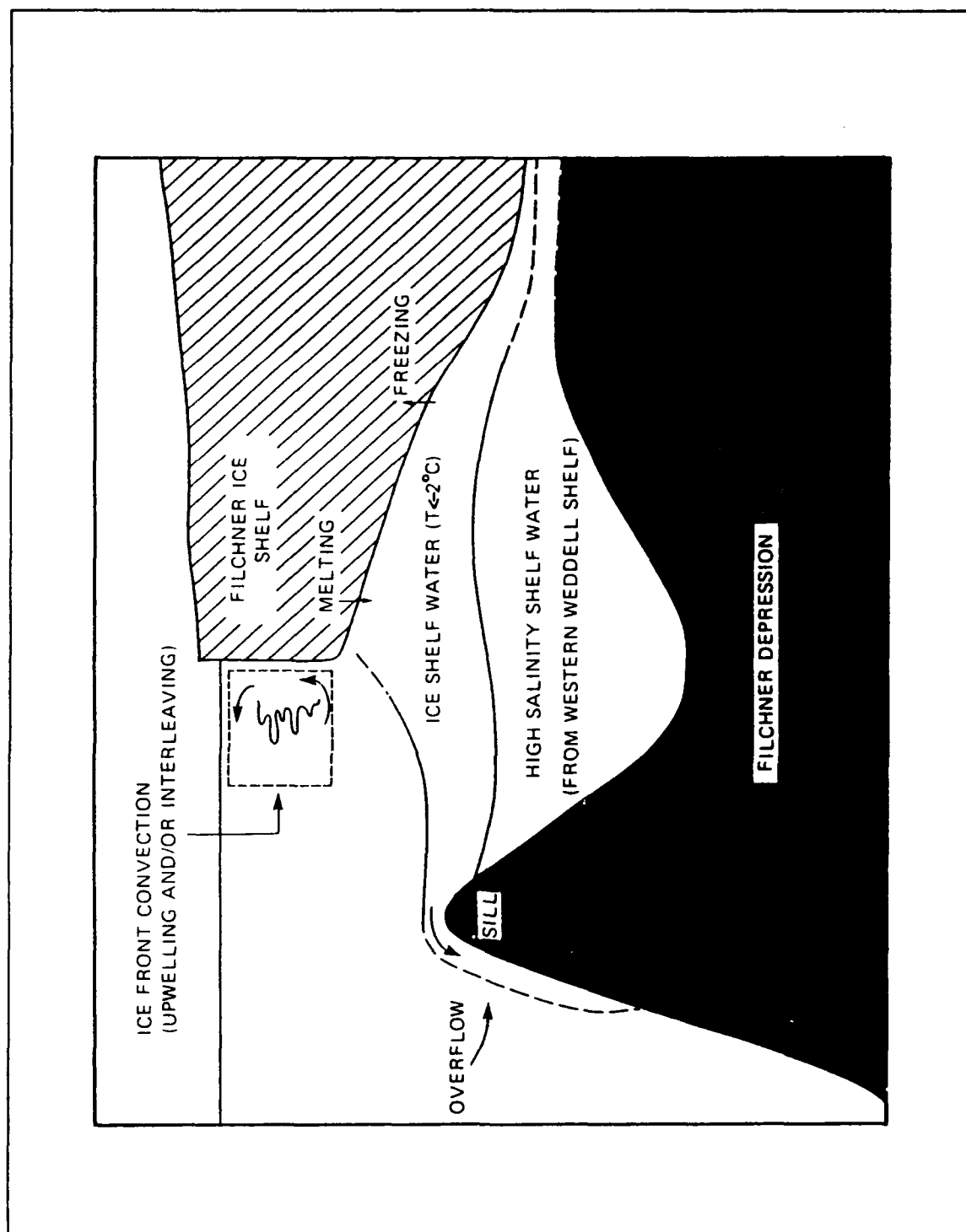
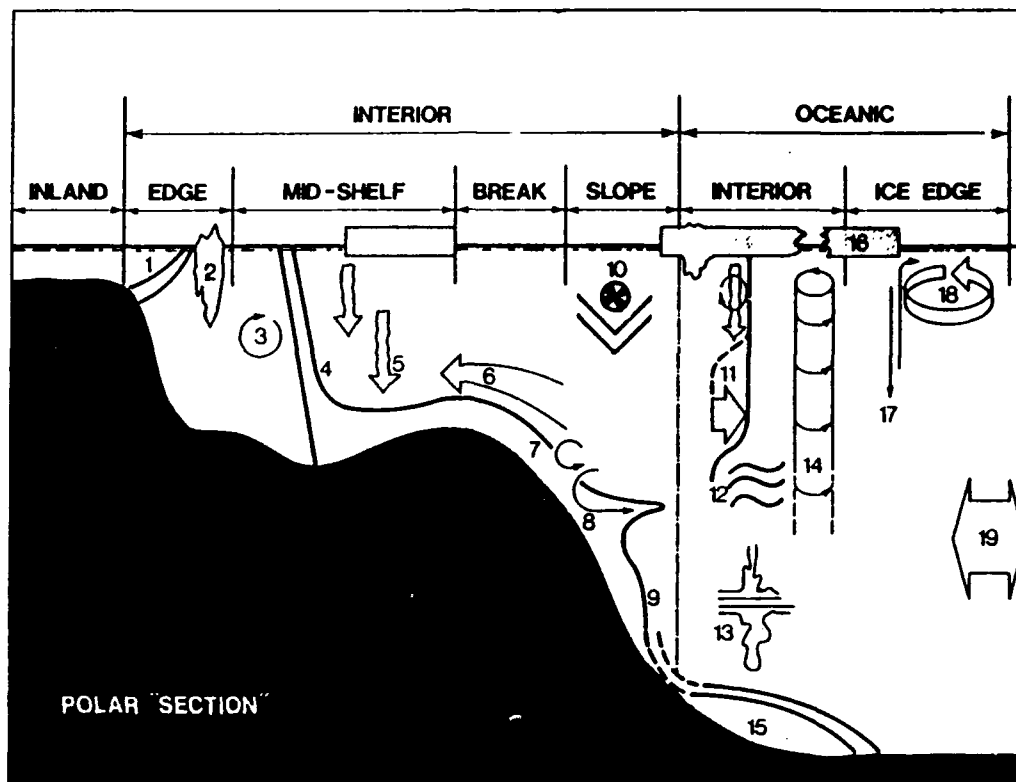


Figure 21. A schematic illustrating glacial melting/freezing processes involved in the formation of AABW (after Carmack, 1986).



- (1) glacial freezing; (2) glacial melting; (3) coastal circulation; (4) shelf front; (5) haline convection; (6) shelf-break upwelling; (7) shelf drainage; (8) mid-depth intrusion; (9) gravity plumes; (10) shelf-break jet; (11) mixed-layer dynamics; (12) halocline formation by lateral advection; (13) double diffusion; (14) chimney; (15) thermohaline circulation; (16) ice-drift; (17) ice-edge upwelling; (18) eddies; (19) exchange with the world ocean.

Figure 22. A schematic summary of the physical process effecting AABW formation (modification on Carmack, 1986).

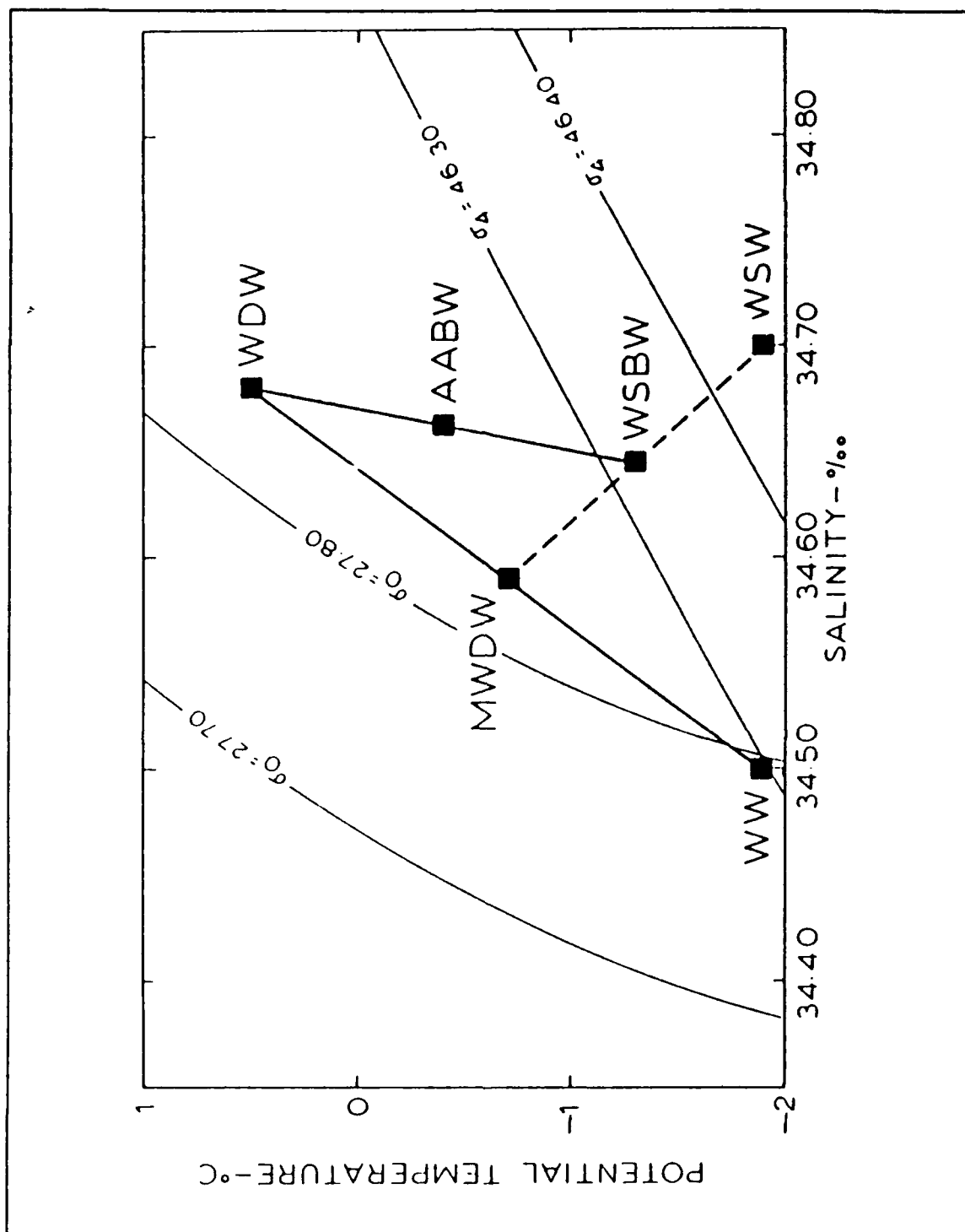


Figure 23. A schematic illustrating the shelf break process mixing scheme involved in the formation of AABW (after Foster and Carmack, 1976).

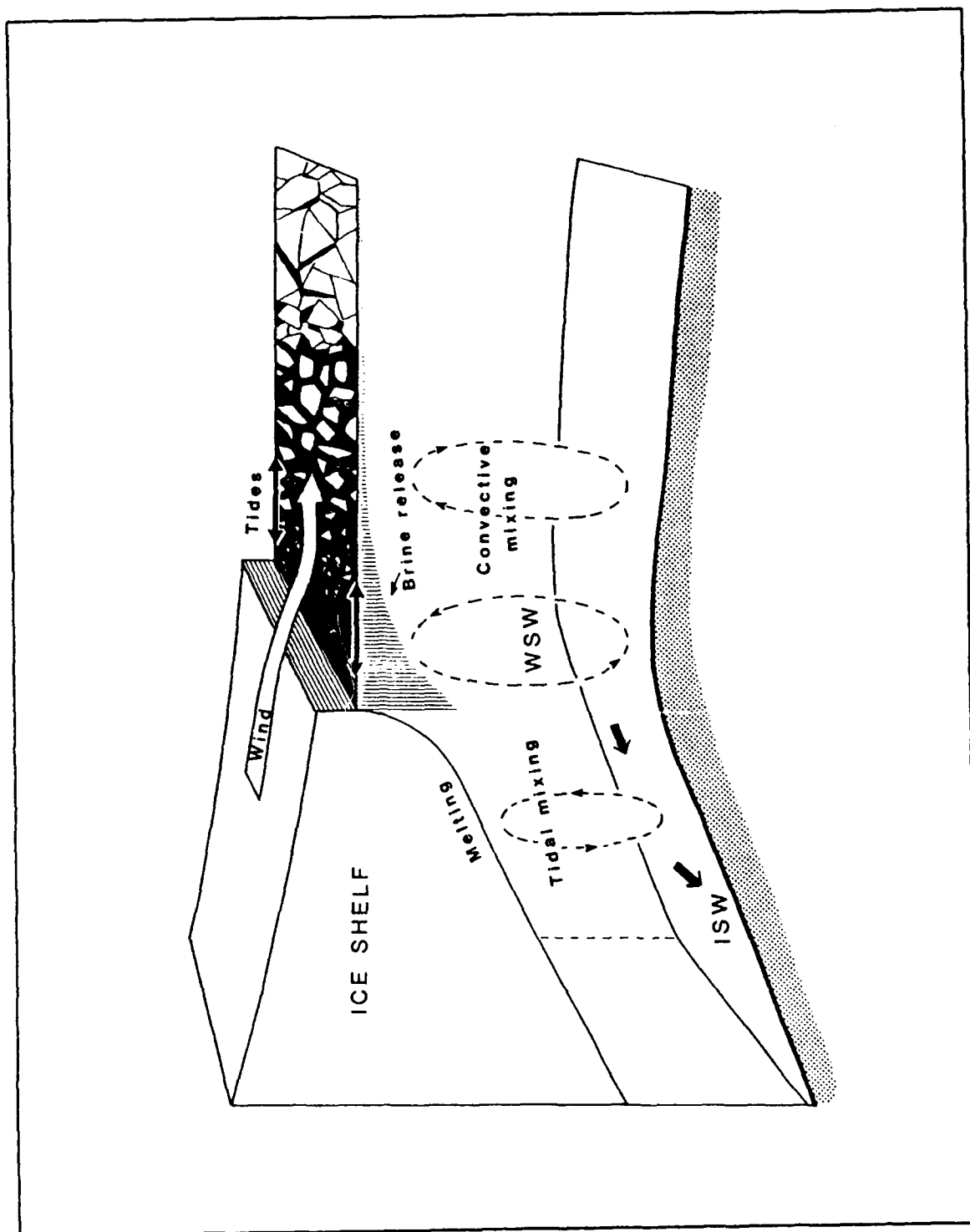


Figure 24. A schematic illustrating the ice shelf processes involved in the formation of AABW (after Foldvik and Gammelsrød, 1988).

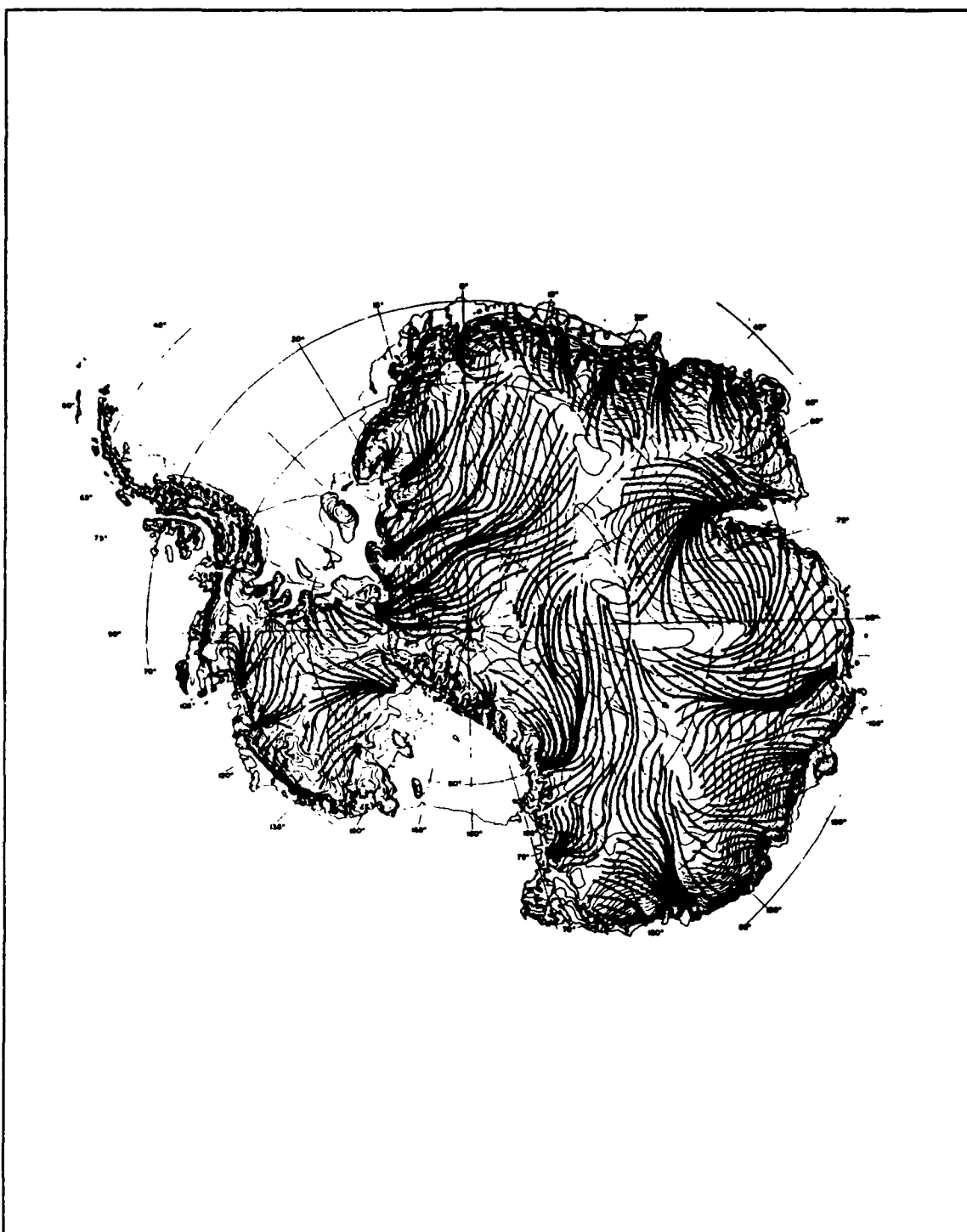


Figure 25. Katabatic wind regimes of the Antarctic continent (after Parrish and Bromich, 1987). Note: Time-averaged near surface streamlines (heavy lines) of cold air drainage over Antarctica.

III. DATA ACQUISITION, ANALYSIS METHODOLOGY AND LIMITATIONS

A. FORCING FUNCTION DATA SOURCES AND DATA PRESENTATION

Data were obtained from various sources for the different forcing functions in the Ross and Weddell Seas. Data sources and presentation schemes are detailed below.

1. Geography

The physical geography and open ocean continental shelf bathymetry of the two basins were obtained from the GEBCO Bathymetric Sheet 5.18, as presented by Vanney and Johnson (1985).

2. Surface Air Temperatures

Monthly archives of surface air temperature for the two basins were retrieved from the National Center for Atmospheric Research, Southern Hemisphere Climatology Data Base (NCAR, 1989). The data were gridded in 1° by 2° latitude longitude cells with 56 grid points in the Ross Sea and 40 grid points in the Weddell Sea. A tabular presentation was made of basin zonal averages and sub-zonal distinctions were made between ocean regimes and regimes at the land/ice shelf barrier. This data base was chosen as preferable to the routinely cited "actual observations" data base of the U.S. Navy (1965) which lacks alongshore ice shelf resolution.

3. Surface Winds

Monthly archives of surface wind information in the Ross and Weddell Seas were obtained from the NCAR (1989) Southern Hemisphere Climatology Data Base and at the same grid points as the surface air temperatures cited above. However, only *u* (east, west) and *v* (north, south) components of the true wind vector were available. Therefore computer-generated vector summations were accomplished and graphical results were projected on to a polar stereographic map. These graphics are presented in the analysis chapter. Relative maximum vector magnitudes are presented for comparison between basins and months. Care should be taken when viewing these graphics as the scales between months and basins are slightly different as indicated on the charts. This data base was also preferable to the U.S. Navy data base of 1965 due to the same resolution problems.

4. Ice Concentration

Quality ice concentration information for the two basins was available from two sources. NASA (1983) produced charts of monthly average concentrations of sea ice around Antarctica from analysis of satellite passive microwave observations made from 1973 to 1976. DMA (1985) published charts of monthly concentrations of sea ice for the same area from analyses of satellite ice data supplemented with aerial and ship-based ice concentration reports from 1973 to 1982. These charts were the result of a collaboration between the U.S. Navy and the National Oceanic and Atmospheric Administration (USN/NOAA).

Both of these sources were compared and found to produce essentially the same analyses. The presentation in this work will consist of a selection of charts and statistical analyses performed on these charts for interbasin comparisons.

5. Hydrography

General hydrographic data are presented by selected vertical cross sections of temperature, salinity, and density (σ_t) values which were produced graphically from the one degree latitude by one degree longitude Grid Point Data Set compiled by Gordon and Baker (1986, data tape). Gordon and Baker's Grid Point Data Set was objectively computed from the Gordon and Molinelli (1986) interpretively contoured Atlas Data Set from 33,866 hydrographic station reports. Due to the desire to show fine scale structure at depth, cross section data intervals were selected which resulted in a blurring of near surface data values. Presentation of surface values is made with horizontal surface charts published by DMA (1985). These charts do not reflect the precise Gordon and Baker Grid Point Data Set values but are similar enough for graphical representation of surface conditions.

Charts of the surface circulation within the Ross and Weddell Seas were obtained from DMA (1985) and are presented as representative of the general subsurface circulation as an alternative to horizontal cross sections at varying depths (as a previously described alternative cited by Deacon (1937)).

No under-ice-shelf hydrographic comparisons were possible due to the total lack of such data in the Weddell Sea. Limited Ross Sea under-ice hydrography exists from the Ross Ice Shelf J-9 Hole project as reported by Jacobs (1989) and winter under-ice-shelf measurements made at McMurdo Sound as reported by Neal et al. (1976). However, due to the lack of comparable Weddell Sea data, no comparisons were possible.

6. Under-Ice-Shelf Bathymetry

The bathymetry beneath the Ross Ice Shelf is the best charted of any Antarctic ice shelf. Information was available from GEBCO Bathymetry Sheet 5.18 (Vannev and Johnson, 1985) and Jacobs' (1989) report of the combined works of Greischar, Bently, Jezek and Shabtaie (from surveys taken from 1980 to 1987) which were at much finer scales than the GEBCO chart.

The bathymetry under the Ronne and Filchner ice shelves has not been extensively researched and currently quite different bathymetries have been reported by varying sources. Robin et al. (1983) presented a compilation of results of seismic and radio-echo testing and data from historical records. Drewry (1983) presented a similar compilation. However, in 1987, Herrod (1987) reported the results of an entirely new survey he recently undertook designed to precisely measure the bathymetry under the Ronne and Filchner Ice Shelves. His work is combined with the GEBCO (previously cited) data for the outflow region of the Filchner Depression (Weddell Sea) as the data base selected for analysis. Presentation will consist of selected reproductions of Herrod's work and results of visual analysis and measurement.

7. Tides

Tidal information was obtained in the form of corange and cotidal values and maps for eight major tidal constituents (Table 2) from Schwiderski (1979, 1981a-h). Grid point data at 1° latitude by 1° longitude of amplitude and phase were selected along the ice shelf barrier in both the Ross and Weddell Seas. Presentation includes a selection of cotidal and corange maps, tabulated values of tidal phase tendencies and tabulated values of tidal amplitude comparison statistics (explained in the following subchapter on data limitations).

Table 2. MAJOR TIDAL CONSTITUENTS

Tidal Mode	Description
M_2	Semidiurnal Principal Lunar
S_2	Semidiurnal Principal Solar
N_2	Semidiurnal Elliptical Lunar
K_2	Semidiurnal Luni-Solar
K_1	Diurnal Declination Luni-Solar
O_1	Diurnal Principal Lunar
P_1	Diurnal Principal Solar
Q_1	Diurnal Elliptical Lunar

B. METHOD OF DATA ANALYSIS

1. Zonation

Due to striking similarities in the physical geography of the Ross and Weddell Seas, a scheme was devised to divide each basin into four zones and perform zonal comparisons between similar zone numbers in each basin, in addition to basin-wide comparisons. Data on most of the forcing functions were available in sufficient resolution to make this approach practical. All data on each forcing function were either arithmetically averaged to obtain a representative zonal value or selected data from that zone were used to represent the entire zone.

Zone selection was accomplished by contrasting the shelf break proximity to land and from land to the ice shelf as detailed below (Figures 26 and 27).

ZONE A: The eastern side of the basin from where the continental shelf moves off land to the first land ice shelf boundary and then offshore perpendicular to the shelf break at 1000m.

ZONE B: From the western boundary of Zone A west to the next land ice shelf boundary then offshore perpendicular to the shelf break at 1000 m.

ZONE C: From the western boundary of Zone B west to the next ice shelf land boundary then offshore approximately perpendicular to the shelf break at 1000 m.

ZONE D: From the western boundary of Zone C west and northwest to where the continental shelf moves towards land.

From Table 3 it can be seen that Zones A through C have almost identical alongshore dimensions. (Offshore dimensions are averages for each zone.) Zone D was

selected to provide a western closure for each basin but has limited use for interbasin comparisons since most of Zone D in the Weddell Sea falls in the data sparse region of the Larsen Ice Shelf while the Ross Sea Zone D falls within a data rich zone. Additionally, the two D Zones have different relative orientations to their respective basins. Thus Zone D information, when available, will be reported for information purposes only. It should also be noted that neither bottom water theories envision substantial AABW formation to occur in either Zone D area.

Table 3. ZONE DIMENSIONS (KM)

Zone	Ross alongshore	Ross offshore	Weddell alongshore	Weddell off- shore
A	550	125	550	145
B	200	200	250	375
C	550	300	500	400
D	900	160	950	400
Total	2200		2250	

Vertical cross sections of temperature, salinity and density (σ_t) for the Ross and Weddell Seas were produced to represent conditions present in each zone. Points were selected within a zone following a track from the coast or ice shelf barrier offshore or perpendicular to the shelf break and continuing to the abyssal plain. In addition, cross sections alongshore from either side and across the ice shelf barrier were produced to analyze conditions near the ice shelf barrier. Table 4 lists the correlation between zone and vertical section for each basin¹¹. Tables 5 and 6 list the locations of each station used in the cross sections for the Ross and Weddell Seas.

¹¹ As previously stated, Zone D information is provided for information only. However, the Ross Sea Zone D is augmented with an additional cross section running approximately perpendicular to the initial section to provide better understanding of the complex nature of the Ross basin's western shelf. Zone D in the Weddell Sea is represented on its far eastern side due to the total lack of source data used in Gordon and Baker's (1986) Grid Point Data Set for the region in front of the Larsen Ice Shelf on the western shelf of the Weddell Sea.

Table 4. ZONE TO CROSS SECTION CROSS REFERENCE

Zone	Ross Sea Cross Section	Weddell Sea Cross Section
Zone A	Ross Sea 1	Weddell Sea 1
Zone B	Ross Sea 2	Weddell Sea 2
Zone C	Ross Sea 3	Weddell Sea 3
Zone 4	Ross Sea 4	Weddell Sea 4 and 6
Ice Barrier	Ross Sea 5	Weddell Sea 5

Table 5. ROSS SEA HYDROGRAPHIC STATION LOCATIONS

#	lat lon	#	lat lon	#	lat lon	#	lat lon
101	77S 152E	201	78S 164E	301	77S 180	501	77S 158E
102	76S 154E	202	77S 164E	302	76S 176E	502	78S 164E
103	75S 154E	203	76S 164E	303	75S 174E	503	78S 166E
104	74S 156E	204	75S 164E	304	74S 172E	504	78S 168E
105	73S 156E	205	74S 164E	305	73S 170E	505	78S 170E
106	72S 158E	206	73S 164E	306	72S 168E	506	78S 172E
		207	72S 164E			507	78S 174E
						508	78S 176E
401	76S 164W	601	76S 180			509	78S 178E
402	75S 170W	602	75S 178W			510	78S 180
403	74S 172W	603	74S 176W			511	77S 174W
404	73S 176W	604	73S 174W			512	77S 172W
405	72S 178W	605	72S 172W			513	77S 170W
406	71S 178W					514	77S 168W
407	70S 176W					515	77S 166W
						516	77S 164W

Table 6. WEDDELL SEA HYDROGRAPHIC STATION LOCATIONS

#	lat lon	#	lat lon	#	lat lon	#	lat lon
		200	77S 36W				
101	75S 28W	201	76S 36W	301	77S 50W	501	73S 20W
102	74S 28W	202	75S 36W	302	76S 48W	502	74S 22W
103	73S 28W	203	74S 36W	303	75S 46W	503	75S 26W
104	72S 28W	204	73S 36W	304	74S 44W	504	76S 30W
105	71S 28W	205	72S 36W	305	73S 44W	505	77S 36W
		206	71S 36W	306	72S 42W	506	77S 38W
		207	70S 36W	307	71S 40W	507	77S 40W
				308	70S 40W	508	77S 42W
						509	77S 44W
401	74S 60W					510	77S 46W
402	73S 56W					511	77S 48W
403	72S 52W					512	77S 50W
404	71S 48W					513	76S 56W
405	70S 46W					514	75S 60W
406	69S 44W					515	74S 60W

2. Tidal Comparison Statistic

Due to phase and frequency differences of the tidal constituents, a linear addition of tidal constituent amplitudes would not reflect the true tidal forcing regime of the total tide. Upon close examination of the raw data, it was determined that the four semi-diurnal constituents all had phases that were roughly comparable and the four diurnal constituents had phases that were also comparable to each other though significantly different from the semi-diurnal type. To account for the minor differences in phase and frequency, the diurnal and semi-diurnal constituents were each grouped and the root mean square (rms) constituent maximum amplitudes calculated. This statistic is not considered a true measure of the amplitude but is a relative measure for comparison to other such measures calculated for different locations. An assumption was hence made that a larger rms value for one location compared to the same statistic calculated for a different location would provide a valid measure of the relative strength of the tidal regime at each location.

C. LIMITATIONS OF DATA AND METHODOLOGY

1. NCAR Temperature and Wind Fields.

The grid point values found in the NCAR data base were generated from algorithms that incorporated limited empirical values due to the dearth of observational data from this remote location of the world. In addition, the global numerical models that produced these grid point values are subject to all the same restrictions as weather prediction models as well as inherent difficulties that most numerical models have when operating near numerical singularities such as 90°S.

The determination of zonal surface air temperature and wind vector averages for both the open ocean and barrier regimes was an interpretive procedure, not an objective analysis due to the lack of spatial resolution in grid point data.

2. Satellite Blended Ice Concentrations

Due to inadequate spatial resolution of the satellite imagery, about 30 km by 30 km per pixel (NASA, 1985, p.vii), leads and polynyas smaller than this scale are not revealed. This is a scale at which, unfortunately, both theories of AABW formation can operate.

3. Hydrographic Data Limitations

Though Gordon and Baker (1986, p. 18) claim the best data available were used in their data set, there are basic limitations to its use as follows:

- The number of stations taken during the austral summer exceed those of the austral winter by a ratio of four to one.
- The distribution of winter stations is predominantly to the north of the sea ice cover.
- Grid point data are average annual values; no seasonal signal is preserved. However, southern points are mainly generated by summer observations.
- The number of hydrographic stations reported for the southern Ross Sea were an order of magnitude greater than the number reported for the southern Weddell Sea.
- The objective nature of the computer-generated grid point data set must be modified to account for the fact that the input data to that model was from an interpretively contoured data base. As Gordon and Molinelli (1986, p. vii) state:

"The term interpretive contouring is used to denote contouring of an array of data points by an experienced individual rather than by mathematical algorithm of an objective contouring method. The interpretive contouring method involves rather complex, perhaps poorly understood, decisions regarding the weights to give various data during contouring. Oceanographic experience and intuition, as well as somewhat preconceived ideas of how the

ocean should look are contributing factors in the final shape of the contours."

- Though using surface horizontal circulation patterns to reflect subsurface horizontal circulation has been held as acceptable, the effect will be to infer the horizontal circulation in one data set (Gordon and Baker, 1986) by another (DMA, 1985). This has been done in the current analysis by design since the assumption was made that production and analysis of horizontal cross sections would not generate significantly different results.

4. Limitations on Tidal Information

Schwiderski has produced a non-linear tidal model that has interpolated empirical tide data at over 2000 tide stations world wide and claims an open ocean accuracy of 5 cm with 10 cm accuracy everywhere else (Schwiderski, 1978, p. iii). However, Schwiderski admits that empirical coverage is marginal at the Antarctic shoreline and therefore accuracy of his model drops near the coast. It is also less accurate where effects of large ice sheets cause tidal distortion and retardation. (Schwiderski, 1978, p. 37; 1981a, p. 5)

Due to concern over these caveats, the entire International Hydrographic Office's Antarctic Tidal Observations Data Base (IHO, 1989) was obtained and compared to Schwiderski's model output at observation locations. With the exception of one observation point at Wilkes Station (66S, 110E), all IHO observation data agreed with Schwiderski's model output.

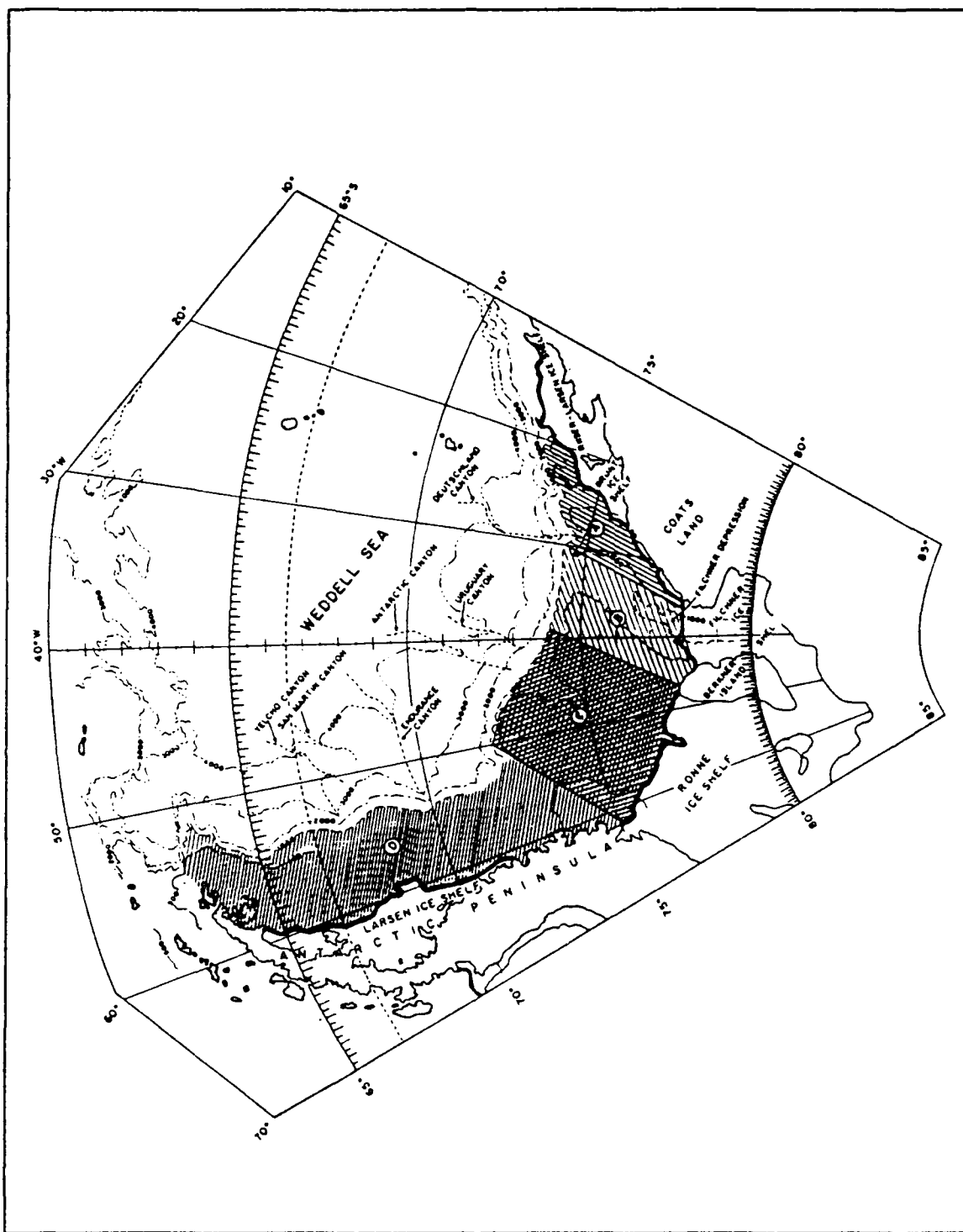


Figure 27. Map of the Weddell Sea showing zonation scheme. Note: Zonation limits are indicated by hatched lines.

IV. RESULTS OF ANALYSIS

A. GEOGRAPHY

Results of the basin wide and zonal geography comparisons revealed the following:

1. Continental Shelf

The Weddell Sea contains 1.8 times more shelf area than the Ross Sea. However, if Zone D is ignored (Larsen Ice Shelf area in the Weddell Sea and Victoria Land area in the Ross Sea), then the basin shelf sizes are comparable (Table 7). Note that the Weddell Sea continental shelf is generally shallower than the Ross Sea continental shelf and only the eastern zones (A and B) are comparable (Table 8).

Table 7. CONTINENTAL SHELF SIZE: (km^2)

Zone	Ross	Weddell
A	70,000	80,000
B	40,000	100,000
C	165,000	200,000
D	145,000	380,000
TOTAL	420,000	760,000

Table 8. PERCENTAGE OF SHELF AREA VERSUS DEPTH

Zone	Ross	Weddell
A	75% < 500m	75% < 500m
B	50% \geq 500m	50% \geq 500m
C	75% > 500m	75% < 500m
D	50% \geq 500m	75% < 500m
Total	50% \geq 500m	75% < 500m

2. Shelf Bathymetry.

The Weddell Sea has one highly organized outflow channel existing from beneath the ice shelf to the shelf break in Zone B. The Ross Sea shows only two small

organized outflow channels, one lying between the Mawson Bank and Cape Adare on the far northwest corner of the basin and the other lying in the Little America Basin between Roosevelt Island and Edward VII Land (Figure 28). The Weddell Sea shelf has no major sills which can prevent bottom shelf water from flowing seaward to the shelf break. This is in direct contrast to the Scott Shoal, a substantial sill in the Ross Sea which prevents the seaward flow of dense shelf water over approximately one half of the basin (Figures 28 and 29). Finally, both basins show roughly the same bathymetries from the shelf break seaward to their respective abyssal plains with many well organized downslope channels.

3. Latitude Considerations

The average position of the Ross and Weddell ice shelf barriers are at approximately the same latitude (Ross Sea barrier 76.5° to 79°S; Weddell Sea barrier 75° to 78°S) except for the Zone D orientation differences referred to in Chapter III. The Ross and Weddell Sea shelf breaks are at approximately the same latitude (Ross Sea 75° to 76°S; Weddell Sea 72° to 74°S) except for Zone D as noted above.

4. Ice Shelves

The Weddell Sea ice shelves (the Ronne and Filchner ice shelves) are slightly smaller than the Ross Ice Shelf (470,000 km^2 versus 525,000 km^2), however, the Weddell Sea ice shelves have a greater volume (307,300 km^3 versus 224,500 km^3) (Robin et al., 1983, p. 583).

In summary, the Weddell Sea has slightly shallower but far more organized (as defined in Chapter II) shelf bathymetry than the Ross Sea but the overall dimensions of the Ross and Weddell basins are remarkably similar. In addition, both basins exhibit similar bathymetries beyond the shelf break which generally permit unimpeded flow to the abyssal plain.

B. SURFACE AIR TEMPERATURE.

The results of the surface air temperature analysis are presented below and the data are summarized in Tables 9, 10 and 11.

- Climatological surface air temperatures when categorized by month, zone, oceanic or land ice barrier regimes show remarkably small differences between the two basins. No more than 9°C differences occur when similar zone numbers are compared by month or oceanic versus land ice barrier regimes. In addition, all of these differences occur between zonal averages which are well below the freezing point of sea water.
- When monthly zonal averages of oceanic versus land ice shelf regimes are arithmetically averaged to produce a total basin average, analysis reveals a range of

monthly temperature differences, by regime, between the Ross and Weddell Seas from 0.5°C to 8.0°C. The Weddell Sea is marginally colder than the Ross Sea in both oceanic and land ice shelf regimes except for the months of August and September and the oceanic regime in October.

- When basin averages combining the two regimes are calculated, the results reveal the Weddell Sea to be marginally colder than the Ross Sea in all months except August through October when the trends reverse. The range of monthly temperature differences, by basin, is from 0.8°C to 7.8°C. However, all air temperatures are significantly below the freezing point of sea water.
- In no month do the mean air temperatures of either basin or their respective zones rise above the freezing point of sea water.
- These results indicate that virtually no effective freezing differences exist between the basins due to surface air temperatures during the entire year. Also, effective surface freezing should occur in both basins throughout the year if the surface air temperature is the only forcing function being considered. Due to the lack of significant differences in surface air temperatures between the two basins, calculation of Zubov's ice thickness was deemed superfluous as a comparison tool.

Table 9. AVERAGE ZONAL AND BASIN SURFACE AIR TEMPERATURES (°C) FOR JANUARY THROUGH APRIL: (with comparisons of total basin and oceanic versus land/ice shelf regime monthly averages).

ZONE	January				February			
	Ocean Regime		Land, Ice Shelf Regime		Ocean Regime		Land, Ice Shelf Regime	
	Ross	Wedd	Ross	Wedd	Ross	Wedd	Ross	Wedd
A	-5	-5	-6	-7	-7	-8	-10	-10
B	-3	-5	-6	-8	-6	-8	-9	-11
C	-3	-5	-5	-8	-5	-7	-8	-11
D	-2	-5	-5	-10	-6	-7	-10	-13
Total basin average	-3.25	-5.0	-5.5	-8.25	-6.0	-7.5	-9.25	-11.25
Re-gime comparison	W colder by 1.75		W colder by 2.75		W colder by 1.50		W colder by 2.00	
Total basin comparison	W colder by 2.25				W colder by 1.75			
	March				April			
A	-10	-18	-14	-22	-17	-20	-19	-23
B	-9	-18	-15	-24	-16	-19	-21	-25
C	-10	-17	-15	-24	-16	-20	-20	-25
D	-12	-18	-21	-27	-17	-20	-24	-28
Total basin average	-10.25	-17.75	-16.25	-24.25	-16.50	-19.75	-21.00	-25.25
Re-gime comparison	W colder by 7.50		W colder by 8.00		W colder by 3.25		W colder by 4.25	
Total basin comparison	W colder by 7.75				W colder by 3.75			

Table 10. AVERAGE ZONAL AND BASIN SURFACE AIR TEMPERATURES (°C) FOR MAY THROUGH AUGUST: (with comparisons of total basin and oceanic versus land ice shelf regime monthly averages).

ZONE	May				June			
	Ocean Regime		Land Ice Shelf Regime		Ocean Regime		Land Ice Shelf Regime	
	Ross	Wedd	Ross	Wedd	Ross	Wedd	Ross	Wedd
A	-22	-25	-25	-28	-23	-26	-26	-29
B	-21	-25	-26	-29	-22	-25	-27	-29
C	-20	-26	-25	-29	-22	-26	-25	-29
D	-22	-26	-28	-32	-23	-26	-28	-32
Total basin average	-21.25	-25.50	-26.00	-29.50	-22.50	-25.75	-26.50	-29.75
Re-gime comparison	W colder by 4.25		W colder by 3.50		W colder by 3.25		W colder by 3.25	
Total basin comparison	W colder by 3.88				W colder by 3.25			
	July				August			
A	-25	-26	-27	-29	-29	-28	-31	-29
B	-24	-25	-27	-29	-29	-27	-33	-30
C	-23	-25	-26	-29	-27	-26	-31	-30
D	-24	-25	-30	-30	-27	-26	-30	-31
Total basin average	-24.00	-25.25	-27.50	-29.25	-28.00	-26.75	-31.25	-30.00
Re-gime comparison	W colder by 1.25		W colder by 1.75		R colder by 1.25		R colder by 1.25	
Total basin comparison	W colder by 1.50				R colder by 1.25			

Table 11. AVERAGE ZONAL AND BASIN SURFACE AIR TEMPERATURES (°C) FOR SEPTEMBER THROUGH DECEMBER: (with comparisons of total basin and oceanic versus land/ice shelf regime monthly averages).

ZONE	September				October			
	Ocean Regime		Land Ice Shelf Regime		Ocean Regime		Land/Ice Shelf Regime	
	Ross	Wedd	Ross	Wedd	Ross	Wedd	Ross	Wedd
A	-27	-23	-29	-27	-21	-18	-23	-20
B	-25	-23	-29	-28	-19	-18	-22	-22
C	-23	-24	-27	-28	-18	-18	-21	-22
D	-24	-24	-30	-30	-18	-18	-21	-25
Total basin average	-24.75	-23.50	-28.75	-28.25	-19.00	-18.00	-21.75	-22.25
Re-gime comparison	R colder by 1.25		R colder by 0.50		R colder by 1.00		W colder by 0.50	
Total basin comparison	R colder by 0.88				R colder by 0.25			
	November				December			
A	-12	-11	-13	-13	-5	-7	-7	-9
B	-9	-9	-11	-13	-4	-6	-5	-9
C	-8	-10	-10	-13	-3	-6	-4	-9
D	-8	-10	-14	-16	-2	-6	-5	-11
Total basin average	-9.25	-10.00	-12.00	-13.75	-3.50	-6.25	-5.25	-9.50
Re-gime comparison	W colder by 0.75		W colder by 1.75		W colder by 2.75		W colder by 4.25	
Total basin comparison	W colder by 1.25				W colder by 3.50			

C. SURFACE WINDS

Climatological surface winds were compared between the two basins and their respective zones in order to determine the wind stress and related sea ice deflection angles. The results are summarized below (Figures 30 through 33 reflect January through December climatological surface winds over the Ross and Weddell Seas):

- In the Weddell Sea during most of the year the winds have a component along or towards the barrier, whereas in the western part of the Ross Sea the winds are directed seaward away from the barrier. If we assume that the average deflection angle is 30° to the left of the wind direction, then the sea ice drift will be towards the barrier in the Weddell Sea, whereas in the Ross Sea the sea ice (and surface water) drift will have a component off the barrier tending to open the sea ice cover. This difference between the two basins is clearly revealed by the entirely different break-up of the pack ice in spring with the pack ice in the Ross Sea disappearing first near the barrier possibly due to off-barrier winds and wind-induced upwelling of warm water (Figures 34 and 35).
- From August through October the wind and ice flow pattern in the Weddell Sea continues to follow the above scenario. However, in the Ross Sea the oceanic regime appears to be sufficiently different from the Weddell Sea oceanic regime to warrant further analysis. It appears a cyclone is established over the shelf break region of the east central Ross Sea during this period. A similar occurrence is not observed in the Weddell Sea. The Ross Sea zonal oceanic surface wind vectors appear to be 45° to 90° out of phase with their Weddell Sea zonal counterparts. However the net effect of these differences appear concentrated in Zones B and C of the Ross Sea. It should be noted that the magnitude of the winds in this outer area are much smaller than in previous months and since it has been shown empirically that deflection angles increase as wind speed decreases, it is entirely possible that the outer B and C Zones of the Ross Sea maintain a borderline convergent divergent flow field when measured at the land barrier.

D. ICE CONCENTRATION

No zonation comparisons of ice concentration have been attempted due to resolution problems of the satellite data source as previously described. Twelve monthly ice charts are presented in Figures 34 and 35. Analyses of ice concentration reveal the following:

- An anomalous total dissipation of the pack ice from the ice barrier seaward in the western Ross Sea during the austral summer (January and February) which finds no counterpart in the Weddell Sea (which maintains a 1.10 to 9.10 coverage during the same period).
- In the Weddell Sea the ice edge advances toward the northeast during the growth season and retreats westward during the decay season. In the Ross Sea the ice edge advances westward during ice growth and poleward during retreat except for the anomalous case cited above.

- During austral winter there appears to be little difference between the two basins with 9-10 ice coverage present in both areas.
- The Weddell basin has a greater amount of ocean area covered by ice and a greater concentration of sea ice than the Ross Sea throughout the year but especially in austral winter when it reaches 1.5 times the ice coverage at 1.5 times greater concentration (Figure 36).
- The maximum ice growth rate occurs from March to April in the Ross Sea which is two months earlier than in the Weddell Sea (Figure 36). The maximum decay rate occurs from December to January in the Ross Sea which is one month later than in the Weddell Sea. The interannual variability in the mean sea ice concentration is greater in the Ross Sea during late austral summer while the Weddell Sea experiences its greatest variability in early austral summer (Figure 37).

In summary, the Ross and Weddell Basins show distinctly different spatial and temporal ice cover characteristics at various times of the year.

E. HYDROGRAPHY

Utilizing the water mass definitions provided in Chapter II, analysis of the hydrographic conditions in each basin revealed the following:

1. Horizontal Circulation and Water Masses

- The basin-wide horizontal circulation of the Weddell Sea is characterized by an elongated cyclonic gyre bounded to the south by the continent and to the west by the Antarctic Peninsula. Its closure to the east is uncertain but extends perhaps to 20 to 30° E. The horizontal circulation of the Ross Sea is similar demonstrating a cyclonic gyre bounded by the continent to the south and by Victoria Land to the west. The seaward boundary is not as well defined and appears to be split with a portion returning along the 90°W recirculation boundary (as seen in Figure 11) and a portion continuing to the west (Figure 38).
- Both basins show low density, warm, low salinity shelf water present on the eastern side of the basin grading to high density, cold, high salinity water on the western side (Figures 39 through 41). These are relative comparisons with each basin with interbasin comparisons showing that the Ross Sea is generally 0.5° to 1 °C warmer and more saline.

2. Vertical Circulation and Water Masses

Cross section track locator maps are provided in Figures 42 and 43.

- ZONE A: Significantly warmer WDW exists in the Ross Sea from 500 m to the bottom while WDW is contained between 750 to 2000 m in the Weddell Sea (Figure 44). Both basins show evidence of downwelling at the shelf at mid-depth (downwelling is seen as the downturning of contours of temperature and salinity at the slope). Classic AABW (temperatures < 0.0 °C, salinities > 34.6 in Figure 44) is present from 2000 m to the bottom only in the Weddell Sea.
- ZONE B: In the Ross Sea significantly warmer WDW intrudes on to the continental shelf then downwells south of the shelf break with apparent extension

down the slope (Figure 45). In the Weddell Sea WDW is constrained between 500 to 1500 m then downwells at the shelf break. Again, only the Weddell Sea shows indication of classic AABW and it is found between the bottom and 1500 m (though the salinity values are comparable between the two basins, the Ross Sea bottom temperatures are too warm to be AABW). In addition, ESW exists along the barriers in both basins as identified by its salinity range. However, the shelf waters of the Ross Sea are warmer, by as much as 0.5 °C, than the Weddell Sea. Within the shelf break region of Zone B in the Weddell Sea, MWDW is clearly evident (temperatures colder than -0.7 °C, salinities > 34.59) but in the Ross Sea it is not so evident. It is difficult to state whether MWDW is present at the shelf break in the Ross Sea at the time of these observations. An organized plume of ISW is clearly visible near the bottom in the vicinity of Zone B, Filchner Depression, stations 505 to 510 of the Weddell Sea transect 5 (Figure 47). This plume can be readily identified by its extremely cold temperatures (colder than -2.0 °C) and high densities (> 27.90). No such plume exists in the Ross Sea. The only outflow channel in this zone is in the region of the Little America Basin. Bottom temperatures in this region are in excess of 0.2 °C indicating that no cold outflow from the shelf seaward appears to occur in this region.

- **ZONE C:** Significantly warmer WDW, extending to the bottom, intrudes on to the shelf in the Ross Sea with a weak signal of possible upwelling (as seen from the upturned 0.4 °C temperature contour) at mid-depth on the slope (Figure 46). In the Weddell Sea, WDW is colder than normal and is confined to a band between 500 to 1500 m with downwelling evident along the slope. AABW is also evident from 1500 m to the bottom in the Weddell Sea with no such signal present in the Ross Sea. MWDW is clearly evident south of the shelf break in the Weddell Sea with downwelling extending seaward to the slope. In the Ross Sea a warm water version of WSW is clearly observed (temperatures colder than -1.5 °C, salinities > 34.7) but existence of MWDW at the shelf break is not clear. An anomalous core of relatively warm water (temperatures warmer than -1.0 °C) is seen at 250 m depth on Ross Sea transect 5 (Figure 47).
- **ZONE D:** The Weddell Sea shows evidence of WDW intruding onto the shelf but no evidence of mixing or other processes at the shelf break (Figure 49). Transects 4 and 6 in the Ross Sea (Figure 48) demonstrate that extremely dense water is present (temperatures colder than -1.7 °C, salinities > 34.9) but appears to remain in the McMurdo Sound region being trapped at the Scott Shoal. The only outflow channel in this zone is between Cape Adare and the Mawson Bank. Bottom temperatures in this region are in excess of 0.6 °C indicating that no cold outflow from the shelf seaward appears to occur in that region.

Basin to basin comparisons reveal that the Ross Sea is warmer at the bottom with no AABW except for a small pocket of water with AABW characteristics trapped by the Scott Shoal. In the Weddell Sea AABW is present in all transects. Also, the Ross Sea is much warmer and more saline than the Weddell Sea at almost all depths. The Ross Sea shows a small, relatively warm core of mid-depth water running under the ice shelf at one location of the barrier while in the Weddell Sea a near-bottom cold plume issues from the ice shelf at roughly the same relative location at the barrier.

Both basins show similar signs of downwelling at the slope with a weak localized upwelling possible in one section of the Ross Sea. Finally, no clear evidence of AABW flowing downslope from the shelf break in either basin can be seen. However, the scale and orientation of the plume of ISW found at the barrier in the Weddell Sea was insufficient to be reflected in the data set of Zone B.

F. UNDER-ICE-SHELF BATHYMETRY

The following points were revealed during analysis of the Ross and Weddell Sea under-ice bathymetries (Figure 50).

- The depth of the water column beneath the ice shelf reveals that in both basins the ice shelves grow thicker and the bottom depths get deeper towards the continent.
- Under the Ronne Ice shelf a path is present which allows ice shelf water to progress in geostrophic balance (shallower water to the left) from under the Ronne Ice shelf around Berkner Island to the Filchner Depression (the Filchner Depression bathymetry is shown in Figure 29).
- The Ross Sea bathymetry indicates a similar but smaller channel around Roosevelt Island. However, the shelf area west of Roosevelt Island is much deeper (600 to 800 m) than the Ronne Ice Shelf (300 to 400 m west of Berkner Island). This implies that the production of dense shelf water is slower at this location than at the Ronne Ice Shelf due to the longer residence time required to transform the deeper water column into dense shelf water.
- In the western part of the Ross Sea two depressions connecting deep water from the ice barrier to the Antarctic coast line are bisected by a shallow rise (Figure 28). The most likely path for ISW produced under the western Ross Ice Shelf would be to flow east of McMurdo Sound, turn westward into the depression west of Mawson Bank and finally flow down the continental slope east of Cape Adare. However, no observations of a cold outflow in this region have been reported.

G. TIDES

The results of the tidal analysis are presented below and a summary of tidal amplitude statistics and constituent phase comparisons are provided in Tables 12 and 13. Representative semi-diurnal and diurnal components (specifically the M_2 and K_1 modes), corange and cotidal maps are found in Figures 51 through 54.

1. Barrier Comparisons

- The dominant tidal constituent in the Ross Sea is the diurnal component (specifically the K_1 mode with a secondary mode of O_1). The Weddell Sea has a dominant semi-diurnal component (specifically the M_2 mode with a secondary S_2) (Table 12). The total rms tidal amplitude of approximately 1.5 m agrees with observations (Foldvik, Gammelsrød, Slotsvik and Tørresen, 1985, p. 218).

- The diurnal amplitudes in the Weddell Sea are similar to those in the Ross Sea (Figure 52).
- The semi-diurnal amplitudes in the Weddell Sea are an order of magnitude greater than those in the Ross Sea (Figure 51).
- The Ross Sea is located much closer to its diurnal and semi-diurnal amphidromic points than is the Weddell Sea to its amphidromic points (Figures 52 and 54).
- All of the Ross Sea diurnal constituents propagate from east to west while in the Weddell Sea, the major diurnal constituents approach the basin as a wave front approximately parallel to the ice shelf with only minor exceptions (Table 13).
- The dominant M_2 mode in the Weddell Sea is a progressive wave traveling east to west. However, the second dominant mode, S_2 , arrives approximately parallel to the wave front (not shown).

2. Zonal Comparisons

- Both the semi-diurnal and diurnal amplitudes show a monotonic increase from east to west (Zone A to Zone C) in both the Ross and Weddell Seas except for a very minor amplitude fluctuation at the eastern end of Zone B in the Weddell Sea.
- Zone D in the Ross Sea shows a monotonic decrease east to west along its southern coastline. Zone D in the Weddell Sea has no southern coast.
- The rms diurnal tidal amplitude averaged over Zones A, B and C indicate nearly identical values for both the Ross and Weddell Seas. However, the rms zonal average for the semi-diurnal tide shows the amplitude in the Weddell Sea to be an order of magnitude larger.

In summary, there are significant tidal differences between the two basins with two features unique to the Weddell Sea. (1) The semi-diurnal tidal forcing (which dominates over diurnal tidal forcing in the Weddell Sea) is an order of magnitude larger in the Weddell Sea compared to the Ross Sea and (2) the Weddell Sea tidal crests have a significant component arriving parallel to the ice shelf while all the Ross Sea modes are waves progressing east to west.

Table 12. AVERAGE TIDAL AMPLITUDE (CM) IN THE ROSS AND WEDDELL SEAS: (range shown in parentheses).

Zone	Type	Ross Sea	Weddell Sea
A	Semi-Diurnal	10.1 (10.5 - 9.7)	91.9 (101.5 - 73.9)
	Diurnal	46.2 (48.2 - 43.9)	47.2 (48.8 - 42.9)
B	Semi-Diurnal	13.4 (14.3 - 11.3)	107.3 (121.1 - 101.6)
	Diurnal	50.9 (52.6 - 48.2)	44.8 (49.6 - 42.7)
C	Semi-Diurnal	13.4 (14.9 - 14.5)	145.7 (171.5 - 123.9)
	Diurnal	60.0 (70.9 - 52.6)	55.3 (59.3 - 50.3)
Total A - C	Semi-Diurnal	12.3 (9.7 - 14.9)	114.0 (101.5 - 73.9)
	Diurnal	53.7 (43.9 - 70.9)	49.1 (42.7 - 59.3)
D	Semi-Diurnal	7.1 (5.4 - 9.1)	no data available
	Diurnal	40.7 (34.6 - 54.4)	no data available

Table 13. TIDAL PHASE COMPARISONS BETWEEN THE ROSS AND WEDDELL SEAS

Semi-Diurnal		Cotidal Wave Orientation to Barrier	Basin Relation to Amphidromic Point
M_2	Ross	parallel	> 1000km
	Weddell	propagating E→W	> 1000km
S_2	Ross	propagating E→W	> 1000km
	Weddell	parallel	> 1000km
N_2	Ross	propagating E→W	≪ 1000km
	Weddell	propagating E→W	> 1000km
K_2	Ross	propagating E→W	≪ 1000km
	Weddell	propagating E→W	> 1000km
Diurnal			
K_1	Ross	propagating E→W	≪ 1000km
	Weddell	parallel	> 1000km
O_1	Ross	propagating E→W	≪ 1000km
	Weddell	parallel	> 1000km
P_1	Ross	propagating E→W	≪ 1000km
	Weddell	propagating E→W	> 1000km
Q_1	Ross	propagating E→W	≪ 1000km
	Weddell	propagating E→W	> 1000km

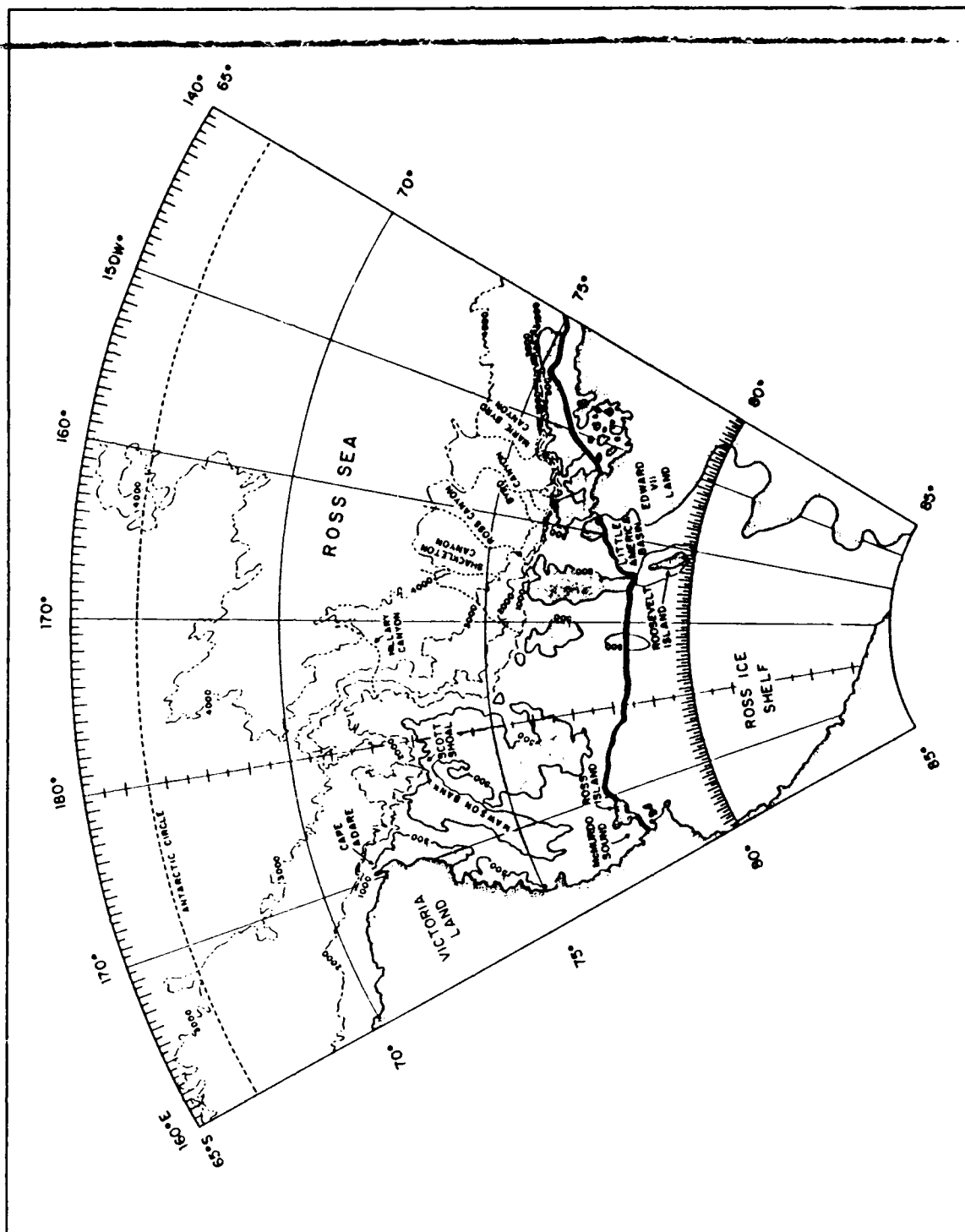


Figure 28. Continental shelf bathymetry for the Ross Sea (shaded areas represent shelf depths < 500 m).

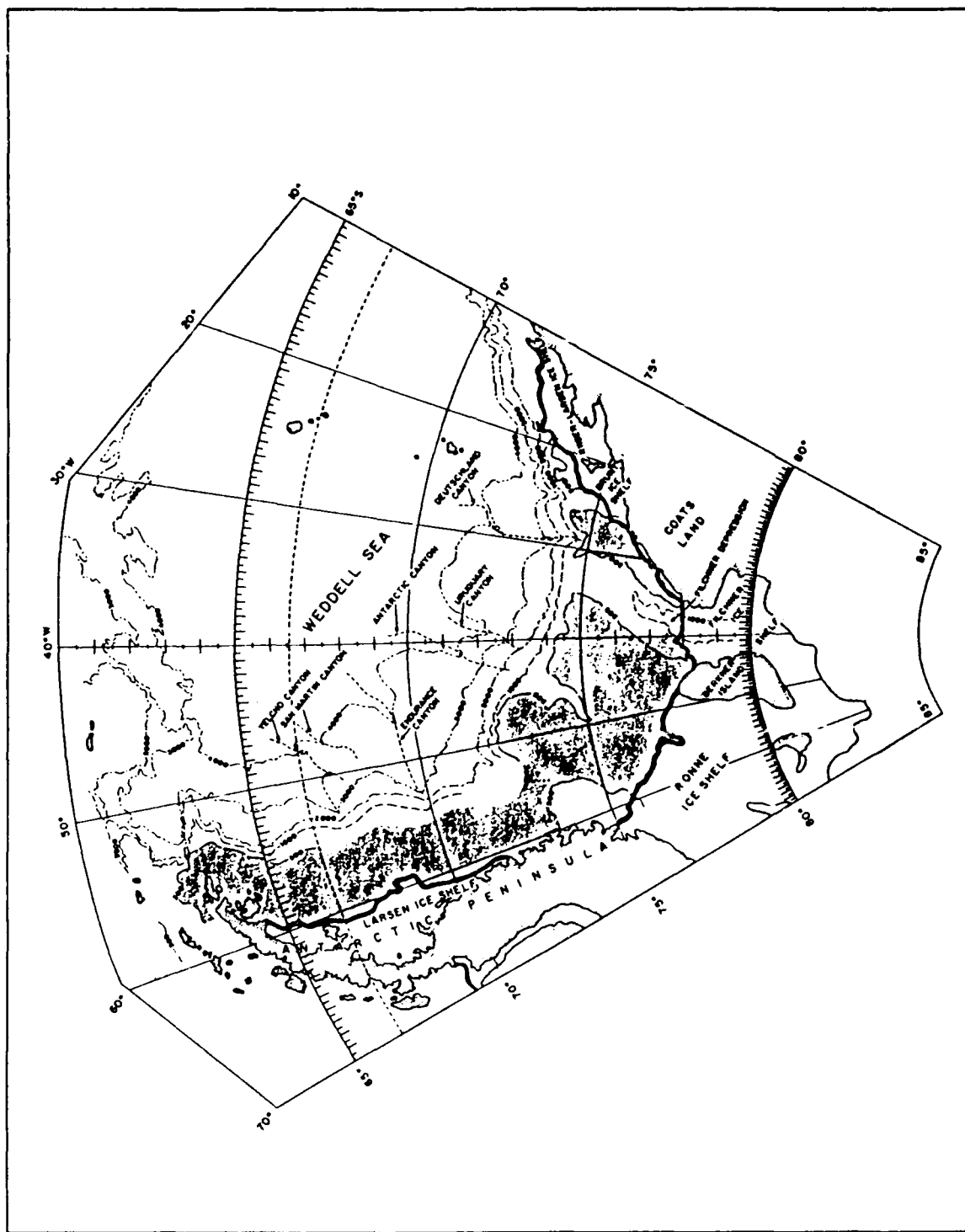


Figure 29. Continental shelf bathymetry for the Weddell Sea (shaded areas represent shelf depths < 500 m).

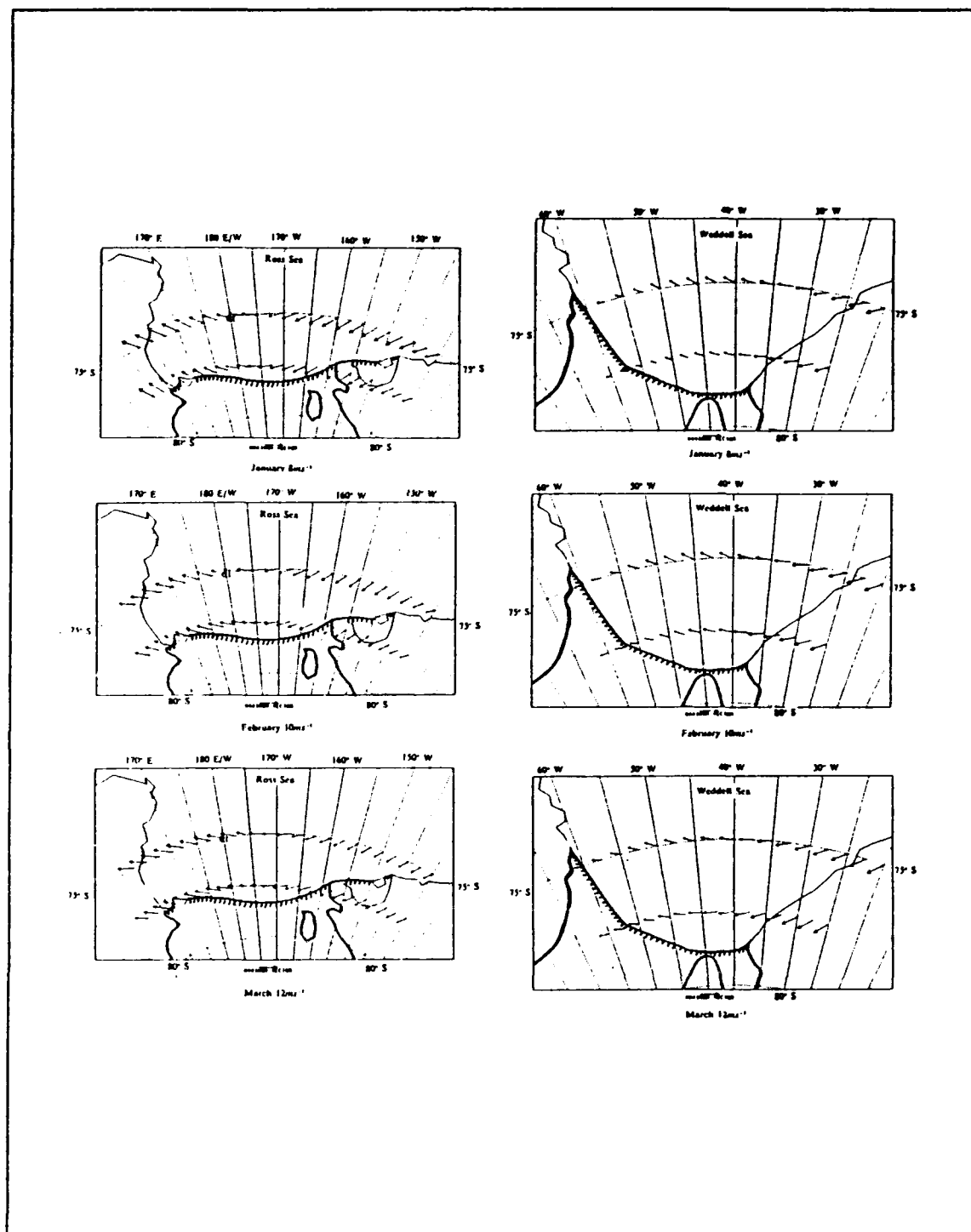


Figure 30. Climatological surface wind velocities in the Ross and Weddell Seas for January through March. Note: Monthly vector lengths were scaled with the longest vector indicating the maximum speed for that month.

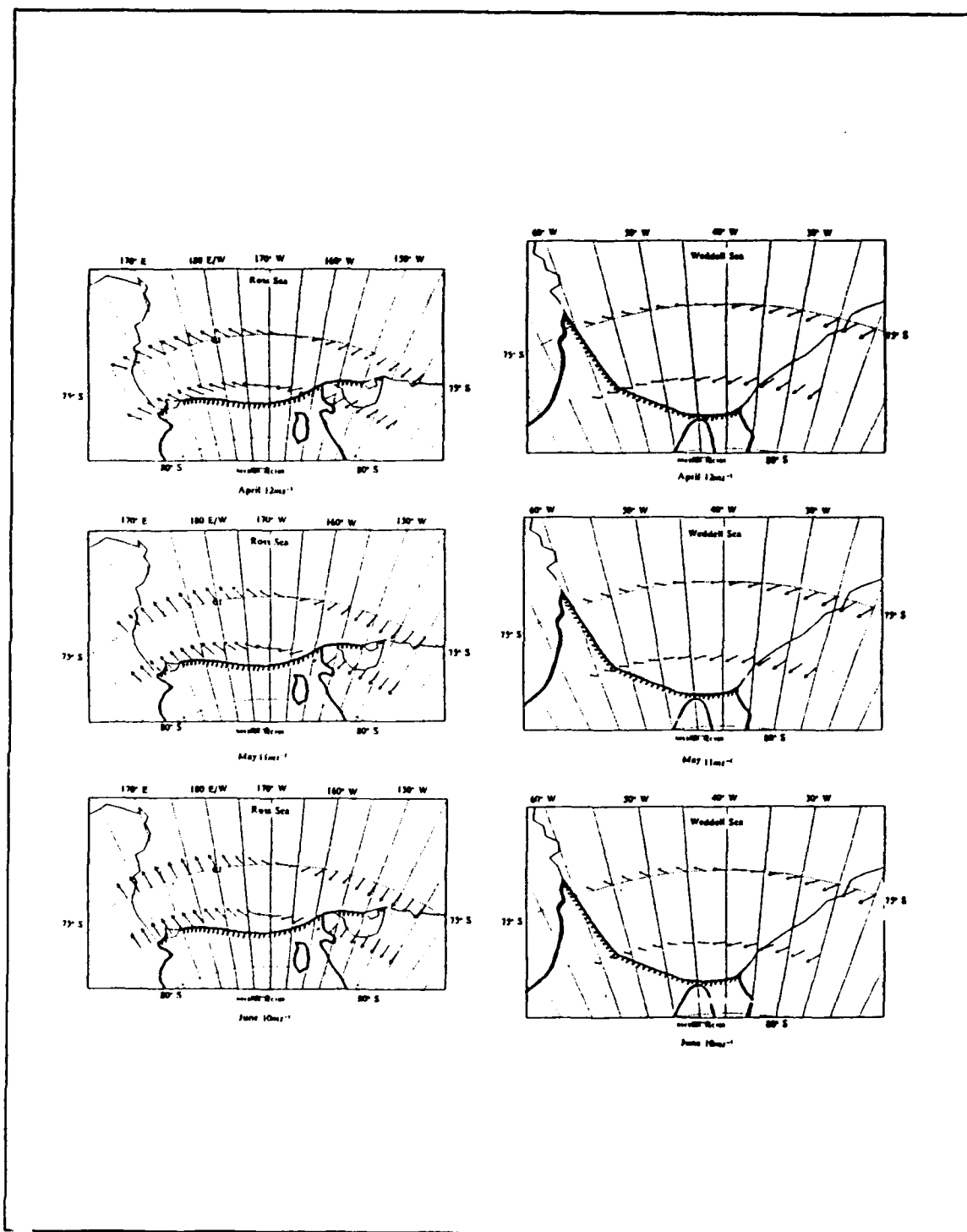


Figure 31. Climatological surface wind velocities in the Ross and Weddell Seas for April through June. Note: Monthly vector lengths were scaled with the longest vector indicating the maximum speed for that month.

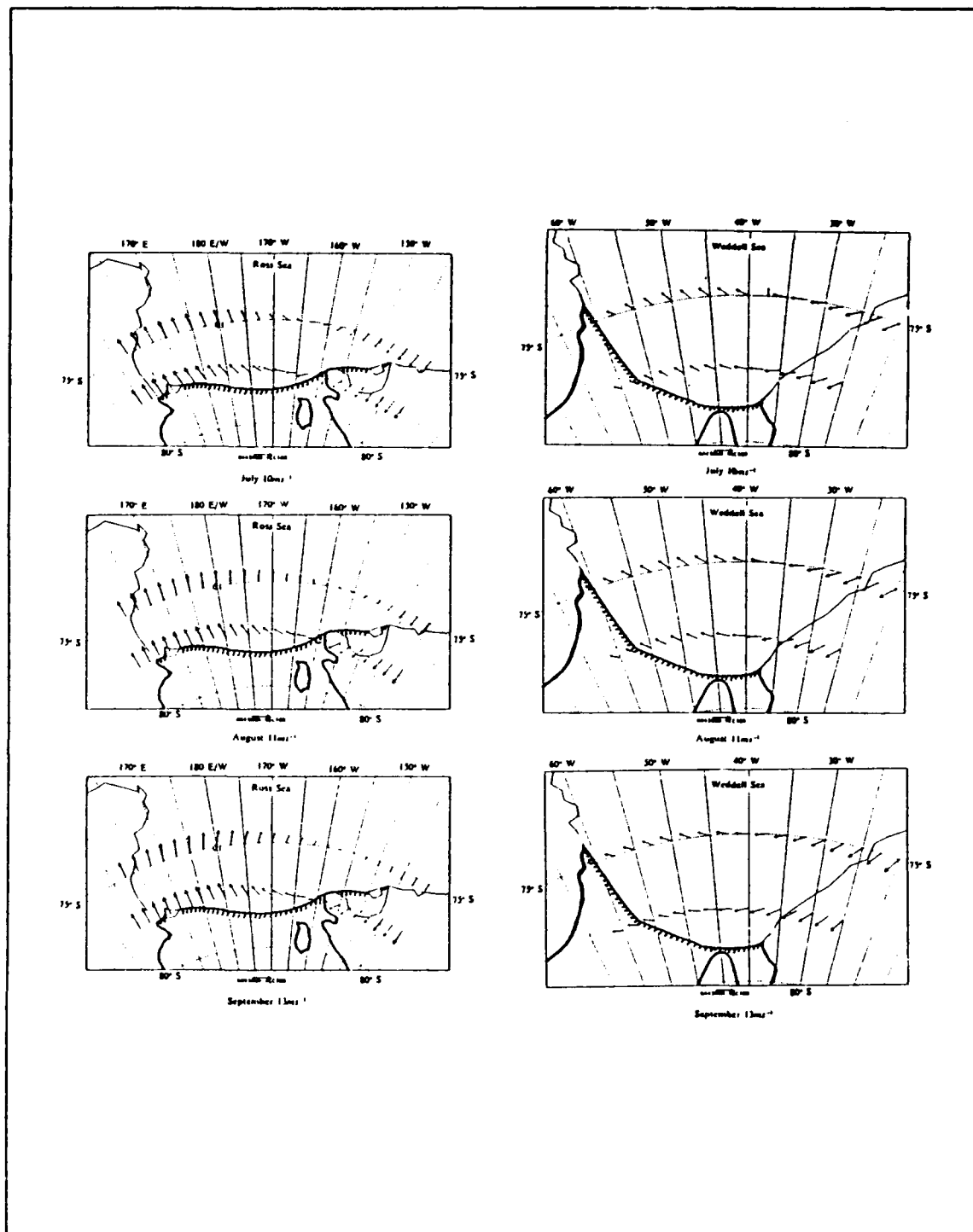


Figure 32. Climatological surface wind velocities in the Ross and Weddell Seas for July through September. Note: Monthly vector lengths were scaled with the longest vector indicating the maximum speed for that month.

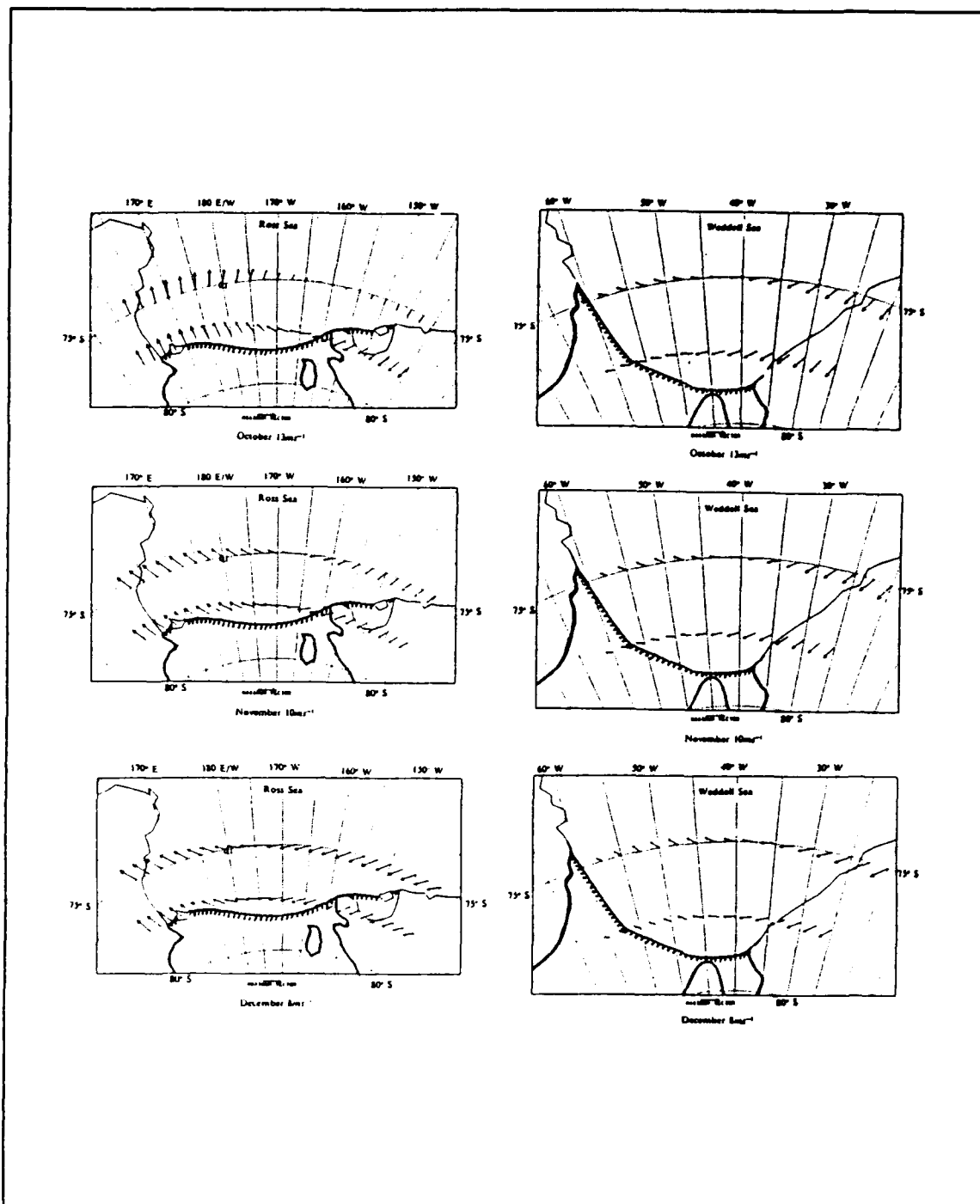


Figure 33. Climatological surface wind velocities in the Ross and Weddell Seas for October through December. Note: Monthly vector lengths were scaled with the longest vector indicating the maximum speed for that month.

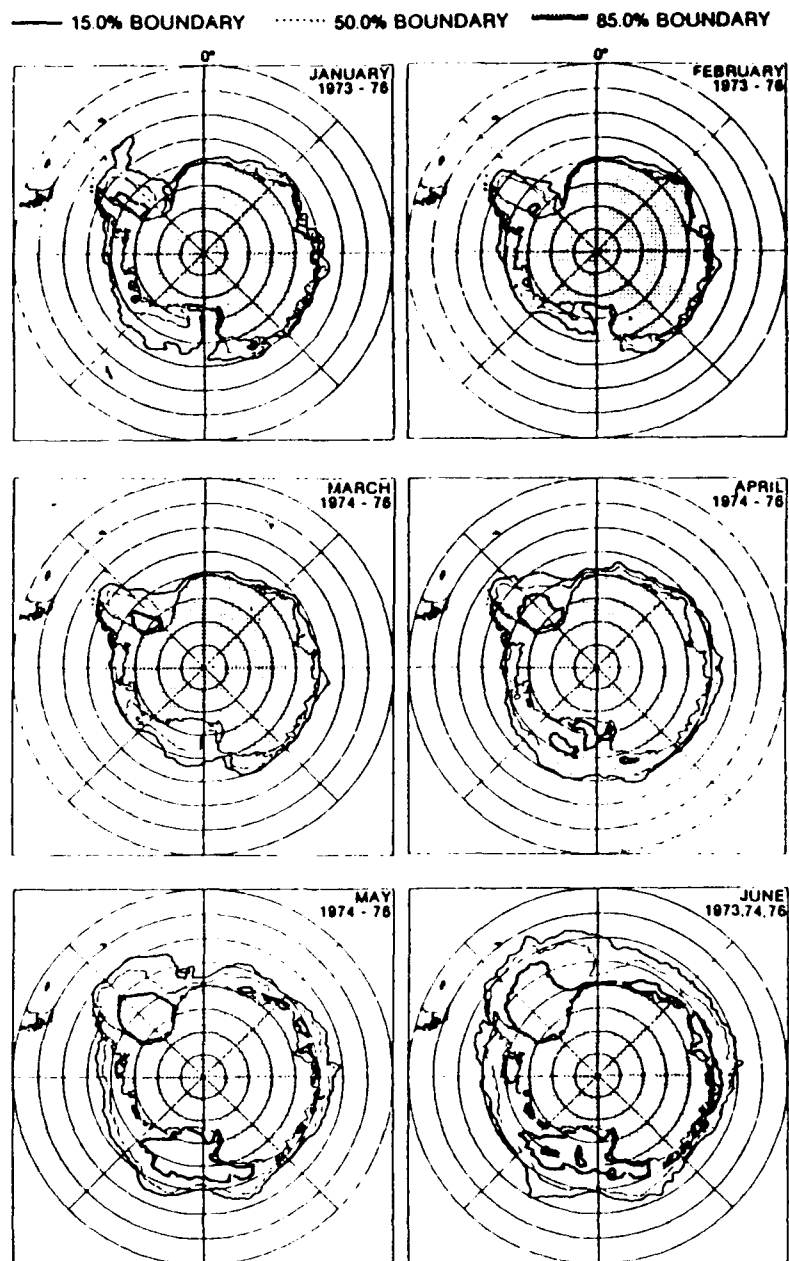


Figure 34. Mean monthly ice concentration contours for January to June for 15, 50, and 85 % levels. Note: Contours averaged for years indicated (after NASA, 1983).

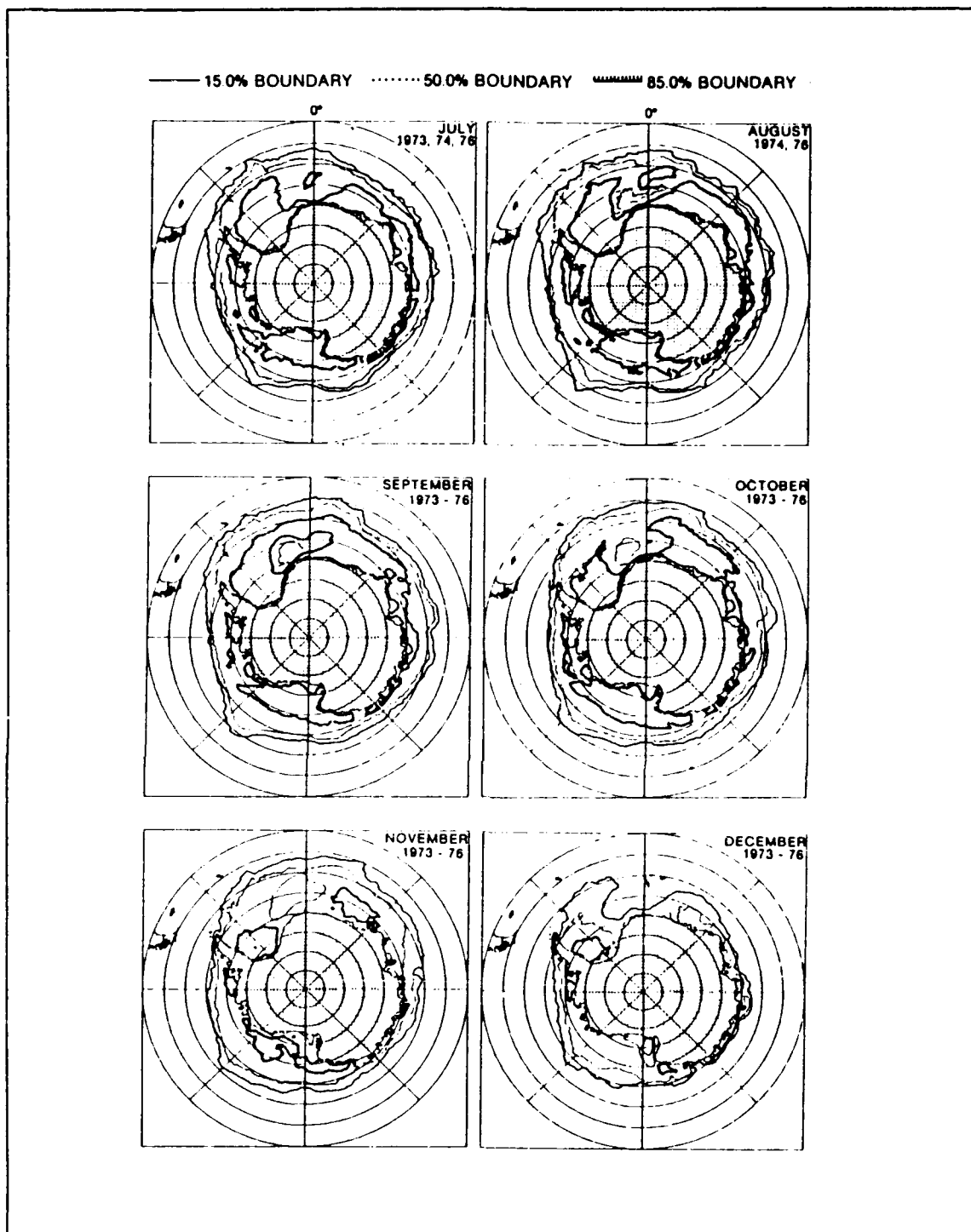


Figure 35. Mean monthly ice concentration contours for July to December for 15, 50, and 85 % levels. Note: Contours averaged for years indicated (after NASA, 1983).

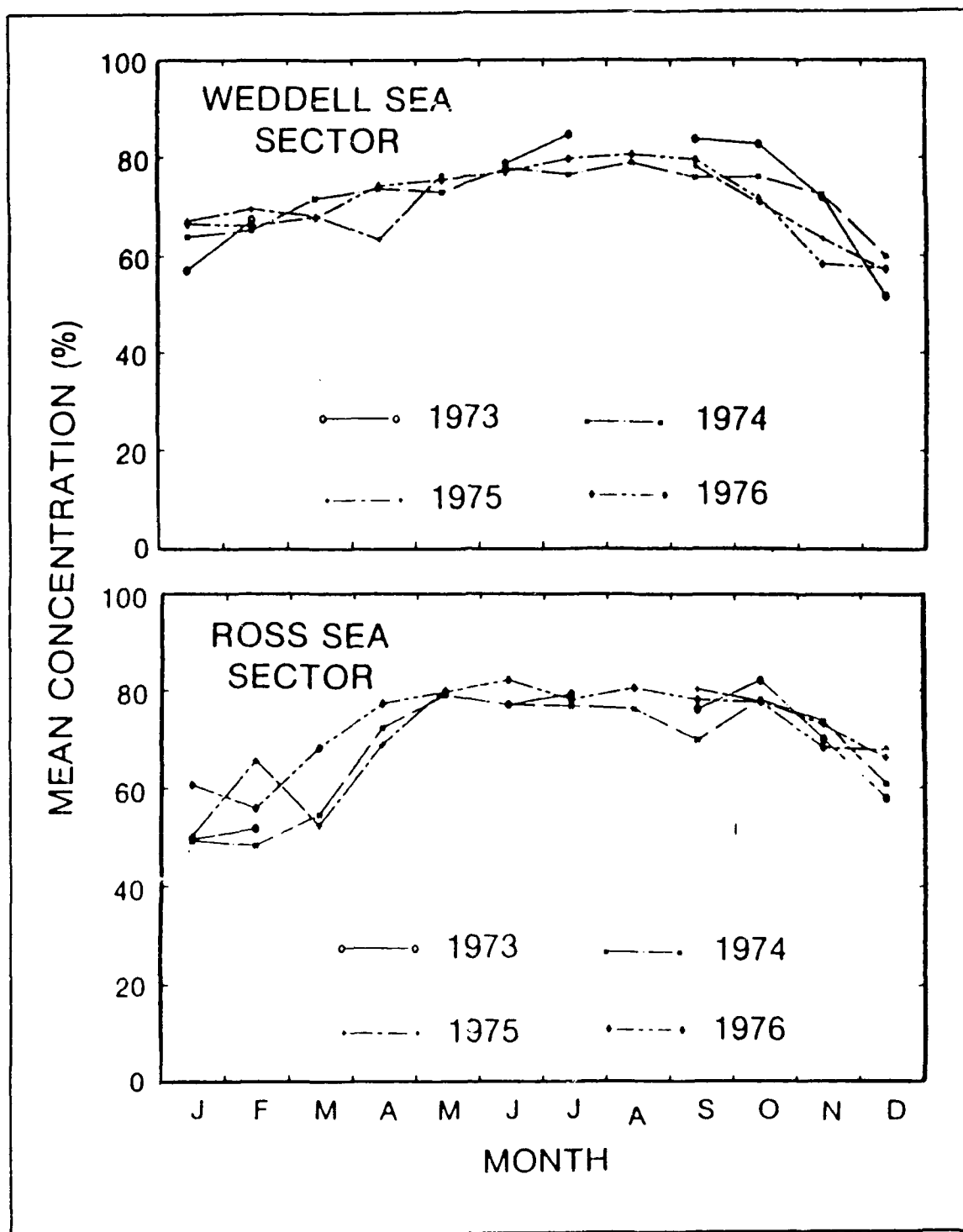


Figure 36. Yearly cycle of area covered by sea ice in the Ross and Weddell Seas (modification of NASA, 1983).

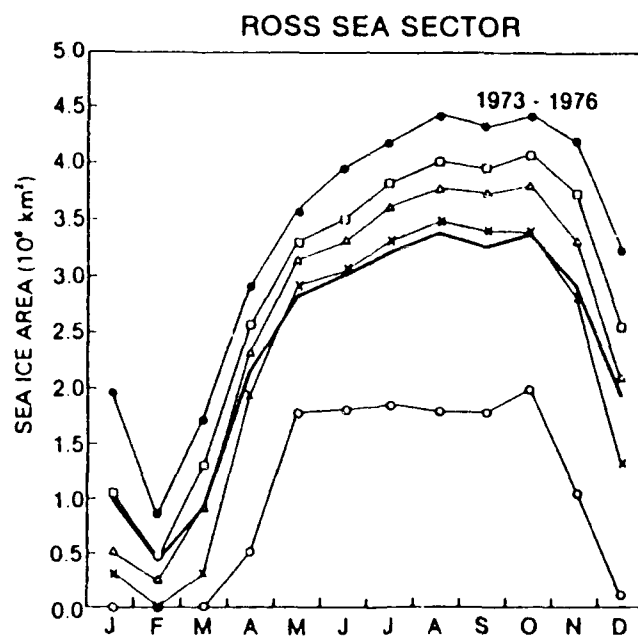
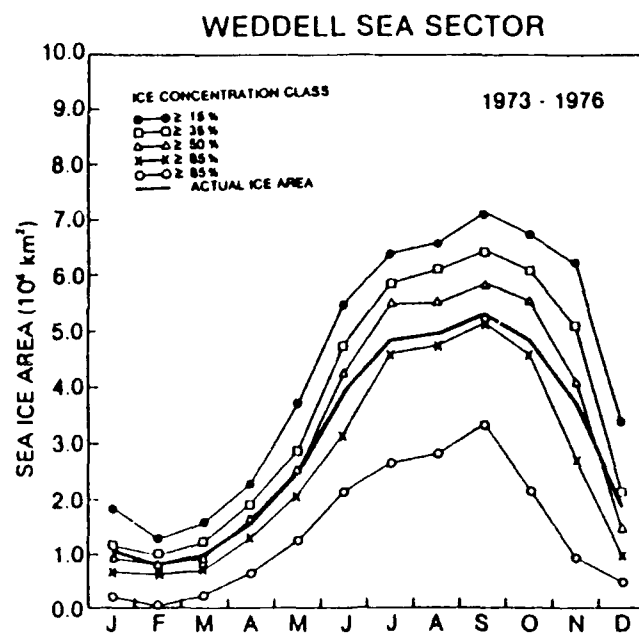


Figure 37. Interannual variation of mean sea ice concentration in the Ross and Weddell Seas (modification of NASA, 1983).

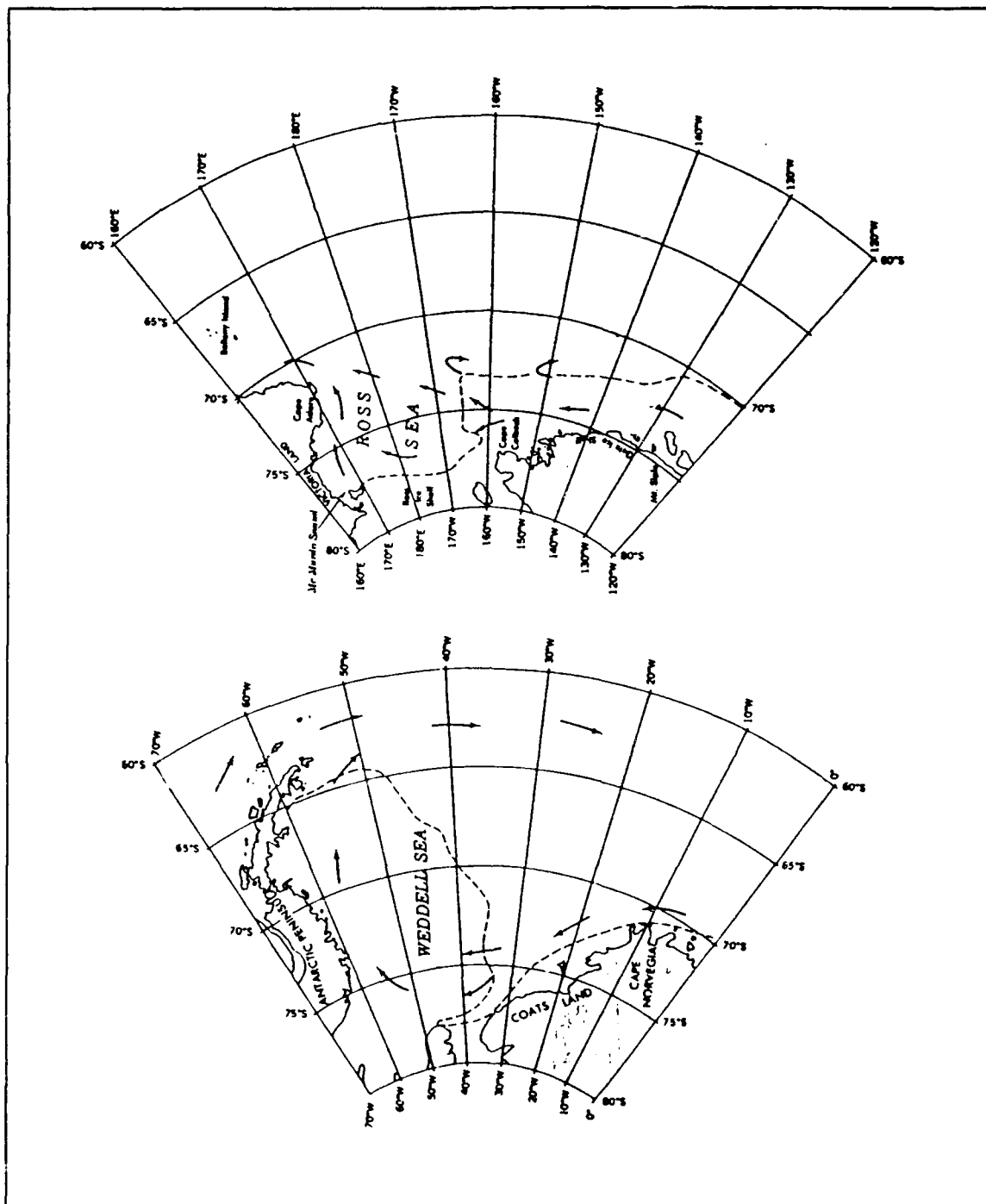


Figure 38. Mean summer surface circulation for the Ross and Weddell Seas based on the Southern Ocean Atlas Observed Data Set (SOAODS). Note: Typical mid-summer 7/10 ice concentration limit is shown as a dashed line (after DMA, 1985).

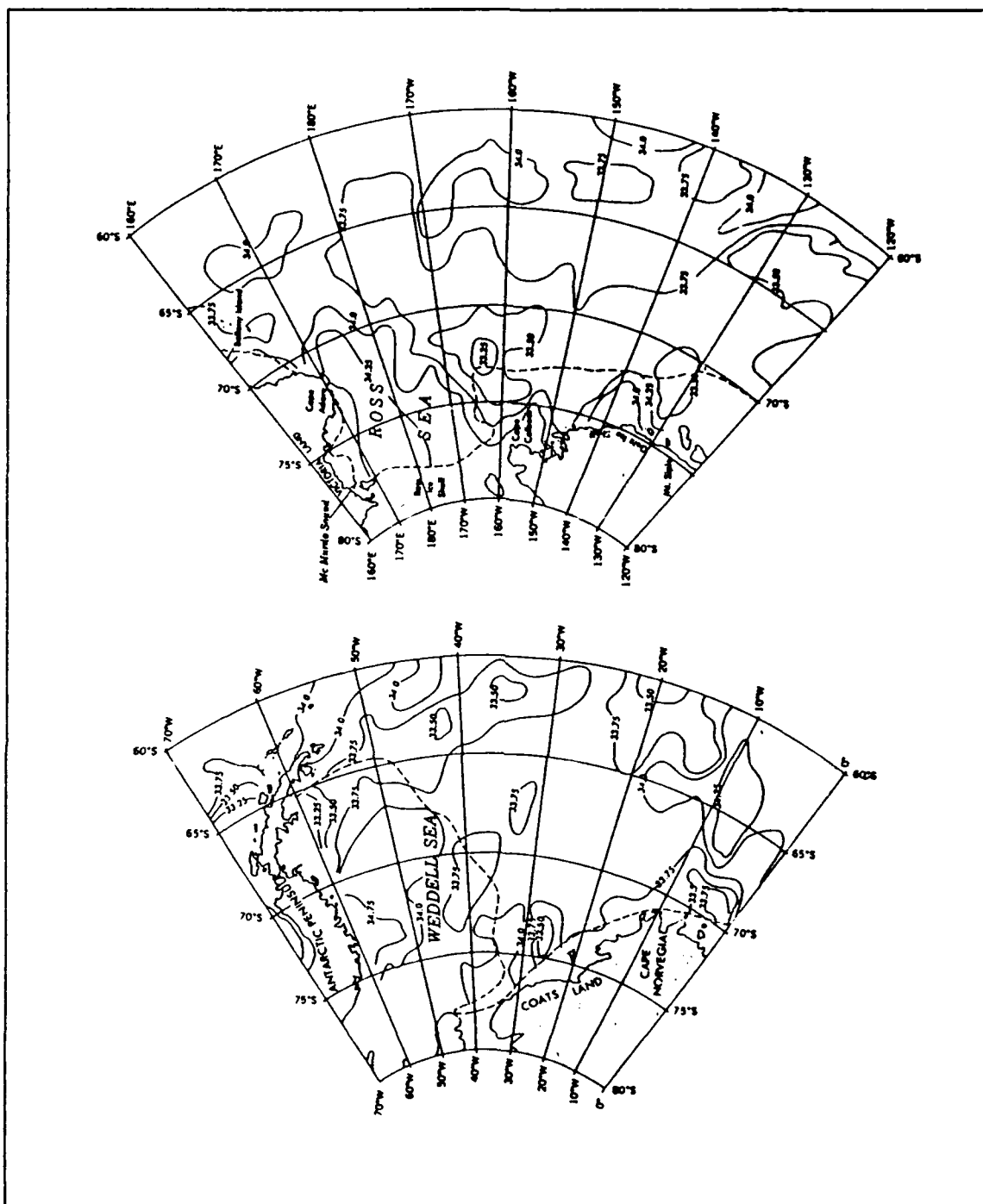


Figure 39. Mean summer surface salinities for the Ross and Weddell Seas based on the Southern Ocean Atlas Observed Data Set (SOAODS). Note: Typical mid-summer 7/10 ice concentration limit is shown as a dashed line (after DMA, 1985).

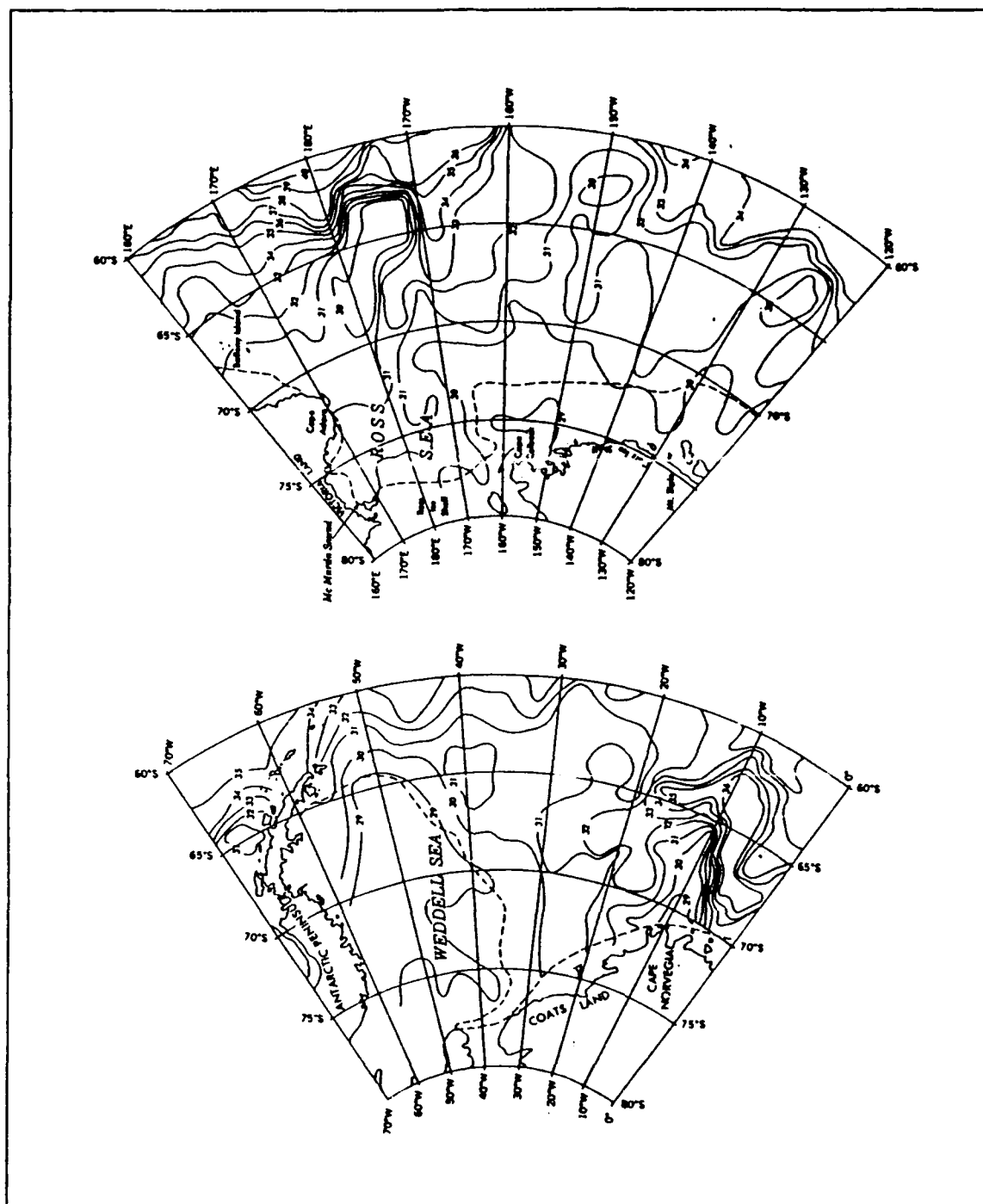


Figure 40. Mean summer sea surface temperature (°F) for the Ross and Weddell Seas based on the Southern Ocean Atlas Observed Data Set (SOAODS). Note: Typical mid-summer 7/10 ice concentration limit is shown as a dashed line (after DMA, 1985).

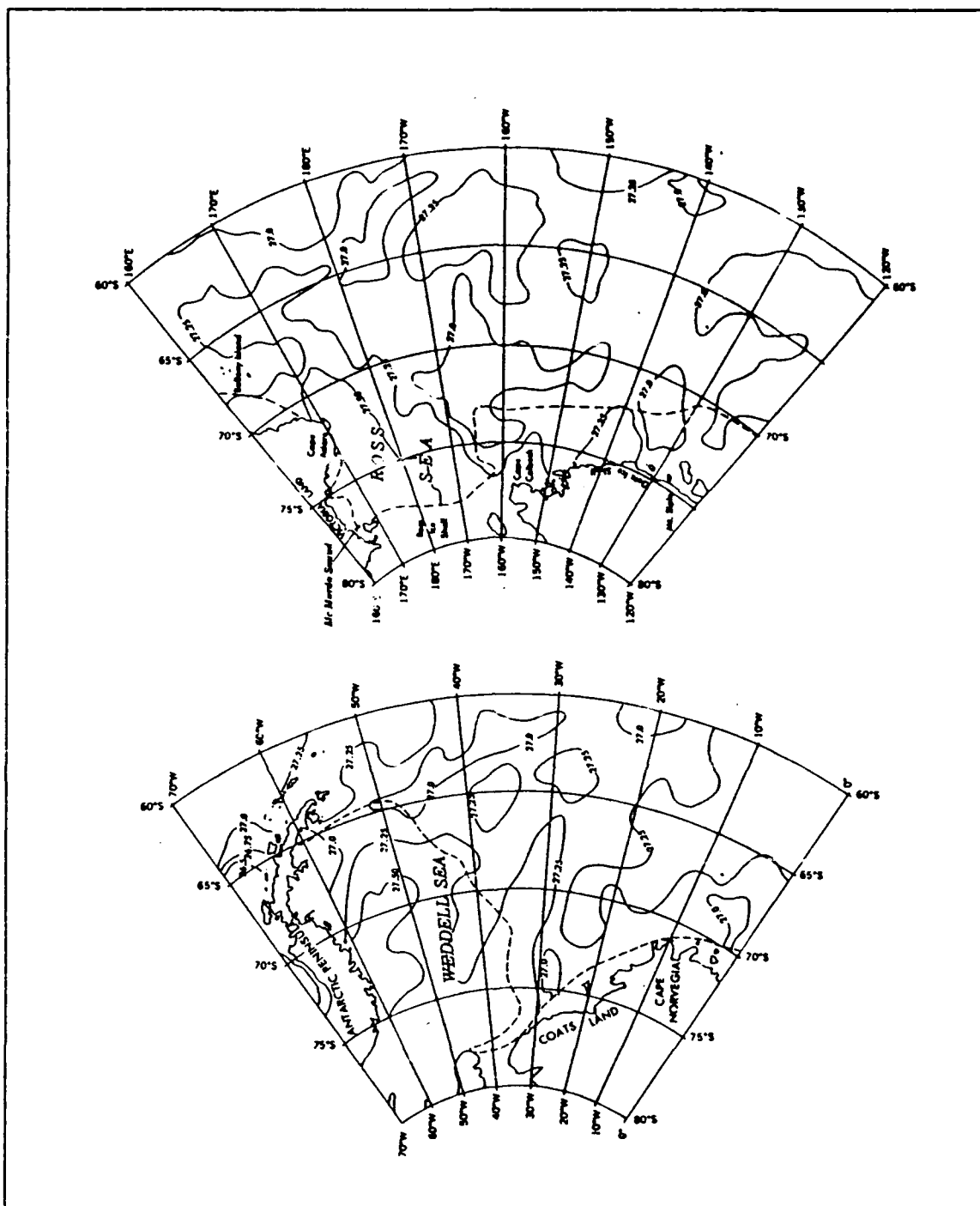


Figure 41. Mean summer sea surface densities (σ_t) for the Ross and Weddell Seas based on the Southern Ocean Atlas Observed Data Set (SOAODS). Note: Typical mid-summer 7/10 ice concentration limit is shown as a dashed line (after DMA, 1985).

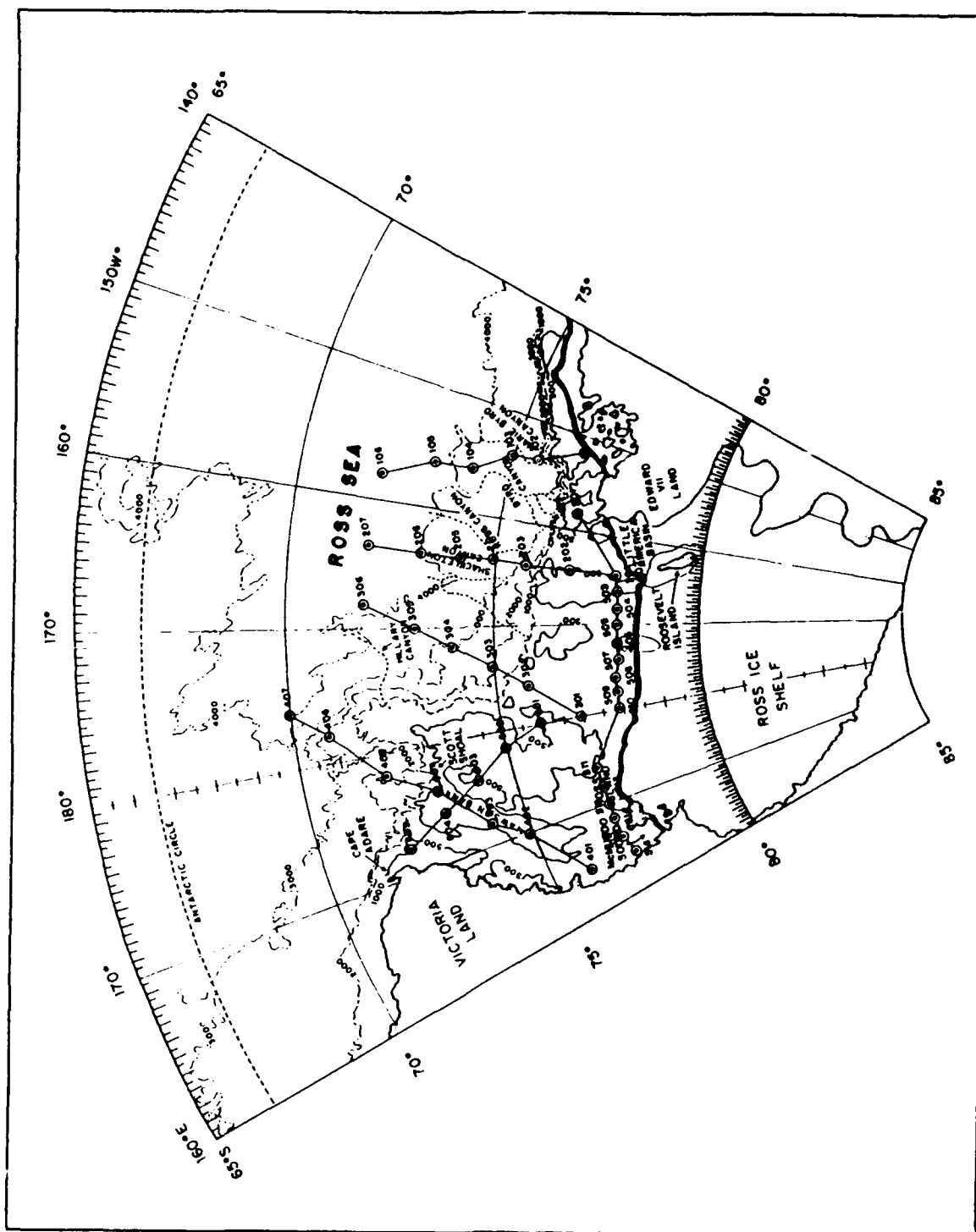


Figure 42. Hydrographic station locator map shown for the Ross Sea. Note: The transect number is indicated by the first digit in the station number. Shaded areas represent shelf depths < 500 m.

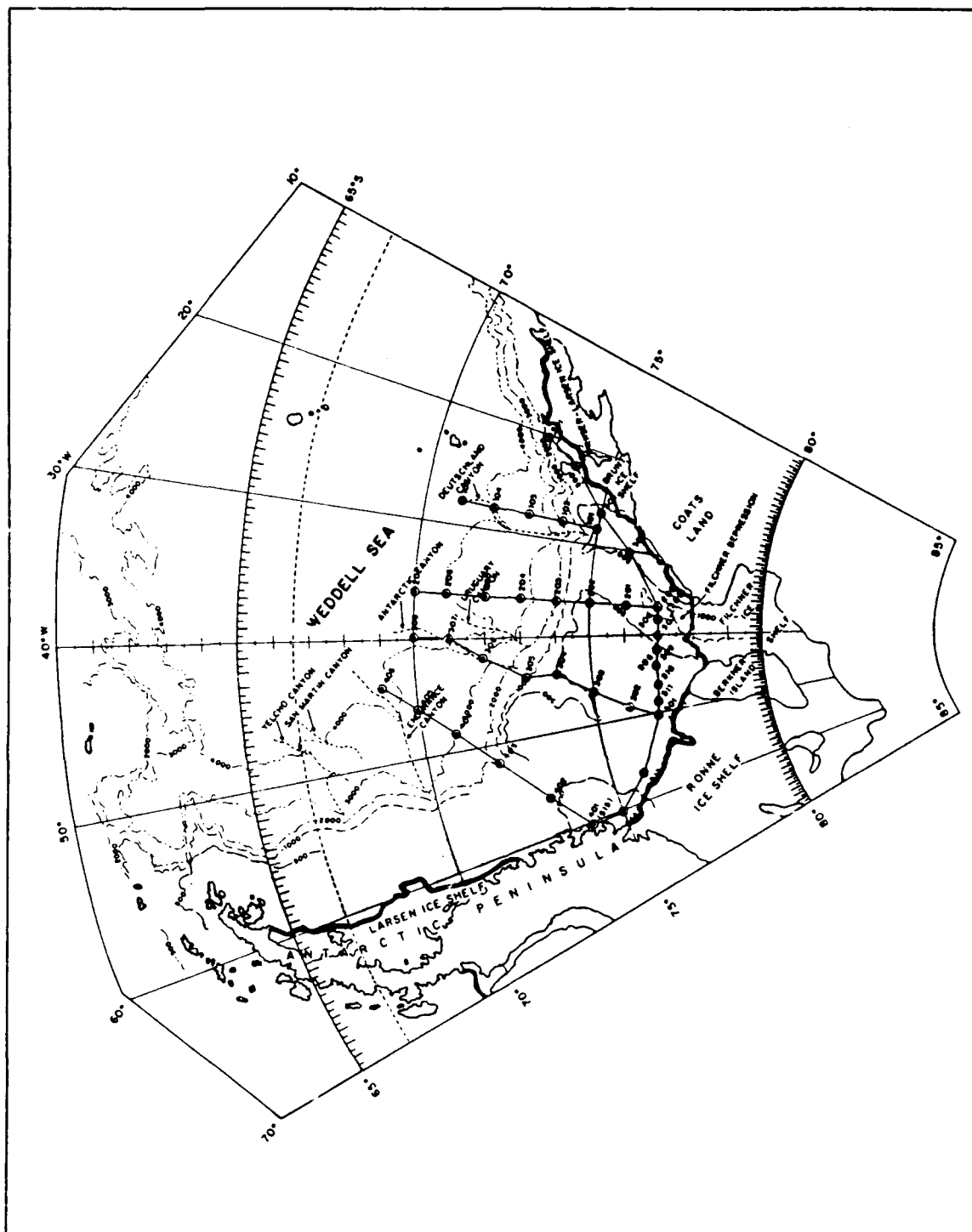
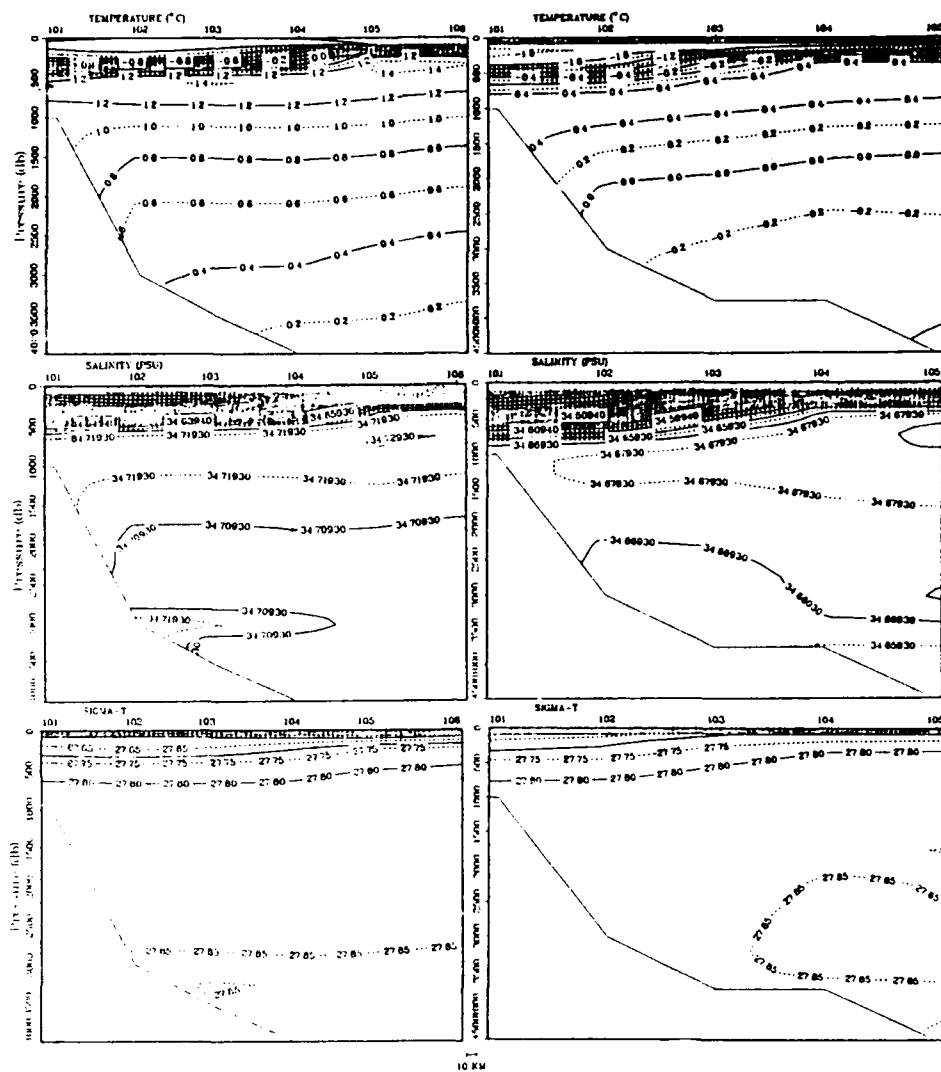


Figure 43. Hydrographic station locator map shown for the Weddell Sea
 Note: The transect number is indicated by the first digit in the station number. Shaded areas represent shelf depths < 500 m.



Ross Sea

Weddell Sea

Figure 44. Temperature, salinity, and density (sigma-t) cross-sections for Track 1 in the Ross and Weddell Seas (note vertical scale difference).

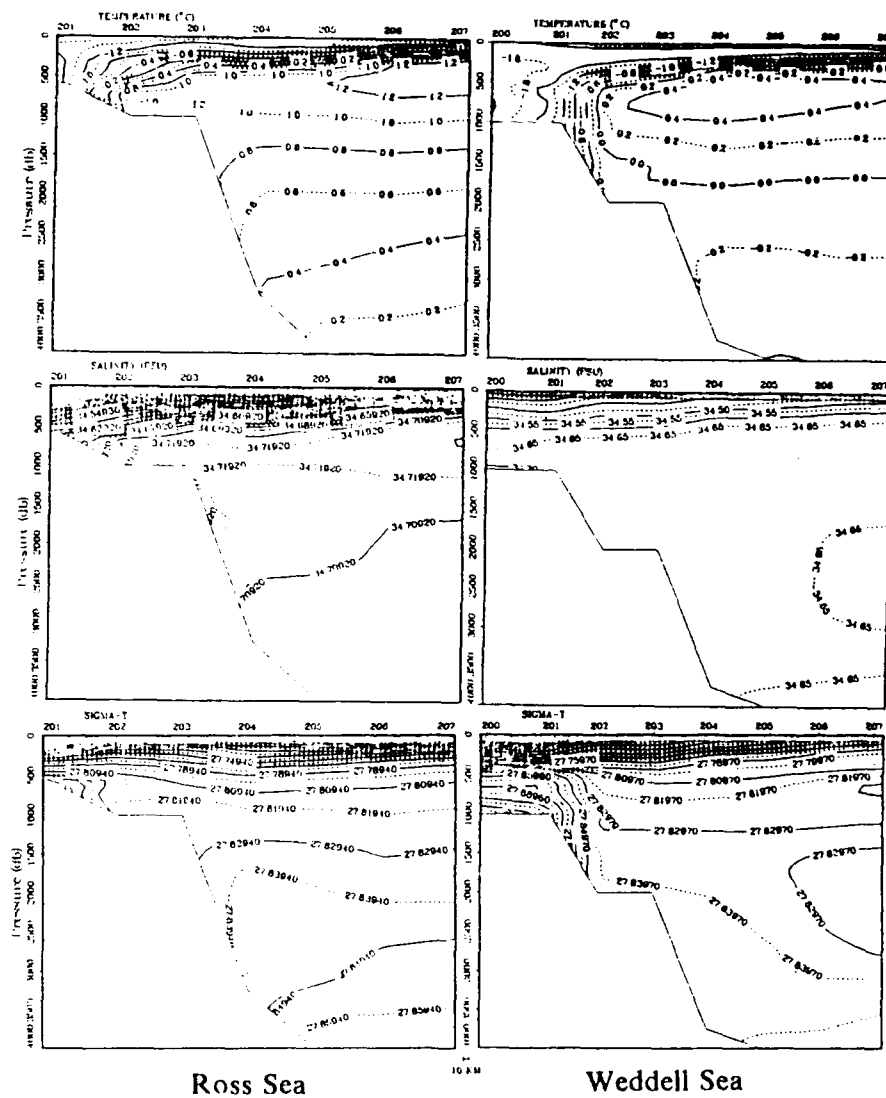


Figure 45. Temperature, salinity, and density (sigma-t) cross-sections for Track 2 in the Ross and Weddell Seas (note vertical scale difference).

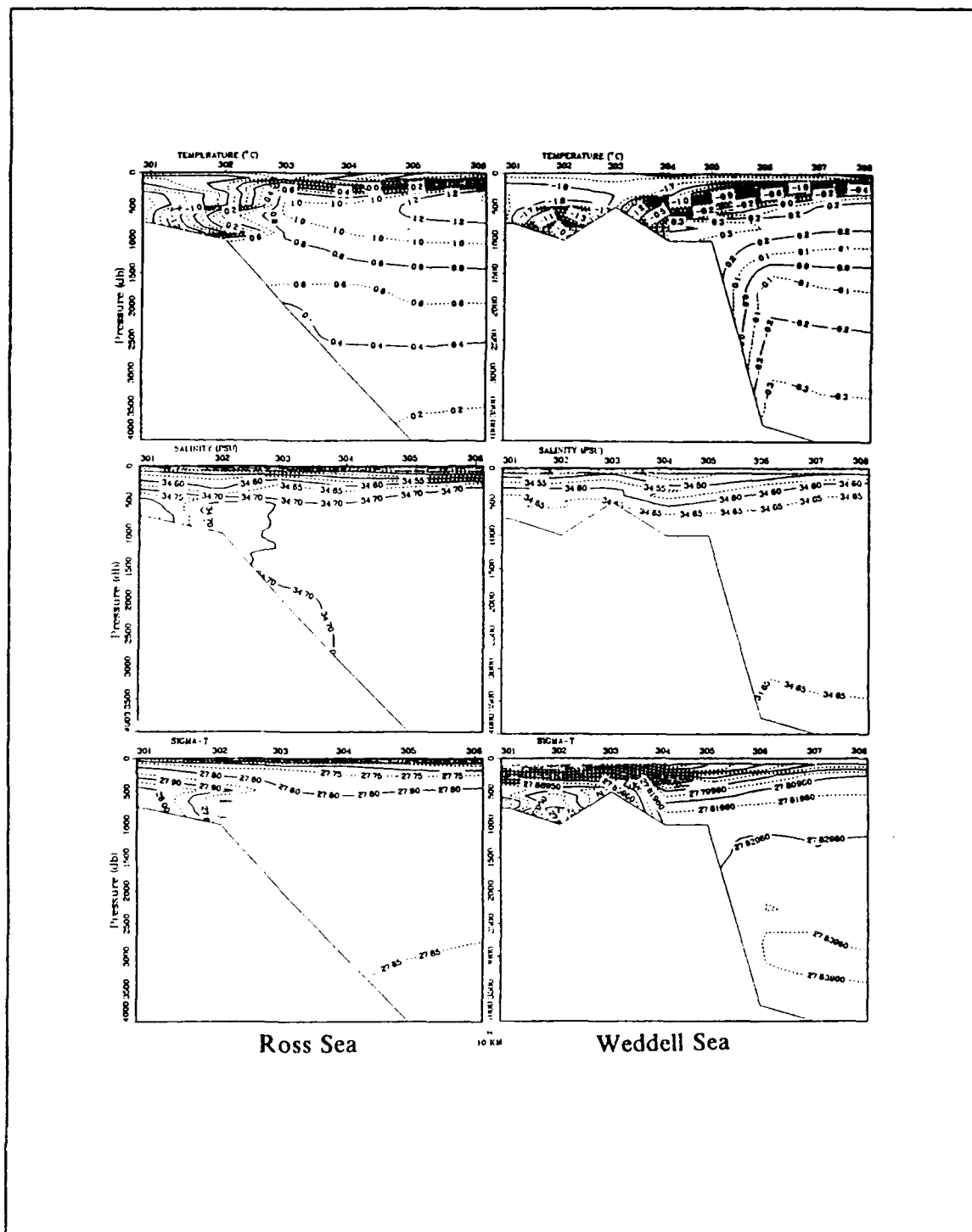


Figure 46. Temperature, salinity, and density (sigma-t) cross-sections for Track 3 in the Ross and Weddell Seas (note vertical scale difference).

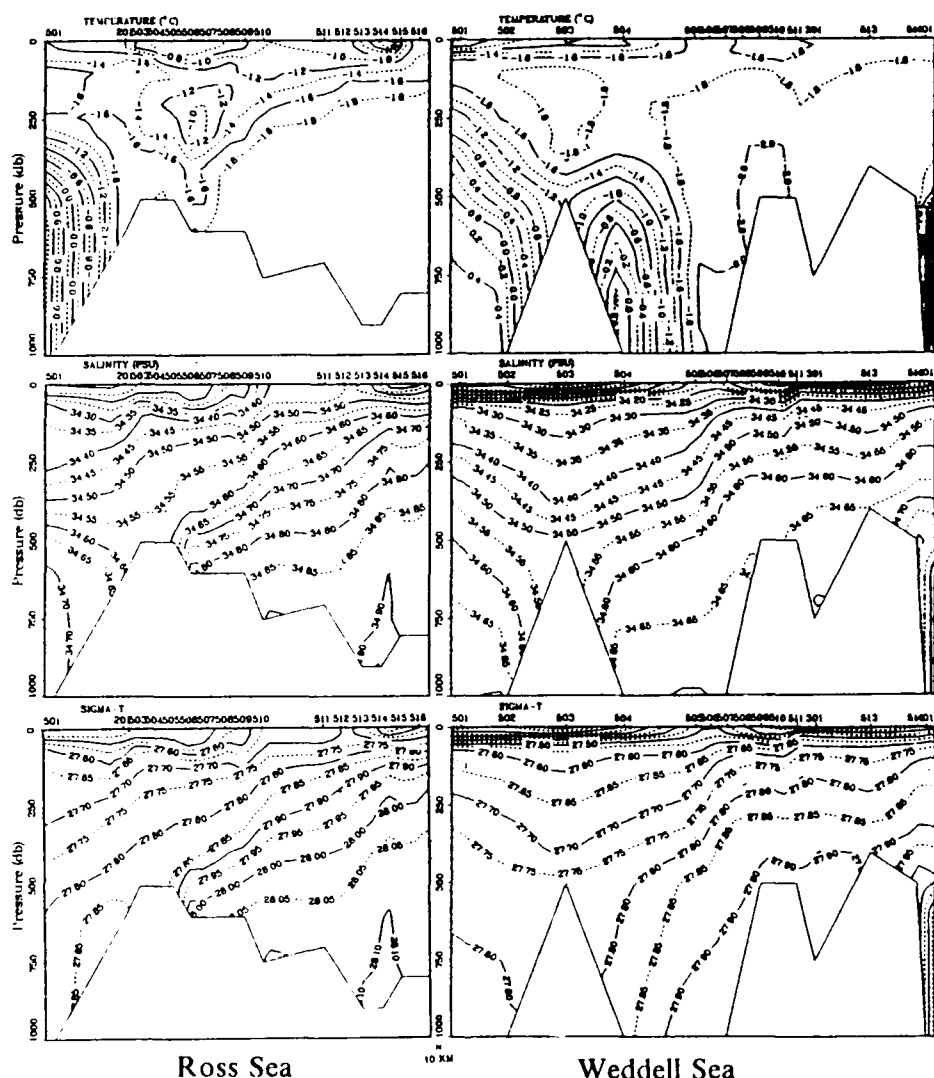


Figure 47. Temperature, salinity, and density (sigma-t) cross-sections for Track 5 in the Ross and Weddell Seas.

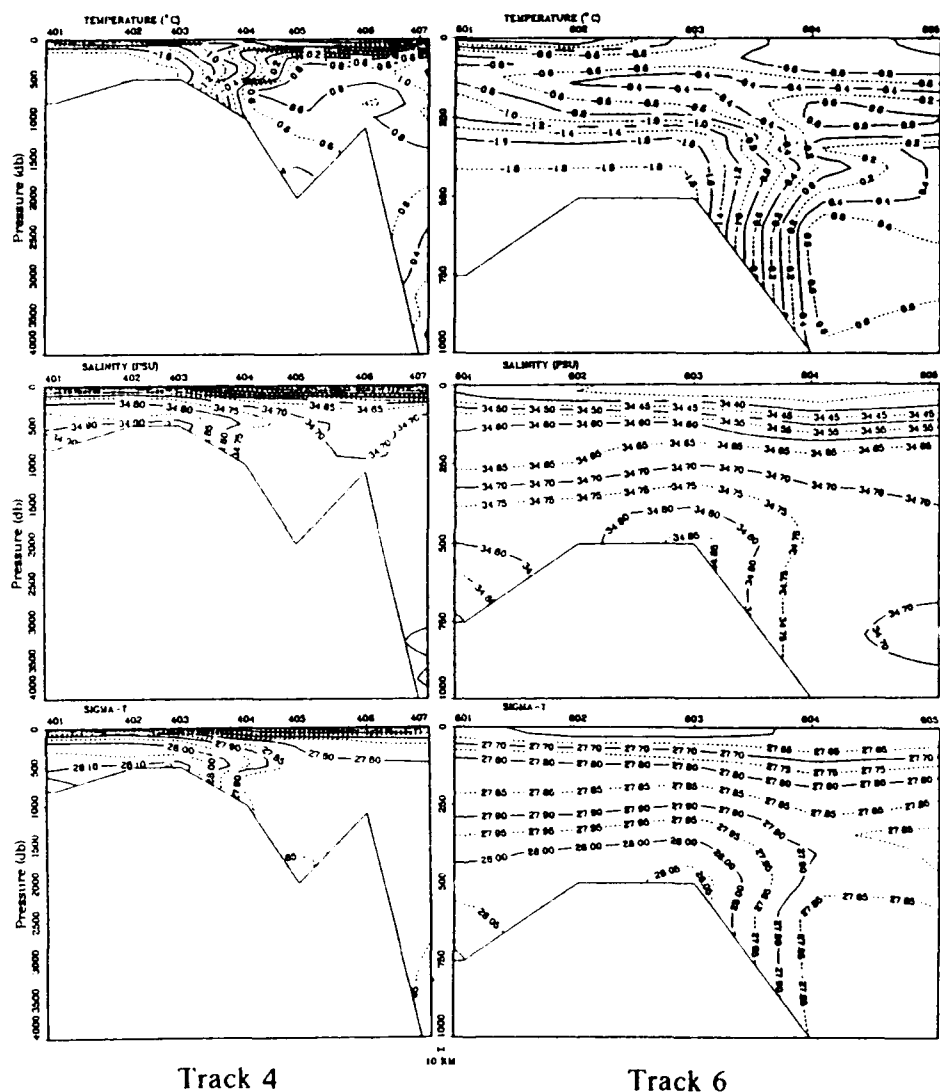


Figure 48. Temperature, salinity, and density (sigma-t) cross-sections for Tracks 4 and 6 in the Ross Sea (note vertical scale difference).

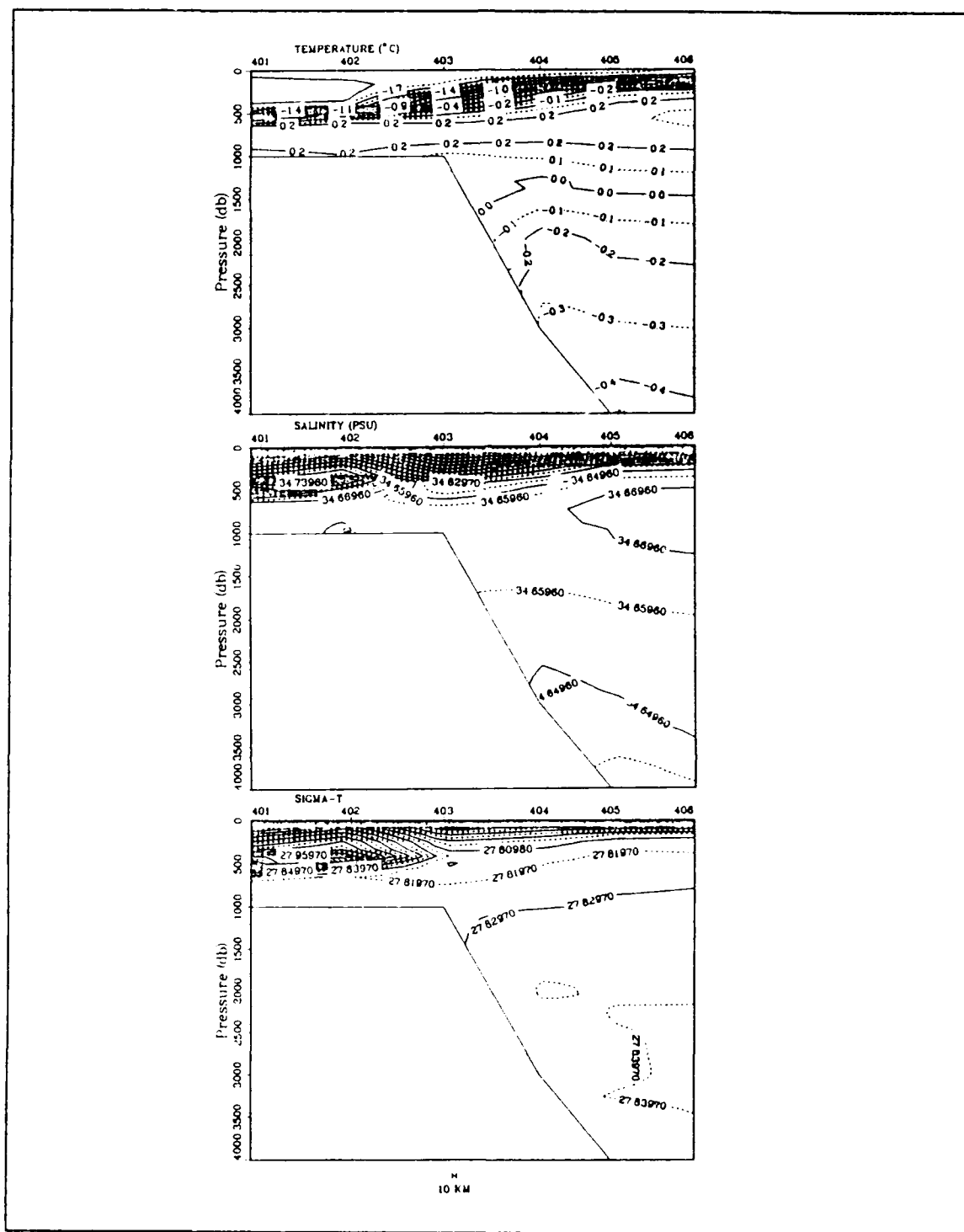


Figure 49. Temperature, salinity, and density (sigma-t) cross-sections for Track 4 in the Weddell Sea.

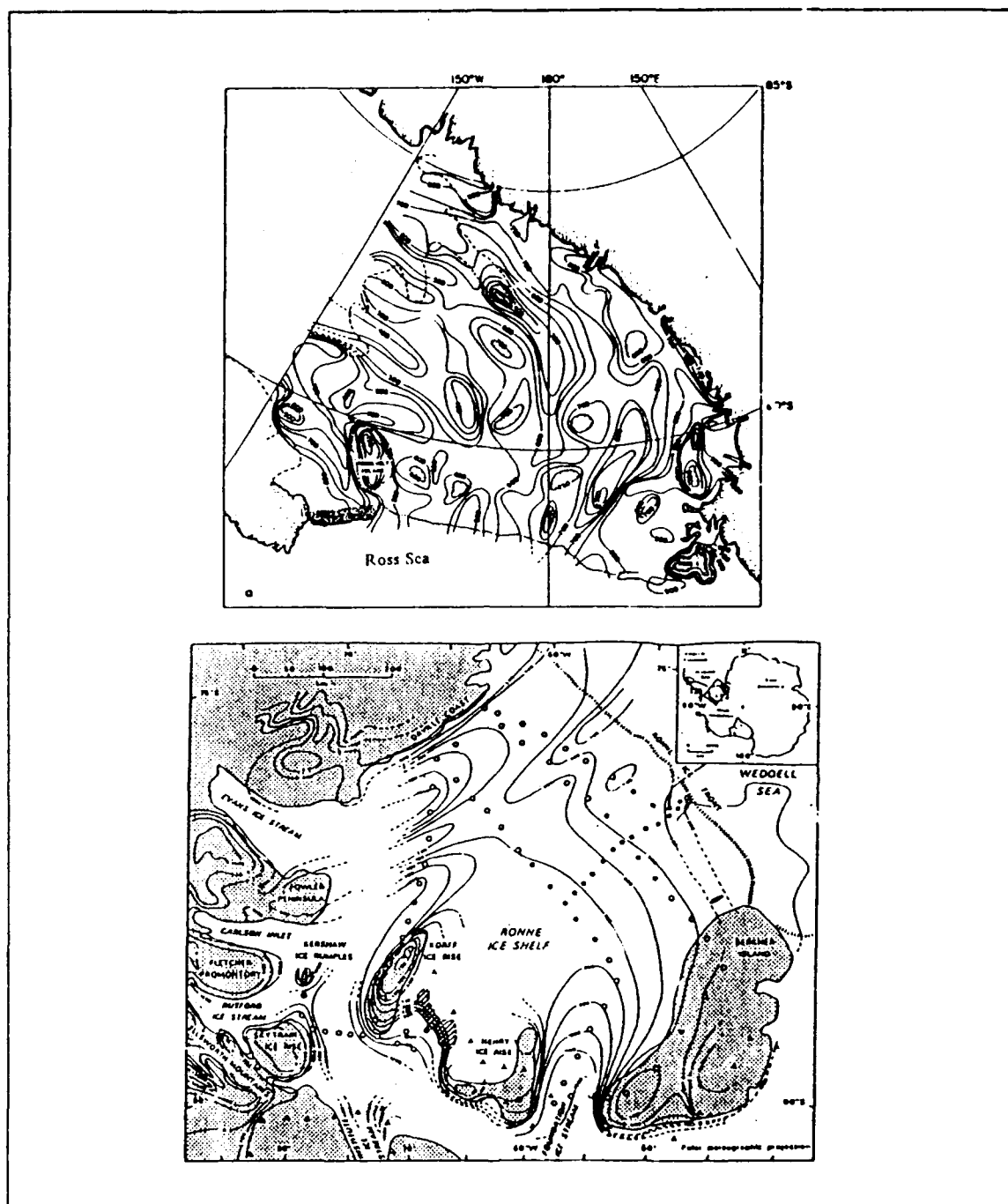


Figure 50. Contours (meters) of bottom depth for the Ross Ice Shelf (top) (after Jacobs, 1989) and the Ronne Ice shelf (bottom) (after Herrod, 1987). Note: The open and closed circles on the bottom map indicate locations where soundings were made beneath the Ronne Ice Shelf.

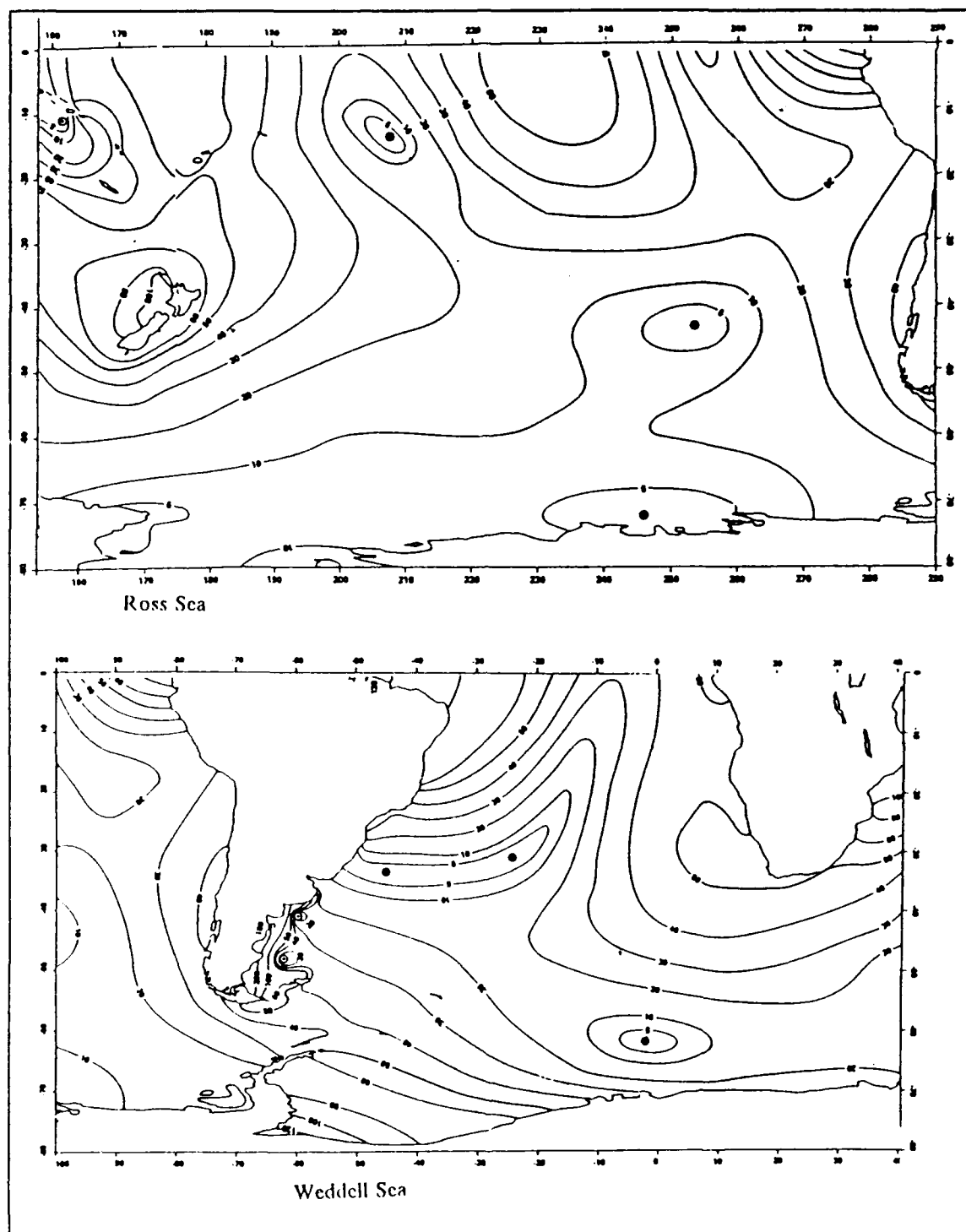


Figure 51. Semi-diurnal corange map for the Ross Sea (top) and Weddell Sea (bottom) (M_2 mode) (modification of Schwiderski, 1979).

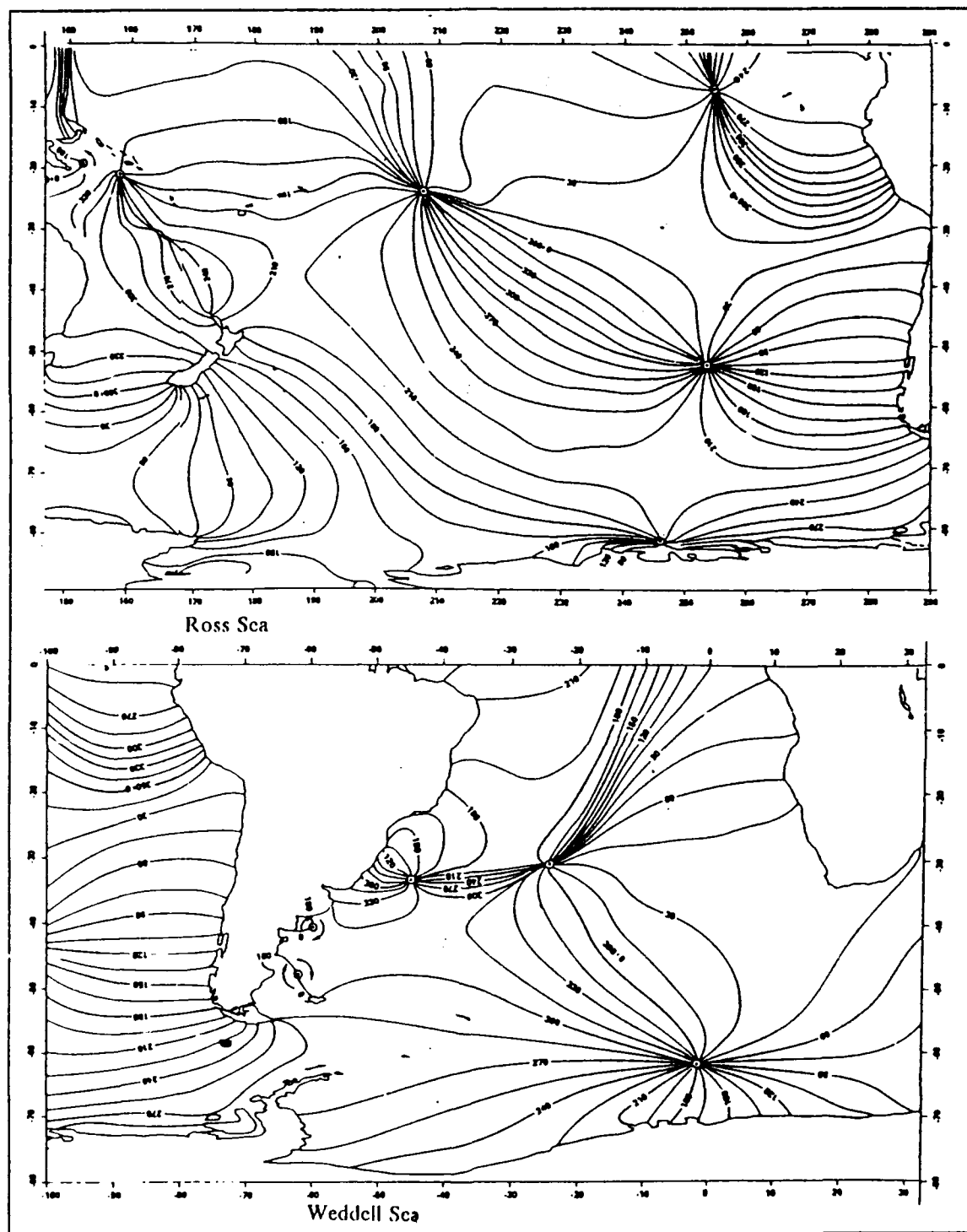


Figure 52. Semi-diurnal cotidal map for the Ross Sea (top) and Weddell Sea (bottom) (M_2 mode) (modification of Schwiderski, 1979).

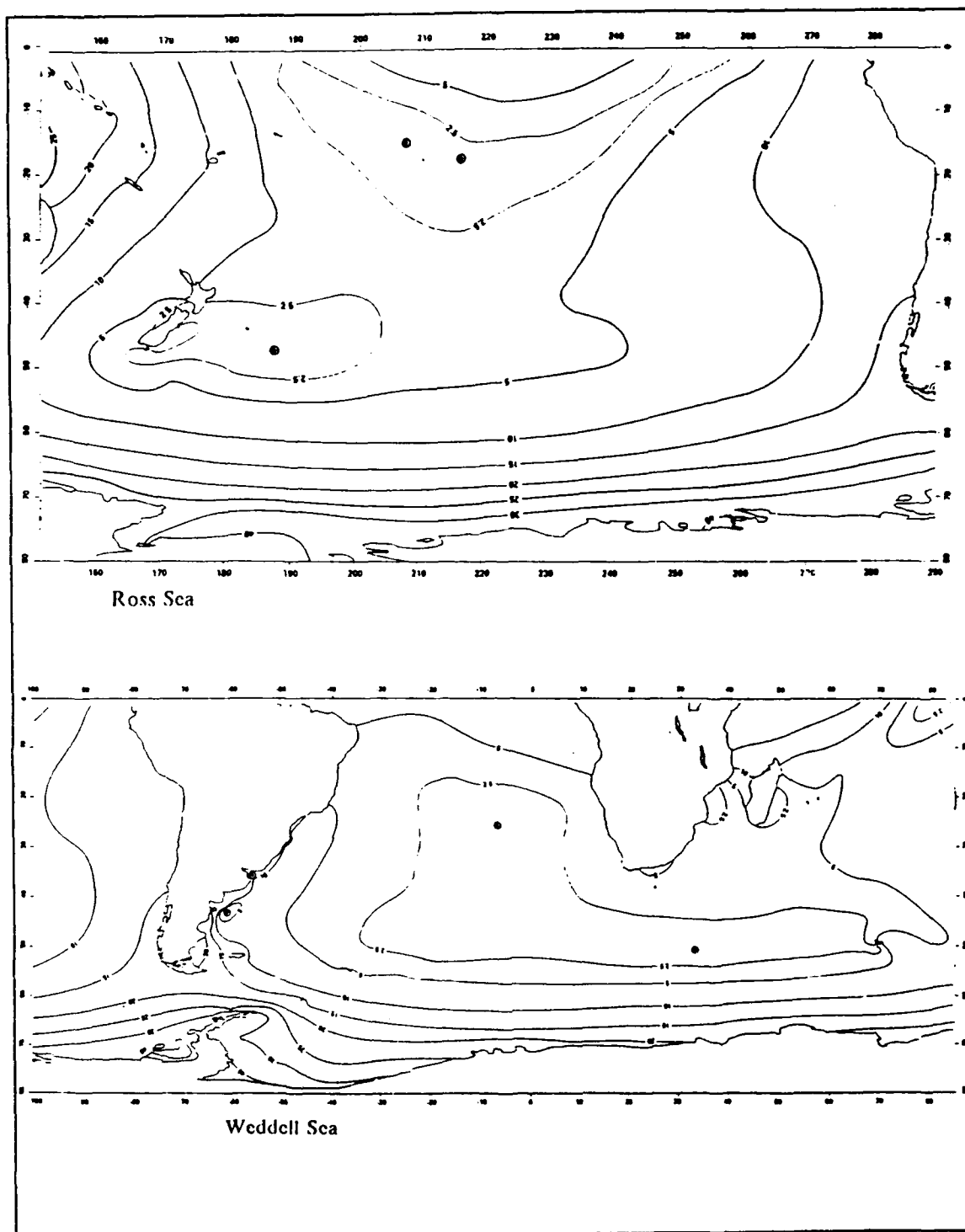


Figure 53. Diurnal corange map for the Ross Sea (top) and Weddell Sea (bottom) (K_1 mode) (modification of Schwiderski, 1981c).

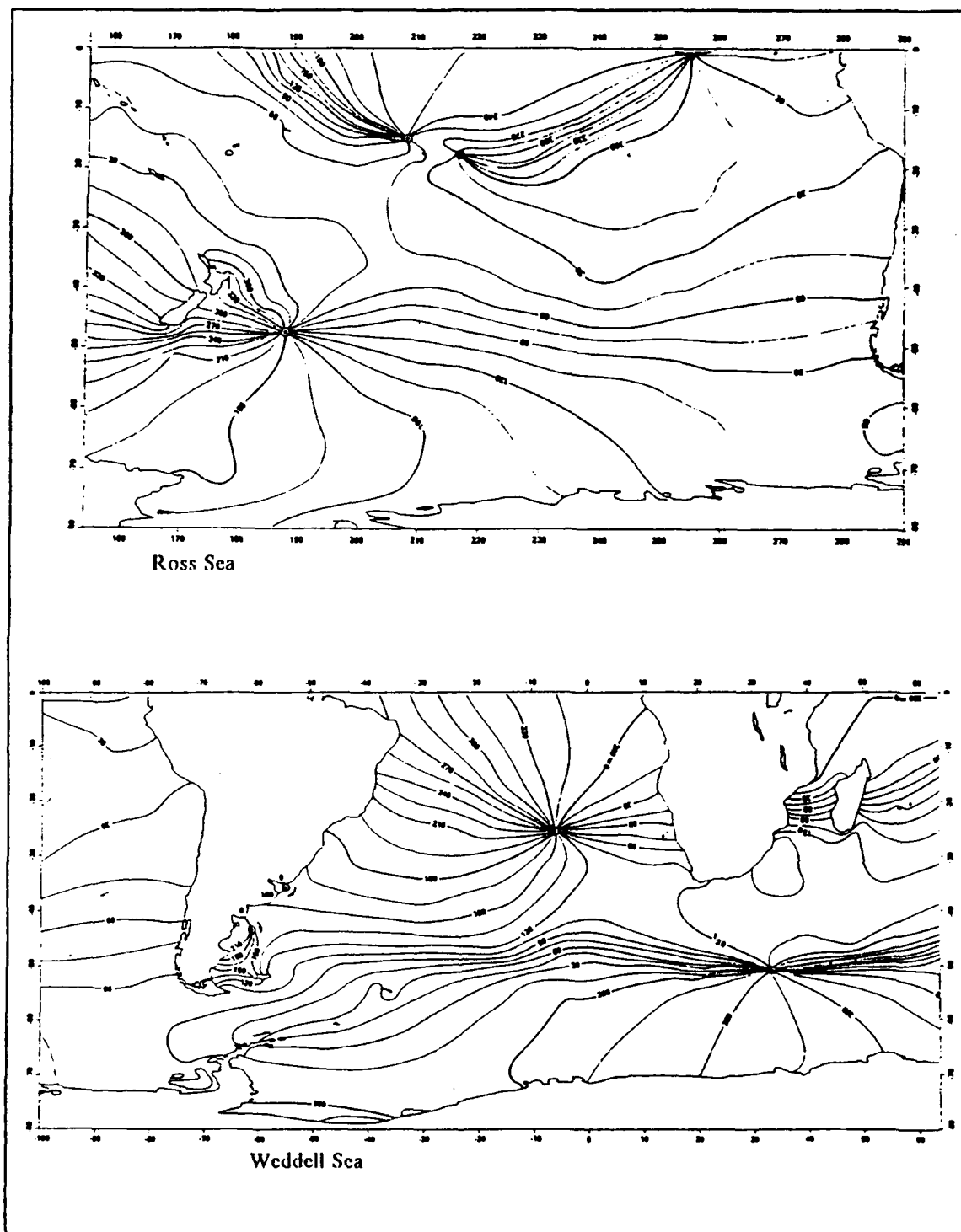


Figure 54. Diurnal cotidal map for the Ross Sea (top) and Weddell Sea (bottom) (K_1 mode) (modification of Schwiderski, 1981e).

V. DISCUSSION

A. UNIQUENESS OF THE WEDDELL SEA

1. Non-Unique Forcing Functions

Forcing functions having parameters similar in both the Ross and Weddell Seas shed little light on why the Weddell Sea is unique as the source of AABW. The following forcing functions were assessed as having features so similar in the two basins that their contribution towards elucidating the uniqueness problem is limited. This is not to say that these forcing functions are not important to the formation of AABW. But it is potentially the combination of other, more unique, forcing functions with one or more of these forcing functions which are required for the production of AABW.

a. Geography

The size of shelf, the nature of the bathymetry beyond the shelf break to the abyssal plain, latitudinal considerations, and ice shelf dimensions are essentially the same between the two basins.

b. Hydrography

The horizontal surface and subsurface circulation patterns appear quite similar. The vertical circulation shows similar relative structures. The small warm core at mid-depth at the Ross Ice Shelf barrier does contrast with the cold bottom plume at the Filchner Ice Shelf barrier, but though these two features are potentially significant on one scale, they are small on the basin scale and do not subvert the general conclusion that the two basins have similar relative circulation structures.

c. Surface Air Temperatures

Differences in air temperatures at the surface are so small between the two basins that this function can not be considered crucial to uniqueness of the Weddell Sea though it is crucial to all AABW formation theories.

2. Surface Winds Revisited

There are no climatologically significant differences (speeds or directions) in the surface wind fields between the two basins. However, the direction of the wind stress relative to the ice shelf barrier is systematically different, especially along the western margins of the barriers. The wind stress appears to have a component directed towards the barrier in the Weddell Sea and a component directed off the barrier in the

Ross Sea. For the Weddell Sea this finding is contrary to earlier investigations. In 1967 Mather and Miller (as reported by Gill, 1973, p. 126) claimed that a prevailing off-ice-shelf wind flow regime existed over the Weddell Sea. Their claim appears to have gone unchallenged and has been accepted as fact (Killworth, 1977, p.179; Foldvik, Gammelsrød, and Tørresen, 1985a, p. 7; Foldvik, Gammelsrød, Slotsvik and Tørresen, and 1985, p. 224). However, an investigation by this author revealed that the wind system over the Weddell Sea was largely unknown at that time, and that Mather and Miller estimated its direction from katabatic considerations. (Killworth, 1979a, p. 180).

Therefore, whereas the above mentioned offshore wind regimes have lead scientists to assume that the advection of new ice away from the barrier in the Weddell Sea was wind stress induced, evidence has been presented that questions that conclusion. Another mechanism (tidal forcing, discussed later) is proposed to be responsible for the advection of new ice away from the barrier (i.e., the generation of leads) in the Weddell Sea.

3. Hydrography Revisited

A relatively warm core of mid-depth water runs under the ice shelf at one location of the barrier in the Ross Sea while in the Weddell Sea a cold bottom plume exits the ice shelf at roughly the same relative location at the barrier. This demonstrates that fundamentally different processes dominate at these locations at the Ross and Weddell Sea ice shelf barriers. In addition, the fact that the Ross Sea is warmer and more saline than the Weddell Sea and the fact that the Ross Sea does not have AABW over its abyssal plain is puzzling. The temperature and salinity differences between the two basins are not easily explained, although it is tempting to speculate that a relationship exists between the unusual warm core of water flowing towards the Ross Ice Shelf barrier and the anomalous melting of the Ross Sea pack ice from the barrier equatorward.

4. Austral Summer Ice Concentration Revisited

The arrival of austral summer marks the beginning of a large difference in the ice cover of the Ross and Weddell Seas. At the end of summer the Ross Sea becomes virtually ice free while the Weddell Sea retains a substantial amount of ice. In addition, the two basins experience a large difference in the magnitude and direction of the ice edge retreat.

Causes for these differences have been attributed to a basic difference in the austral summer ocean circulation within the Ross Sea. Jacobs and Fairbanks (1985,

p. 80) and Pillsbury and Jacobs (1985) have shown that the intermediate depth intrusions on to the continental shelf are warmer in the Ross Sea than those in the Weddell Sea. This has also been seen in the yearly averaged data presented here which were derived mainly from summer observations. As noted above, melting of the Ross Sea pack ice, which initiates from within the interior of the pack ice, may be explained by the off-barrier wind stress. The resulting northward surface transport in response to the wind stress may be compensated by a southward transport and upwelling of WDW as has frequently been observed. Mixing of the surface waters with the upwelled WDW would provide the heat necessary to melt the ice. In the absence of this compensatory flow, the ice pack should remain year round as in the Weddell Sea because, as has been previously described, sufficient cooling of the atmosphere is present even in the summer to keep the pack ice intact.

5. Continental Shelf and Under-Ice-Shelf Bathymetry Revisited

Similar topographic steering features exist around both Roosevelt Island under the Ross Ice Shelf and around Berkner Island under the Ronne/Filchner Ice Shelves. However, the thickness of the water column at the Ronne Ice Shelf barrier is approximately 300 m compared to 600 m at the Ross Ice Shelf barrier. This difference in water column thickness should lead to different circulation patterns under each ice shelf barrier.

With the same surface cooling stress at the barrier (and thus the same brine production), the Weddell Sea should produce a denser water column per unit time since the brine is distributed in a shallower water column. Hence, a denser water should flow under the Ronne Ice Shelf. Furthermore, the density difference between an inflowing water column at the Ronne Ice Shelf barrier and an outflowing water column at the Filchner Ice Shelf barrier would be large due to their much different depths (300 m versus 1000 m). This density difference should be sufficient to drive an under-ice-shelf flow. In the Ross Sea the water column thicknesses at the barrier on either side of Roosevelt Island are comparable (~ 600 m). Therefore the driving force for the under-ice-shelf flow should be substantially less.

The vertical descent from a bottom depth of approximately 300 m to one of 1000 m under the Ronne/Filchner Ice Shelf around Berkner Island is 700 m and has a steep landward slope. This compares to the 100 to 200 m vertical descent and gentle landward slope under the Ross Ice Shelf around Roosevelt Island from a bottom depth of 600 m to one of 700 to 800 m. This difference in vertical excursions could

be reflected in lower temperatures of outflowing ISW in the Weddell Sea due to the depression of the local freezing point of sea water with depth.

In summary, the volume of ISW produced should be greater and its temperature lower in the Weddell Sea compared to the Ross Sea. A possible flow path under the Weddell Sea ice shelves with a return flow to the continental shelf break is illustrated in Figure 55.

6. Tidal Forcing Revisited

The dominant semi-diurnal tidal forcing at the ice shelf barrier in the Weddell Sea is an order of magnitude stronger than in the Ross Sea. It appears that this tidal forcing is possibly one of the major forcing functions in the Weddell Sea that accounts for its uniqueness along with its under-ice-shelf bathymetry and wind stress field.

The Weddell Sea has major semi-diurnal and diurnal modes with cotidal lines indicating a tidal wave progression that can approach the barrier approximately parallel to it, thus: (1) moving the newly formed ice away from the barrier on a periodic basis and (2) forcing water (WSW) under the ice shelf front on a periodic basis.

The opening up of new leads along the barrier by the tidal motion is essential to enhance the brine production. Also, tidal forcing of the WSW under the ice shelf is needed to accomplish the mixing of glacial meltwater into the water column and thus enhance the production of ISW. Foldvik, Gammelsrød, Slotsvik and Tørresen (1985, p. 218) found a mixed tidal amplitude of 1.5 m at the ice shelf barrier in the Weddell Sea, whereas Lewis and Perkins (1986) found that tidal motion at the Ross Sea ice shelf barrier was insufficient to force the outflow of ISW which was produced under the Ross Ice Shelf at that time, a feature corroborated by MacAyeal (1985a,b).

7. Summary of the Uniqueness of The Weddell Sea

In summary, this study shows, objectively, the unique nature of the Weddell Sea when compared to the Ross Sea.

- The Weddell Sea is generally colder and less saline at all depths than the Ross Sea.
- There is a systematic difference in the direction of the wind stress field at the ice shelf barrier between the two basins. The wind stress has a dominant component directed towards the entire length of the barrier in the Weddell Sea whereas in the Ross Sea the wind stress has a dominant component directed seaward, i.e., off-shore from its western barrier.
- The bottom water seaward of the shelf break in the Ross Sea does not have the characteristic features of the AABW found in the Weddell Sea. Ross Sea bottom water is too warm to be considered AABW.

- The austral summer ice cover in the Weddell Sea is substantially greater than that in the Ross Sea. Also, the Weddell Sea shows less interannual variability in ice concentration and greater yearly overall mean ice concentration levels.
- Both the continental shelf and under-ice-shelf bathymetries of the Weddell and Ross Seas have well organized channels for topographically steering a shelfward flow from an entrance under the ice-shelf, around and out from under the ice-shelf and remaining focused all the way seaward to the shelf break. However, in the Weddell Sea the shallower inflow and deeper outflow provide a larger driving force for the ISW than in the Ross Sea. In addition, the only other two outflow channels in the Ross Sea are either blocked just at the shelf break (Scott Shoal) or show no signs of an outflow of any deep or bottom water which might originate from either under the ice shelf or from anywhere on the southern shelf even though easy access to the abyssal plain is available starting at the shelf break (Cape Adare/Mawson Bank).
- Finally, the Ross Sea is an area of weak tidal activity whereas the Weddell Sea is a zone of relatively significant tidal forcing.

B. RELEVANT THEORY

The following discussion details how successful the two theories of AABW formation are in explaining why the unique qualities of the Weddell Sea are crucial to the formation of AABW.

1. Shelf Break Process

The Ross Sea basin has all the required forcing functions present for the formation of AABW according to the shelf break process theory. This theory does not require special bathymetries of the continental shelf nor does it require an ice shelf. The fact that the water temperatures at depth are higher in the Ross Sea is compensated for by their higher salinities. Double-diffusion and cabbeling are processes that should operate at any similar relative temperature and salinity ratios, hence the higher salinities of the Ross Sea alone would indicate a higher production of dense bottom water if sinking started from near-freezing surface water.

The intrusion of WDW onto the continental shelf clearly occurs in the Ross Sea as well as the Weddell Sea. Mixing at the shelf break obviously occurs in the Ross Sea as well as the Weddell Sea. If the melting of the Ross Sea pack ice begins at the barrier due to the surfacing of a tongue of WDW, then the Ross Sea would permit more mixing to occur with sinking high salinity surface water. Again this would lead to the conclusion that the Ross Sea should produce large quantities of dense water, possibly more than produced by shelf break mixing processes in the Weddell Sea. Downwelling at the shelf break is clearly evident in both basins and indicates the downslope flow of newly formed dense water.

Observations show that the dense waters flowing down the continental slope in the Ross Sea do not produce the extremely cold type of bottom water observed in the Weddell Sea. One reason for this is that mixing at the slope in the Ross Sea takes place with considerably warmer water than that found in the Weddell Sea. It should be noted that although dense bottom water (e.g., WSBW) is not observed to form in the Ross Sea, this does not exclude the possibility of the production of significant quantities of intermediate or deep waters.

2. Ice Shelf Process

The ice shelf process theory suggests that the source of AABW is the bottom cold plume exiting at the Filchner Ice Shelf barrier and the theory utilizes the unique tidal regime, wind stress field and continental shelf and under-ice-shelf bathymetries of the Weddell Sea to drive the flow.

To show that the strong tidal forcing at the Weddell Sea ice shelf barrier, combined with the special under ice shelf and continental shelf bathymetric channels, are the key factors in the formation of AABW we begin with the surface freezing levels due to tidal action at the barrier. In Appendix A, a formula and constants are derived for ice production (IP) by tidal constituent forcing per unit length of ice shelf:

$$IP (m^2) = \frac{V_o C}{2} \omega^{-\frac{3}{2}} K \quad \{5\}$$

where V_o equals the maximum tidal mode speed, C equals the ice growth coefficient $\approx 4.7 \times 10^{-4} ms^{-\frac{1}{2}}$, $\omega = \frac{2\pi}{T}$ where T equals the tidal mode period and finally, $K = 3.79$.

If the dominant tidal mode of the Weddell Sea (the M_2 Semi-diurnal Principal Lunar Tide with frequency of $\omega = 1.40519 \times 10^{-4} s^{-1}$) is used as the sole measure of tidal forcing at the ice shelf barrier, and a recently observed, at the Weddell Sea shelf break, maximum tidal speed of $V_o = 0.4 ms^{-1}$ (Foldvik, Kvinge and Tørresen 1985, p. 10)¹² is used, then the area of ice production per unit length of ice shelf equals $\sim 213 m^2$. This would lead to an average displacement value ($\frac{Y}{2}$) or average width of tidally induced lead opening between the barrier and the pack ice of approximately 2.8 km from:

¹² At an earlier date, Foldvik, Gammelsrød, Slotsvik and Tørresen (1985, p. 218) found a $V_o = 0.3 ms^{-1}$ at the Weddell Sea ice shelf barrier.

$$\frac{Y}{2} = \frac{1}{2} \frac{V_o}{\omega} (1 - \cos \omega t) \quad \{6\}$$

Foldvik's (1989) firsthand accounts of the scale of the barrier lead in the Weddell Sea indicate that 2.8 km is a reasonable value. Also, Foldvik, Gammelsrød and Tørresen (1985a, p. 7) documented ice divergence at the barrier in the Weddell Sea brought about by tidal action.

If the ice production (IP) is multiplied by the approximate length (L) of the Ronne Ice Shelf (~ 500 km), then a volume of production (VP) can be obtained as approximately $10^8 m^3$.

To determine a production rate we can use the principal of brine rejection in the freezing process and knowledge of the observed salinity changes occurring at the barrier between surface Winter Water (WW) and Western Shelf Water (WSW) below. If we calculate the amount of brine released into the surrounding waters upon freezing as volume production (VP) multiplied by the salinity of the water (S), then this must equal the volume (V) ($V = L \times \frac{Y}{2} \times D$, where D equals the average depth of water of the barrier lead) multiplied by the change in salinity of the surrounding waters (ΔS) or:

$$VP \times S = V \times \Delta S \quad \{7\}$$

If we assume an average depth of 400 m at the Ronne Ice Shelf barrier lead, we can estimate ΔS by solving equation 7 for ΔS resulting in a value of .00865 PSU per cycle. To convert surface source water having a salinity of 34.5 PSU (WW) to 34.7 PSU (WSW) would take almost exactly 24 semidiurnal cycles or 12 days to be produced. If the wind stress field has a dominant on-barrier component, then no combined wind-induced upwelling of WDW and off-barrier surface water drift circulation will occur. Thus this 12 day residence time requirement to produce an entire column of WSW is possible.

To determine a realistic flow rate that incorporates the added salinity changes due to under-ice-shelf melting in the production of Ice Shelf Water (ISW), we solve equation 7 for the volume (V). To determine the flow rate (FR) divide the volume by the period of the tidal mode:

$$FR (m^3 s^{-1}) = \frac{VP \times S}{\Delta S \times T} \quad \{8\}$$

If we assume the same value for VP of 10^8 m^3 , an outflow salinity of 34.6, an overall ΔS of 0.1 and a period (for M_2) of ~ 12.4 hours, then we find a flow rate of:

$$FR = 0.7 \times 10^6 \text{ m}^3 \text{ s}^{-1} \quad \{9\}$$

or 0.7 Sv (1 Sv or Sverdrup = $10^6 \text{ m}^3 \text{ s}^{-1}$).

This is exactly the value that Foldvik, Gammelsrød and Tørresen (1985c, p. 199) found in a year long (1979-1980), steady (no appreciable seasonal variance) plume of ISW ($T \sim -2.0^\circ\text{C}$, $S \sim 34.65$) exiting the Filchner Depression and traveling down the continental shelf to the shelf break. Foldvik, Gammelsrød and Tørresen (1985a, p. 17) averaged this result with the previous years result to obtain a flow of 1 Sv. If we assume a certain amount of entrainment and allowance for the fact that the M_2 tidal constituent is an underestimation when used as the sole tidal forcing factor, then a realistic flow approximation of 1 Sv is appropriate¹³.

In Appendix B, a simple mixing model using observed temperature-depth profiles of the ISW plumes and WDW shows that Weddell Sea Bottom Water (WSBW) (when defined as $T \sim -0.8^\circ\text{C}$), is formed at a rate of about 5 Sv. This production rate is comparable to most estimates to date of WSBW production (2 to 5 Sv by Carmack and Foster, 1975a, p. 723; 3.5 Sv by Michel, 1978, p. 6198; 3 to 5 Sv by Weiss et al., 1979, p. 1110).

Therefore, it would appear that the ice shelf process theory not only accounts for the necessity of the Weddell Sea's unique features in the formation of AABW, but can also account for the required scale of production of AABW from the Weddell Sea.

Conclusive proof as to the relative importance of ice shelf processes and shelf break processes for the formation of AABW in the Weddell Sea should be available in approximately five years. Dr. Eberhard Fahrback of the Alfred Wegener Institute for Ocean and Polar Research intends to place a string of moored sensing devices across the Weddell Sea in an attempt to measure the ratio of oxygen 18 to oxygen 16 in the outflowing bottom water of the basin (Fahrback, 1989). If the result shows glacial origin of the bottom waters, then the ice shelf process theory of Foldvik and Gammelsrød will be substantiated. If not, then the search will have to continue for the formation mechanism of Antarctic Bottom Water.

¹³ Carmack and Foster (1975b, p. 89) theoretically determined that ISW production for this area should be 0.6 Sv which agrees with the magnitude of our result.

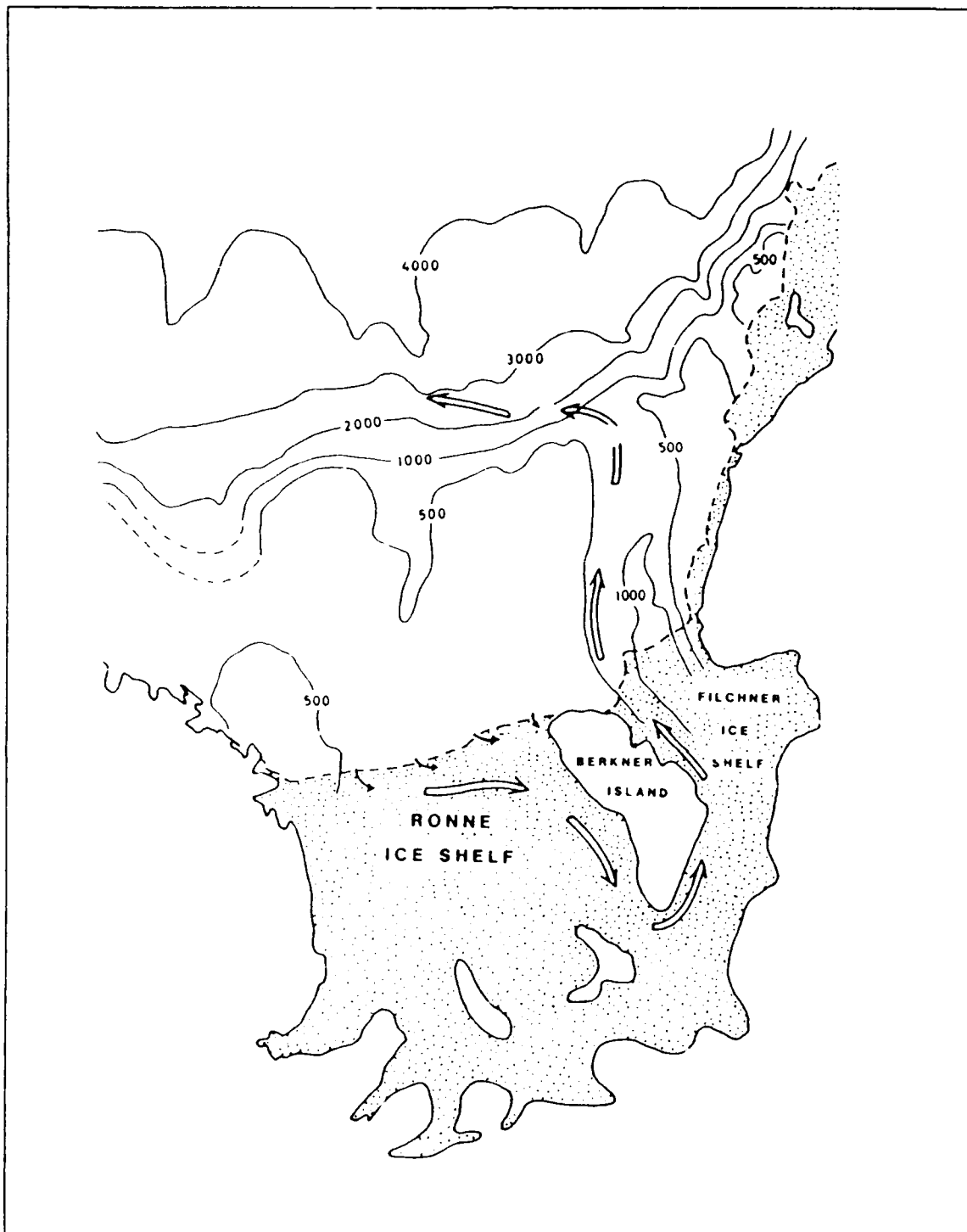


Figure 55. Possible flow path under the Weddell Sea ice shelves with a return flow to the continental shelf break: (modification of Foldvik and Gammelsrød, 1988).

VI. CONCLUSIONS

The abyssal characteristics of the world oceans are strongly influenced by the northward propagation of Antarctic Bottom Water (AABW). The most important source of AABW is Weddell Sea Bottom Water (WSBW) which originates from the shelf areas in the southern Weddell Sea. AABW is not produced in the Ross Sea despite the striking similarities between the two basins.

An attempt was made to assess those differences existing between the two basins that make the Weddell Sea unique compared to the Ross Sea as a production region of AABW. In addition, the two predominant theories of AABW formation, Foster and Carmack's (1977) shelf break process theory and Foldvik and Gammelsrød's (1988) ice shelf process theory, were reviewed with a goal of determining how well each theory could explain the Weddell Sea's effectiveness in forming AABW based on its identified unique qualities.

Individual forcing functions were compared between the two basins and the following were determined to be similar in both the Weddell Sea and the Ross Sea:

- The size of shelf, the nature of the bathymetry beyond the shelf break to the abyssal plain, latitudinal considerations, and ice shelf dimensions are essentially the same between the two basins.
- The horizontal surface and subsurface circulation patterns appear quite similar. The vertical circulation shows similar relative structures.
- Differences in air temperatures at the surface are so small between the two basins that this function can not be considered crucial to the uniqueness of the Weddell Sea though it is crucial to all AABW formation theories.
- There are no climatologically significant differences in the surface wind fields between the two basins.

The unique qualities of the Weddell Sea when compared to the Ross Sea follow:

- The Weddell Sea is generally colder and less saline at all depths than the Ross Sea.
- There is a systematic difference in the direction of the wind stress field at the ice shelf barrier between the two basins. The wind stress has a dominant component directed towards the entire length of the barrier in the Weddell Sea whereas in the Ross Sea the wind stress has a dominant component directed seaward, i.e., off-shore from its western barrier.
- The bottom water seaward of the shelf break in the Ross Sea does not have the characteristic features of the AABW found in the Weddell Sea. Ross Sea bottom water is too warm to be considered AABW.

- The austral summer ice cover in the Weddell Sea is substantially greater than that in the Ross Sea. Also, the Weddell Sea shows less interannual variability in ice concentration and greater yearly overall mean ice concentration levels.
- Both the continental shelf and under-ice-shelf bathymetries of the Weddell and Ross Seas have well organized channels for topographically steering a shelfward flow from an entrance under the ice-shelf, around and out from under the ice-shelf and remaining focused all the way seaward to the shelf break. However, in the Weddell Sea the shallower inflow and deeper outflow provide a larger driving force for the ISW than in the Ross Sea. In addition, the only other two outflow channels in the Ross Sea are either blocked just at the shelf break (Scott Shoal) or show no signs of an outflow of any deep or bottom water which might originate from either under the ice shelf or from anywhere on the southern shelf even though easy access to the abyssal plain is available starting at the shelf break (Cape Adare Mawson Bank).
- Finally, the Ross Sea is an area of weak tidal activity whereas the Weddell Sea is a zone of relatively significant tidal forcing.

The review of the Foster and Carmack theory revealed the following:

- Analysis of the shelf break process theory reveals that the requisite amount of WDW intrusions on to the continental shelf, sufficient mixing at the shelf break, sufficient densities of the mixing water masses and sufficient distance beyond the shelf break are present in such a magnitude that AABW should not only be produced in the Ross Sea but possibly be produced more effectively than in the Weddell Sea. Though dense bottom water (e.g., WSBW) is not observed to form in the Ross Sea, this theory could explain the production of significant quantities of intermediate or deep waters.

The review of the Foldvik and Gammelsrod theory revealed the following:

- The ice shelf process theory can account for the uniqueness of the Weddell Sea and its role in the formation of AABW. This theory can also suggest why it is not produced in the Ross Sea. The theory demonstrates that the strong tidal forcing at the Weddell Sea ice shelf barrier, combined with the wind stress field and special under-ice-shelf and continental shelf bathymetries of the Weddell Sea, permit the formation of AABW in this basin.
- Surface freezing levels due to tidal action at the barrier produce a volume of ice of approximately 10 m^3 .
- Enough ISW is produced to create an outflow down the continental slope of 0.7 Sv which agrees with observations.
- Theoretical calculations using this theory show that Weddell Sea Bottom Water (WSBW) is formed at a rate of about 5 Sv which is comparable to most estimates of WSBW production.
- In summary, Foldvik and Gammelsrod's ice shelf process theory not only can account for the necessity of the Weddell Sea's unique features in the formation of AABW, but it can also account for the required scale of production of Antarctic Bottom Water from the Weddell Sea as well.

APPENDIX A. FREEZING DUE TO TIDES AT THE ICE SHELF BARRIER

The following discussion develops the theory of tidal action at the barrier maintaining open leads for the freezing of surface waters and converts it into a measure of ice production with determination of appropriate constants¹⁴.

A. ICE PRODUCTION

Within a tidal cycle, the maximum displacement (Y) of a water particle due to a tidal constituent velocity (V), a function of time, is:

$$Y = \int_0^t V(t) dt = \frac{V_o}{\omega} (1 - \cos \omega t) \quad \{10\}$$

where t equals time in seconds, ω equals tidal constituent frequency and V_o equals the maximum tidal constituent velocity.

Ice thickness (h) is a function of freezing time Ψ ($h = h(\Psi)$). At a distance X off the barrier, ice has been forming for a time Ψ , where:

$$X = \int_{t-\Psi}^t V(t) dt \quad \{11\}$$

that is:

$$X = V_o \omega^{-1} (\cos \omega(t - \Psi) - \cos \omega t) \quad \{12\}$$

For this relation we get the relation between dx and dt :

$$dx = V_o \sin \omega(t - \Psi) dt \quad \{13\}$$

The total ice production (IP) within one tidal cycle should then be obtained by first summing all changes in ice thickness ($\frac{\delta h}{\delta \Psi}$), the partial derivative of ice thickness with respect to freezing time, taking place over the stretch of freezing water ($0 \leq x \leq Y$), and then integrating over the tidal period (T):

¹⁴ This appendix is the result of a collaborative effort of A. Foldvik and the author.

$$IP = \int_{t=0}^T dt \int_{x=0}^Y \frac{\delta h}{\delta \Psi} dx \quad \{14\}$$

in area per unit length of ice shelf.

Here we replace dx by $d\Psi$ from equation 13 and insert the freezing formula:

$$h = C\Psi^{\frac{1}{2}} \quad \{15\}$$

where C equals the ice growth coefficient. Hence:

$$IP = \frac{V_a C}{2} \int_0^T \Psi^{-\frac{1}{2}} \sin \omega(t - \Psi) d\Psi \quad \{16\}$$

Finally, introducing non-dimensional units: $\omega t = t_1$ and $\omega\Psi = \Psi_1$:

$$IP = \frac{V_a C}{2} \omega^{-\frac{3}{2}} \int_0^{2\pi} dt_1 \int_0^{t_1} \Psi_1^{-\frac{1}{2}} \sin(t_1 - \Psi_1) d\Psi_1 \quad \{17\}$$

For numerical integration we can write:

$$IP = \frac{V_a C}{2} \omega^{-\frac{3}{2}} \int_0^{2\pi} dt \left\{ \sin t \int_0^t \frac{\cos \Psi}{\sqrt{\Psi}} d\Psi - \cos t \int_0^t \frac{\sin \Psi}{\sqrt{\Psi}} d\Psi \right\} \quad \{18\}$$

Note that the integrals are solvable at $\Psi = 0$ because they can be integrated by parts. For example, the first integral can be expressed as:

$$2 \int_0^t \frac{1}{\sqrt{\Psi}} \sin \Psi d\Psi$$

The integral is now a constant (K), independent of any parameter and can be quickly calculated to any desired precision. The Fortran IV program below calculated the value for:

$$K \approx 3.78667$$

therefore:

$$IP = \frac{V_o C}{2} \omega^{-\frac{3}{2}} K \quad \{21\}$$

Thus it should be noted that ice production is proportional to the tidal velocity and to the tidal period to the $\frac{3}{2}$ power.

Program to calculate K

```

REAL*8 K,TOTALA,TOTALB,DT
REAL*8 DPsi,BOXA,BOXB,PI,A,B,AA,BB,PRODA,PRODB
DIMENSION AA(1000),BB(1000),PRODA(1000),PRODB(1000)
PI=4*ATAN(1.)
DT=2*PI/1000.
TOTALA=0.
TOTALB=0.
A=0.
B=0.
DO 10 N=1,1000
    BOXA=(COS(N*DT)/SQRT(N*DT))*DT
    A=A+BOXA
    AA(N)=A
    BOXB=(SIN(N*DT)/SQRT(N*DT))*DT
    B=B+BOXB
    BB(N)=B
    PRODA(N)=AA(N)*SIN(N*DT)
    PRODB(N)=BB(N)*COS(N*DT)
    TOTALA=TOTALA + PRODA(N)
    TOTALB=TOTALB + PRODB(N)
10 CONTINUE
K=(TOTALA-TOTALB)*DT
WRITE(6,*)K
END

```

B. ICE GROWTH COEFFICIENT

To determine an applicable ice growth coefficient (C) for the Weddell ice shelf area, Gill (1973, pg. 126) and Foster (1976b) reports that very rapid freezing of .08m growth in eight hours when a lead opened at the barrier in the Weddell Sea. Manipulating the freezing equation (equation 15) and solving for C, a value of approximately:

$$C \approx 4.7 \times 10^{-4} \text{ ms}^{-\frac{1}{2}}$$

is obtained.

APPENDIX B. PLUME MIXING WITH WARM DEEP WATER

The following discussion develops the theory of the formation of Weddell Sea Bottom Water (WSBW) from a plume of Ice Shelf Water (ISW) entraining Warm Deep Water (WDW) on its descent down the continental slope utilizing observed values¹⁵.

Definitions:

θ_p

Potential temperature of the plume of ISW ($\approx -2.0^\circ\text{C}$).

θ_w

Potential temperature of the WDW ($\approx 0.5^\circ\text{C}$).

θ_{bm}

Potential temperature of the WSBW ($\approx -0.8^\circ\text{C}$).

ρ_o

Density of the observed plume of ISW at depth z_o .

M_p

Mass of the plume of ISW.

V_o

Observed volume transport of the plume of ISW $\approx 1\text{ Sv}$ or $10^6\text{ m}^3\text{ s}^{-1}$ at depth z_o .

Entrainment of WDW can be described by:

$$\theta_p M_p + \theta_w \delta M_p = (\theta_p + \delta\theta_p)(M_p + \delta M_p) \quad \{23\}$$

which can be described in terms of volume transport as:

$$V_1 = V_o \frac{\rho_o}{\rho_1} \exp \int_0^1 \frac{\delta\rho_z}{\theta_w - \theta_p} \quad \{24\}$$

¹⁵ This appendix is the result of a collaborative effort of A. Foldvik and the author.

where V_1 equals the volume transport of the entrained flow and ρ_1 equals the density of the entrained flow, both at depth z_1 .

Integrating from the surface, $z_0 \approx 0$ m, to $z_1 \approx 4000$ m with observed values where both θ_p and θ_w converge to θ_{bm} gives $V_1 \approx 5.0 V_0$ or $V_1 \approx 5$ Sv.

The result is sensitive to bottom water temperature but not to variations on the shape of the θ_p curve. In the extreme case with no mixing above z_1 , we get:

$$V_1 = V_0 \left(\frac{\theta_p - \theta_w}{\theta_{bm} - \theta_w} \right)_{z=z_1} = (5 \text{ to } 8) V_0 \quad \{25\}$$

Thus a simple mixing model using observed temperature-depth profiles of the ISW plumes and WDW shows that 5 to 8 Sv of Weddell Sea Bottom Water (WSBW) when defined as $T \sim -0.8^\circ\text{C}$, can be produced by the entrainment of these two water types.

LIST OF REFERENCES

- Bowditch, N., *American Practical Navigator*, 1, Defense Mapping Agency, Washington DC, 1984.
- Brennecke, W., Excerpt from: The Oceanographic Work of the German Antarctic Expedition (1911), Excerpt from: The Oceanographic Results of the Second French, Swedish, and Scottish Polar Expedition (1918), Excerpt from: The Oceanographic Work of the German Antarctic Expedition, 1911-1912, Weddell Sea (1921), In: G. E. R. Deacon and M. Deacon (editors), *Modern Concepts of Oceanography*, Hutchinson Ross Publishing Company, Stroudsburg, PA, 277-287, 1982.
- Broecker, W. S., Geochemical Tracers and Ocean Circulation, In: B. A. Warren and C. Wunsch (editors), *Evolution of Physical Oceanography*, The MIT Press, Boston, MA, 434-460, 1981.
- Carmack, E. C., Water Characteristics of the Southern Ocean South of the Polar Front, In: Martin Angel (editor), *A Voyage of Discovery*, Pergamon Press, Oxford, England, 15-41, 1977.
- Carmack, E. C., Circulation and Mixing in Ice-covered Waters, In: N. Untersteiner (editor), *The Geophysics of Sea Ice*, Plenum Press, New York, NY, 641-712, 1986.
- Carmack, E. C. and T. D. Foster, On the Flow of Water Out of the Weddell Sea, *Deep-Sea Research*, **22**, 711-724, 1975a.
- Carmack, E. C. and T. D. Foster, Circulation and Distribution of the Oceanographic Properties Near the Filchner Ice Shelf, *Deep-Sea Research*, **22**, 77-90, 1975b.
- Carmack, E. C. and T. D. Foster, Water Masses and Circulation in the Weddell Sea, In: M. J. Dunbar (editor), *Polar Oceans*, Arctic Institute of North America, Calgary, Canada, 151-165, 1977.
- Carmack, E. C. and P. D. Killworth, Formation and Interleaving of Abyssal Water Masses off Wilkes Land, Antarctica, *Deep-Sea Research*, **25**, 357-369, 1978.
- Central Intelligence Agency (CIA), *Polar Region Atlas*, Washington, DC, 1978.
- Chen, C. T. A. and M. R. Rodman, Inhomogeneous Distribution of Traces in the Abyssal Southern Ocean, *Antarctic Journal of the United States*, **19**, (5), 68-69, 1985.
- Coachman, L. K. and K. Aagaard, Physical Oceanography of Arctic and Subarctic Seas, *Marine Geology and Oceanography of the Arctic Sea*, Springer-Verlag, New York, NY, 1974.
- Deacon, G. E. R., The Hydrology of the Southern Ocean, *Discovery Reports*, **XV**, 1-124, Plates I-XLIV, 1937.
- Deacon, G. E. R., The Southern Ocean, In: M. N. Hill (editor), *The Sea*, **2**, Interscience Publishers, New York, NY, 281-296, 1963.
- Deacon, G. E. R., Antarctic Water Masses and Circulation, In: M. J. Dunbar (editor), *Polar Oceans*, Arctic Institute of North America, Calgary, Canada, 151-165, 1977.

- Deacon, G. E. R., Oxygen in Antarctic Water, *Deep-Sea Research*, **31**, 11a, 1369-1371, 1984.
- Defense Mapping Agency (DMA), *Sailing Directions for Antarctica*, Pub. 200, Washington DC, 1985.
- Drewry, D. J. (editor). *Antarctica: Glaciological and Geophysical Folio*. Scott Polar Research Institute, University of Cambridge, Cambridge, England, 1983.
- Duxbury, A. C., *The Earth and Its Oceans*, Addison-Wesley Publishing Company, Reading, MA, 1971.
- Fahrbach, E., Alfred Wegener Institute for Ocean and Polar Research, Bremerhaven, FGR, Interview by D. St.Pierre, 16 February 1989.
- Fofonoff, N. P., Some Properties of Sea Water Influencing the Formation of Antarctic Bottom Water, *Deep-Sea Research*, **4**, (4), 32-35, 1956.
- Foldvik, A., University of Bergen, Bergen, Norway. Interview by D. St.Pierre, 9 June 1989.
- Foldvik, A. and T. Gammelsrød, Notes on Southern Ocean Hydrography, Sea-Ice and Bottom Water Formation, *Paleogeography, Paleoclimatology, Paleoecology*, **67**, 3-17, 1988.
- Foldvik, A., T. Gammelsrød, N. Slotsvik and T. Tørresen, Oceanographic Conditions on the Weddell Sea Shelf during the German Antarctic Expedition 1979 80, *Polar Research*, **3**, 209-226, 1985.
- Foldvik, A., T. Gammelsrød and T. Tørresen, Circulation and Water Masses on the Southern Weddell Sea Shelf. In: S. S. Jacobs (editor), *Oceanology of the Antarctic Continental Shelf, Antarctic Research Series*, **43**, American Geophysical Union, Washington, DC, 5-20, 1985a.
- Foldvik, A., T. Gammelsrød and T. Tørresen, Hydrographic Observations from the Weddell Sea During the Norweign Antarctic Expedition 1976 77, *Polar Research*, **3**, 177-193, 1985b.
- Foldvik, A., T. Gammelsrød and T. Tørresen, Oceanography Studies in the Weddell Sea During the Norweign Antarctic Expedition 1978 79, *Polar Research*, **3**, 195-207, 1985c.
- Foldvik, A. and T. Kvinge, Conditional Instability of Sea Water at the Freezing Point, *Deep-Sea Research*, **21**, 169-174, 1974.
- Foldvik, A. and T. Kvinge, Thermohaline Convection in the Vicinity of an Ice Shelf. In: M. J. Dunbar (editor), *Polar Oceans*, Arctic Institute of North America, Calgary, Canada, 247-255, 1977.
- Foldvik, A., T. Kvinge and T. Tørresen, Bottom Currents Near the Continental Shelf Break in the Weddell Sea. In: S. S. Jacobs (editor), *Oceanology of the Antarctic Continental Shelf, Antarctic Research Series*, **43**, American Geophysical Union, Washington, DC, 21-34, 1985.
- Foldvik, A., J. H. Middleton and T. D. Foster, The Tides of the Southern Weddell Sea, (preliminary draft) June 1989.

- Foster, T. D., An Analysis of the Cabbeling Instability in Sea Water, *Journal of Physical Oceanography*, **2**, (3), 294-301, 1972a.
- Foster, T. D., Haline Convection in Polynyas and Leads, *Journal of Physical Oceanography*, **2**, (4), 462-469, 1972b.
- Foster, T. D. and E. C. Carmack, Frontal Zone Mixing and Antarctic Bottom Water Formation in the Southern Weddell Sea, *Deep-Sea Research*, **23**, 301-317, 1976a.
- Foster, T. D. and E. C. Carmack, Temperature and Salinity Structure in the Weddell Sea, *Journal of Physical Oceanography*, **6**, 36-44, 1976b.
- Foster, T. D. and E. C. Carmack, Antarctic Bottom Water Formation in the Weddell Sea, In: M. J. Dunbar (editor), *Polar Oceans*, Arctic Institute of North America, Calgary, Canada, 167-177, 1977.
- Foster, T. D., A. Foldvik and J. H. Middleton, Mixing and Bottom Water Formation in the Shelf Break Region of the Southern Weddell Sea, *Deep-Sea Research*, **34**, (11), 1771-1794, 1987.
- Foster, T. D. and J. H. Middleton, International Weddell Sea Oceanographic Expedition, 1978, *Antarctic Journal of the United States*, **13**, (4), 82-83, 1978.
- Foster, T. D. and J. H. Middleton, Variability in Bottom Water of the Weddell Sea, *Deep-Sea Research*, **26**, (A), 743-762, 1979.
- Foster, T. D. and J. H. Middleton, Bottom Water Formation in the Western Weddell Sea, *Deep-Sea Research*, **27**, (5A), 367-381, 1980.
- Gascard, J. C., Mediterranean Deep Water Formation Baroclinic Instability and Oceanic Eddies, *Oceanologica Acta*, **1**, (3), 315-330, 1978.
- Gascard, J. C., University de Paris, Paris, France, Interview by D. St.Pierre, 2 February 1989.
- Gill, A. E., Circulation and Bottom Water Production in the Weddell Sea, *Deep-Sea Research*, **20**, 111-140, 1973.
- Gill, A. E., *Atmosphere-Ocean Dynamics*, Academic Press, Inc., Orlando, FL, 1982.
- Gordon, A. L., Structure of Antarctic Waters Between 20°W and 170°W, In: V. Bashnell (editor), *Antarctic Map Folio Series*, Folio 6, American Geographical Society, New York, NY, 1967.
- Gordon, A. L., Spreading of Antarctic Bottom Waters II, In: A. L. Gordon (editor), *Studies in Physical Oceanography*, Gordon and Breach Science Publishers, New York, NY, 1-17, 1972.
- Gordon, A. L., Deep Antarctic Convection West of Maud Rise, *Journal of Physical Oceanography*, **8**, (4), 600-612, 1978.
- Gordon, A. L., The Southern Ocean and Global Climate, *Oceanus*, **31**, (2), 39-46, 1988.
- Gordon, A. L. and T. N. Baker, Objective Contouring and the Grid Point Data Set, In: A. L. Gordon (editor), *Southern Ocean Atlas*, National Science Foundation, Washington, DC, 1986.

- Gordon, A. L. and R. D. Goldberg, Circumpolar Characteristics of Antarctic Waters. In: V. Bushnell (editor), *Antarctic Map Folio Series, Folio 13*, American Geographical Society, New York, NY, 1970.
- Gordon, A. L. and E. J. Molinelli, Thermohaline and Chemical Distribution and the Atlas Data Set, *Southern Ocean Atlas*, National Science Foundation, Washington, DC, 1986.
- Gordon, A. L. and P. Tchernia, Waters of the Continental Margin Off Adélie Coast, Antarctica, In: D. F. Hayes (editor), *Antarctic Oceanology II, Antarctic Research Series, 19*, American Geophysical Union, Washington, DC, 59-69, 1972.
- Guest, P.S. and K. L. Davidson, The Effect of Observed Conditions on the Drag Coefficient in the Summer East Greenland Marginal Ice Zone, *Journal of Geophysical Research*, **92**, (C7), 6943-6954, 1987.
- Herrod, L. D. B., *A Geophysical Reconnaissance of the Ronne Ice Shelf Antarctica*, Ph.D. Dissertation, Darwin College, University of Cambridge, Cambridge, England, June 1987.
- Hofmeyr, W. L., Atmospheric Sea-Level Pressure over the Antarctic, In: M. P. van Rooy (editor), *Meteorology of the Antarctic*, Weather Bureau, Department of Transport, Pretoria, South Africa, 51-70, 1957.
- Ingersoll, A. P., The Atmosphere, *Scientific American*, 164-174, 1983.
- International Hydrographic Office (IHO), *IHO Tidal Constituent Bank*, Ocean and Aquatic Sciences, Marine Environmental Data Services, Department of Fisheries and Oceans, Ottawa, Canada, 1989.
- Jacobs, S. S., Marine Controls on Modern Sedimentation on the Antarctic Continental Shelf, *Marine Geology*, **85**, 121-153, 1989.
- Jacobs, S. S., A. F. Amos and P.M. Bruchhausen, Ross Sea Oceanography and AABW Formation, *Journal of Geophysical Research*, **17**, 935-962, 1970.
- Jacobs, S. S. and R. G. Fairbanks, Origin and Evolution of Water Masses Near the Antarctic Continental Margin: Evidence from $H_2^{18}O/H_2^{16}O$ Ratios in Sea Water, In: S. S. Jacobs (editor), *Oceanology of the Antarctic Continental Shelf, Antarctic Research Series, 43*, American Geophysical Union, Washington, DC, 59-85, 1985.
- Jacobs, S. S. and D. T. Georgi, Observations on the South West Indian Antarctic Ocean, In: M. V. Angel (editor), *A Voyage of Discovery*, Pergamon Press, Oxford, England, 43-84, 1977.
- Jacobs, S. S., A. L. Gordon and A. F. Amos, Effect of Glacial Ice Melting on the Antarctic Surface Water, *Nature*, **277**, 469-471, 1979.
- Killworth, P. D., Some Models of Bottom Water Formation, In: M. J. Dunbar (editor), *Polar Oceans*, Arctic Institute of North America, Calgary, Canada, 179-189, 1977a.
- Killworth, P. D., Mixing on the Weddell Sea Continental Slope, *Deep-Sea Research*, **24**, (5), 427-448, 1977b.
- Killworth, P. D., On "Chimney" Formations in the Ocean, *Journal of Physical Oceanography*, **9**, (3), 531-554, 1979.

Kurtz, D. D. and D. H. Bromwich, A Recurring Atmospherically Forced Polynya in Terra Nova Bay. In: S. S. Jacobs (editor), *Oceanology of the Antarctic Continental Shelf, Antarctic Research Series, 43*, American Geophysical Union, Washington, DC, 177-199, 1985.

Lettau, H. H., A Case Study of Katabatic Flow of the South Polar Plateau. In: M. J. Robin (editor), *Studies in Antarctic Meteorology, Antarctic Research Series, 9*, American Geophysical Union, Washington, DC, 1-11, 1966.

Lewis, E. L. and R. G. Perkin, The Winter Oceanography of McMurdo Sound, Antarctica. In: S. S. Jacobs (editor), *Oceanology of the Antarctic Continental Shelf, Antarctic Research Series, 43*, American Geophysical Union, Washington, DC, 145-165, 1985.

Lewis, E. L. and R. G. Perkin, Ice Pumps and Their Rates, *Journal of Geophysical Research, 91*, (C10), 11756-11762, 1986.

Lutjeharms, J. R. E., C. C. Stavropoulos and K. P. Kolterman, Tidal Measurements Along the Antarctic Coastline. In: S. S. Jacobs (editor), *Oceanology of the Antarctic Continental Shelf, Antarctic Research Series, 43*, American Geophysical Union, Washington, DC, 273-289, 1985.

MacAyeal, D. R., Tidal Rectification Below the Ross Ice Shelf, Antarctica. In: S. S. Jacobs (editor), *Oceanology of the Antarctic Continental Shelf, Antarctic Research Series, 43*, American Geophysical Union, Washington, DC, 109-132, 1985a.

MacAyeal, D. R., Evolution of Tidally Triggered Meltwater Plumes Below Ice Shelves. In: S. S. Jacobs (editor), *Oceanology of the Antarctic Continental Shelf, Antarctic Research Series, 43*, American Geophysical Union, Washington, DC, 133-143, 1985b.

Martinson, D. G., P. D. Killworth and A. Gordon, A Convective Model for the Weddell Polynya, *Journal of Physical Oceanography, 11*, 466-488, 1981.

Michel, R. L., Tritium Distributions in Weddell Sea Water Masses, *Journal of Geophysical Research, 83*, (C12), 6192-6198, 1978.

Middleton, J. H., T. D. Foster and A. Foldvik, Low-frequency Currents and Continental Shelf Waves in the Southern Weddell Sea, *Journal of Physical Oceanography, 12*, 618-634, 1982.

Middleton, J. H., T. D. Foster and A. Foldvik, Diurnal Shelf Waves In the Southern Weddell Sea, *Journal of Physical Oceanography, 17*, 784-791, 1987.

Mosby, H., The Water of the Atlantic Ocean, *Scientific Results of the Norwegian Antarctic Expedition 1927-1928, 1*, 1934.

National Center for Atmospheric Research (NCAR), *Southern Hemisphere Climatology Data Base*, Fleet Numerical Oceanography Center, Monterey CA, 1989.

National Aeronautics and Space Administration (NASA), *Antarctic Sea Ice, 1973-1976*, NASA SP 459, Washington, DC, 1983.

Neal, V. T., H. Crew and R. Broome, Oceanographic Measurements Under Winter Sea Ice in McMurdo Sound, *Antarctic Journal of the United States, 11*, (4), 235-239, 1976.

- Overland, J. E., Atmospheric Boundary Layer Structure and Drag Coefficients Over Sea Ice, *Journal of Geophysical Research*, **90**, (C5), 9029-9049, 1985.
- Parish, T. R. and D. H. Bromwich, The Surface Windfield Over the Antarctic Ice Sheets, *Nature*, **328**, 51-54, 1987.
- Pickard, G. L. and W. J. Emery, *Descriptive Physical Oceanography*, Pergamon Press, Oxford, England, 1982.
- Pillsbury, R. D. and S. S. Jacobs, Preliminary Observations From Long-Term Current Meter Moorings Near the Ross Ice Shelf, Antarctica. In: S. S. Jacobs (editor), *Oceanology of the Antarctic Continental Shelf, Antarctic Research Series*, **43**, American Geophysical Union, Washington, DC, 87-107, 1985.
- Pond, S. and G. L. Pickard, *Introductory Dynamical Oceanography*, Pergamon Press, Oxford, England, 1983.
- Reid, J. L. and R. J. Lynn, On the Influence of the Norwegian-Greenland and Weddell Seas Upon the Bottom Waters of the Indian and Pacific Oceans, *Deep-Sea Research*, **18**, 1063-1088, 1971.
- Robin, G. de Q., C. S. M. Drake, H. Kohnen, R. D. Crabtree, S. R. Jordan and D. Moller, Regime of the Filchner-Ronne Ice Shelves, Antarctica, *Nature*, **302**, 582-586, 1983.
- Schlosser, P., Helium: A new Tracer in Antarctic Oceanography, *Nature*, **321**, 233-235, 1986.
- Schwerdtfeger, W., *Developments in Atmospheric Science 15: Weather and Climate of the Antarctic*, Elsevier, Amsterdam, The Netherlands, 1984.
- Schwiderski, E. W., *Global Ocean Tides, Part I: A Detailed Hydrodynamical Interpolation Model*, NSWC DL TR-3866, Dahlgren, VA, 1978.
- Schwiderski, E. W., *Global Ocean Tides, Part II: The Semidiurnal Principal Lunar Tide (M_2)*, *Atlas of Tidal Charts and Maps* NSWC TR 79-414, Dahlgren, VA, 1979.
- Schwiderski, E. W., *The NSWC Global Ocean Tide Data Tape (GOTD), Its Features and Application*, *Random Point Tide Program* NSWC TR 81-254, Dahlgren, VA, 1981a.
- Schwiderski, E. W., *Global Ocean Tides, Part III: The Semidiurnal Principal Solar Tide (S_2)*, *Atlas of Tidal Charts and Maps* NSWC TR 81-122, Dahlgren, VA, 1981b.
- Schwiderski, E. W., *Global Ocean Tides, Part VI: The Semidiurnal Elliptical Lunar Tide (N_2)*, *Atlas of Tidal Charts and Maps* NSWC TR 81-218, Dahlgren, VA, 1981c.
- Schwiderski, E. W., *Global Ocean Tides, Part VIII: The Semidiurnal Declination Luni-Solar Tide (K_2)*, *Atlas of Tidal Charts and Maps* NSWC TR 81-222, Dahlgren, VA, 1981d.
- Schwiderski, E. W., *Global Ocean Tides, Part IV: The Diurnal Declination Luni-Solar Tide (K_1)*, *Atlas of Tidal Charts and Maps* NSWC TR 81-142, Dahlgren, VA, 1981e.
- Schwiderski, E. W., *Global Ocean Tides, Part V: The Diurnal Principal Lunar Tide (O_1)*, *Atlas of Tidal Charts and Maps* NSWC TR 81-144, Dahlgren, VA, 1981f.

- Schwiderski, E. W., *Global Ocean Tides, Part VII: The Diurnal Principal Solar Tide (P_2)*, *Atlas of Tidal Charts and Maps* NSWC TR 81-220, Dahlgren, VA, 1981g.
- Schwiderski, E. W., *Global Ocean Tides, Part IX: The Diurnal Elliptical Lunar Tide (Q_1)*, *Atlas of Tidal Charts and Maps* NSWC TR 81-224, Dahlgren, VA, 1981h.
- Seehrist, F., Naval Environmental Prediction Research Facility, Interview by D. St. Pierre, 10 January 1989.
- Solomon, H., Vertical Mixed Layer Convection in the Weddell Sea, *Atmosphere-Ocean*, **21**, (2), 187-206, June 1983.
- Sverdrup, H. U., M. W. Johnson and R. H. Fleming, *The Oceans*, Prentice-Hall, Inc., Englewood, NJ, 1942.
- Tchernia, P., *Descriptive Regional Oceanography*, Pergamon Press, Oxford, England, 1980.
- U. S. Navy Hydrographic Office, *Oceanographic Atlas of the Polar Seas, Part I Antarctic*, H. O. Pub No. 705, Washington DC, 1957.
- U. S. Navy Hydrographic Office, *Marine Climate Atlas of the World Volume VII Antarctic*, NAVWLP 50-1C-50, U. S. Government Printing Office, Washington DC, 1965.
- Vannev, J. R. and G. L. Johnson, GELCO Bathymetric Sheet 5.18 (Circum-Antarctic). In: S. S. Jacobs (editor), *Oceanology of the Antarctic Continental Shelf, Antarctic Research Series*, **43**, American Geophysical Union, Washington, DC, 1-3, 1985.
- Warren, B. A., Deep Circulation of the World Ocean, In: B. A. Warren and C. Wunsch (editors), *Evolution of Physical Oceanography*, The MIT Press, Boston, MA, 6-41, 1981.
- Weiss, R. F., H. G. Ostlund and H. Craig, Geochemical Studies of the Weddell Sea, *Deep-Sea Research*, **26**, (A), 1093-1120, 1979.
- Whitworth III, T., The Antarctic Circumpolar Current, *Oceanus*, **31**, (2), 53-58, 1988.
- Worthington, L. V., The Water Masses of the World Oceans: Some Results of a Fine-scale Census, In: B. A. Warren and C. Wunsch (editors), *Evolution of Physical Oceanography*, The MIT Press, Boston, MA, 42-69, 1981.
- Wüst, G., The Origin of the Deep Waters of the Atlantic (1928), In: M. B. Deacon (editor), *Oceanography Concepts and History*, Dowden, Hutchinson and Ross, Inc., Stroudsburg, PA, 65-88, 1978.

INITIAL DISTRIBUTION LIST

		No. Copies
1.	Defense Technical Information Center Cameron Station Alexandria, VA 22304-6145	2
2.	Library, Code 0142 Naval Postgraduate School Monterey, CA 93943-5002	2
3.	Superintendent Attn: Prof. R. H. Bourke (Code 68Bf) Naval Postgraduate School Monterey, CA 93943	4
4.	Prof. Arne Foldvik University of Bergen Institute of Geophysics Department of Oceanography N-5007 Bergen, NORWAY	4
5.	LCDR David B. St.Pierre HQ NAVSOUTH Box 168 FPO, New York 09524	2
6.	Prof. Theodore D. Foster Marine Sciences University of California Santa Cruz, CA 95064	1
7.	Dr. E. Schwiderski Naval Surface Warfare Center Code K104 Dahlgren, VA 22448	1
8.	Superintendent Attn: Prof. C. C. Collins (Code 68Co) Naval Postgraduate School Monterey, CA 93943	2
9.	Commanding Officer Naval Oceanographic Office Stennis Space Center, MS 39529	1
10.	Commander Naval Oceanography Command Stennis Space Center, MS 39529	1

- | | | |
|-----|---|---|
| 11. | Commanding Officer
Naval Ocean Research and Development Activity
Stennis Space Center, MS 39529 | 1 |
| 12. | Commanding Officer
Naval Polar Oceanography Center, Suitland
Washington, DC 20373 | 1 |
| 13. | Commander
Naval Support Force Antarctica
Box 100
FPO San Francisco, CA 96601 | 1 |
| 14. | Prof. Joseph L. Reid Jr.
Scripps Institution of Oceanography
University of California, San Diego
La Jolla, CA 92037 | 1 |
| 15. | Prof. Arnold L. Gordon
Lamont-Doherty Geological Observatory
Palisades, NY 10964 | 1 |
| 16. | Prof. Stanley S. Jacobs
Lamont-Doherty Geological Observatory
Palisades, NY 10964 | 1 |
| 17. | Prof. Eddy C. Carmack
Institute of Ocean Sciences
P.O. Box 6000
9860 West Saanich Road
Sidney, British Columbia V8L 4B2
Canada | 1 |
| 18. | Superintendent
Attn: Chairman, Oceanography Department
U. S. Naval Academy
Annapolis, MD 21402 | 1 |
| 19. | Commanding Officer
Naval Environmental Prediction Research Facility
Monterey, CA 93943 | 1 |
| 20. | Superintendent
Attn: Prof. Robert Renard (Code 63Rd)
Naval Postgraduate School
Monterey, CA 93943 | 1 |